Chapter 1
Introduction

1.1 Ordering by Disorder

The kagomé Heisenberg antiferromagnet has attracted considerable attention in recent years [1]. It is an example of frustrated systems where the classical ground state manifold has macroscopic degeneracies, and where most of these ground states are disordered. The interesting question is whether an unique, ordered state will emerge when either quantum or thermal fluctuations are added to the system. The peculiar ordering effect of fluctuations is usually called "ordering by disorder", and is found in many systems [2], such as the frustrated Ising magnet on a square lattice [3], or the freezing of hard spheres [4].

The qualitative reason why fluctuations tend to select order is quite easy to understand. What we called an "ordered" state refers to the average configuration of a fluctuating system, which is one of the ground states of a classical Hamiltonian. The average configuration could be very well-ordered, yet the fluctuational entropy (in the classical case) or the quantum zero point energy could be very high. In such a case, this ordered state may be the thermodynamic state observed in an experiment. Fluctuational entropy or quantum zero point energy depends on the stiffness of the system against fluctuations. This stiffness is proportional to the curvature of the potential well centered around each average configuration. The smaller the stiffness, the larger the fluctuations, and the

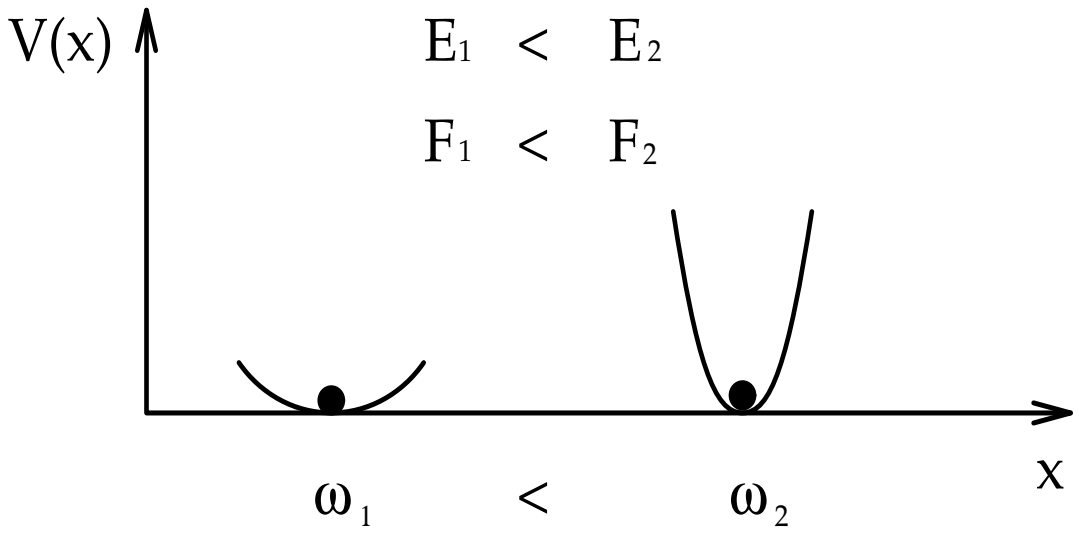

Figure 1.1 Particles in two harmonic potentials, with frequencies $\omega_1 < \omega_2$. Considered as quantum particles, the quantum zero point energy is $E = \frac{1}{2}\hbar\omega$. Considered as classical particles, the thermal free energy is $F = k_B T \ln[1 - e^{-\hbar\omega/k_B T}]$. In both cases, the (free) energy is higher for particle 2.

larger the entropy (or the smaller the free energy and quantum zero point energy.) This situation is illustrated in Figure 1.1 for two 1-dimensional harmonic potential wells. It so happens that in nature, a well-ordered configuration often has a less stiff effective potential well around it[1]. To visualize this, take the example of a sheet of paper. When it is flat (the *ordered* state), it is relatively easy to make waves on it. When it is crumpled (the *disorder* state), it becomes much stiffer. In fact, this analogy with paper folding is exploited quantitatively by Ritchey *et al*[5] and Shender *et al*[6, 7] for the kagomé antiferromagnet, carrying the picturesque name of "spin origami".

[1] This is with the proviso that the different configurations have the same underlying microscopic Hamiltonian. Ferromagnet is stiffer than spin glass: but they have different Hamiltonians.

In the kagomé spin system, an "ordered" state refers to a configuration where the spin orientations (treated as vectors) have certain periodicity. Examples are the "q=0" and the "$\sqrt{3} \times \sqrt{3}$" states depicted in Figure 1.2 . On the other hand, a "disordered" state is one where the spin orientations have no repeating patterns. Our goal in this thesis is to show that quantum fluctuations endow one such ordered state– the "$\sqrt{3} \times \sqrt{3}$" state – with the lowest quantum energy among all states, and this is therefore a case of "ordering by disorder". (This is in conformity with widespread expectation.)

1.2 Regimes of Interest

We have identified two ways[2] of adding fluctuations to the ground states of a classical system: quantum and thermal. In each case there is a control parameter for controlling the magnitude of the fluctuations. For quantum fluctuations in spin systems, it is the spin quantum number S. For thermal fluctuations, it is the temperature T. The quantity $1/S$ for a spin is analogous to the Planck's constant h for a particle: the smaller it is, the less quantum fluctuation there will be. This analogy can be made formal through an uncertainty relation for spins. (See Section[3.1].)

The case of thermal ordering by disorder in the kagomé antiferromagnet has been explored by several authors [8, 9, 10, 11]. The techniques used included spinwave expansion, high temperature expansion, mapping to height models, as well as Monte Carlo simulations. The general conclusion is that the "coplanar" states are selected. (A coplanar state is one in which all the spins are

[2] A third way, not discussed here, is adding quenched disorder such as dilution to the system. See Ref. 2, 3 and 6.

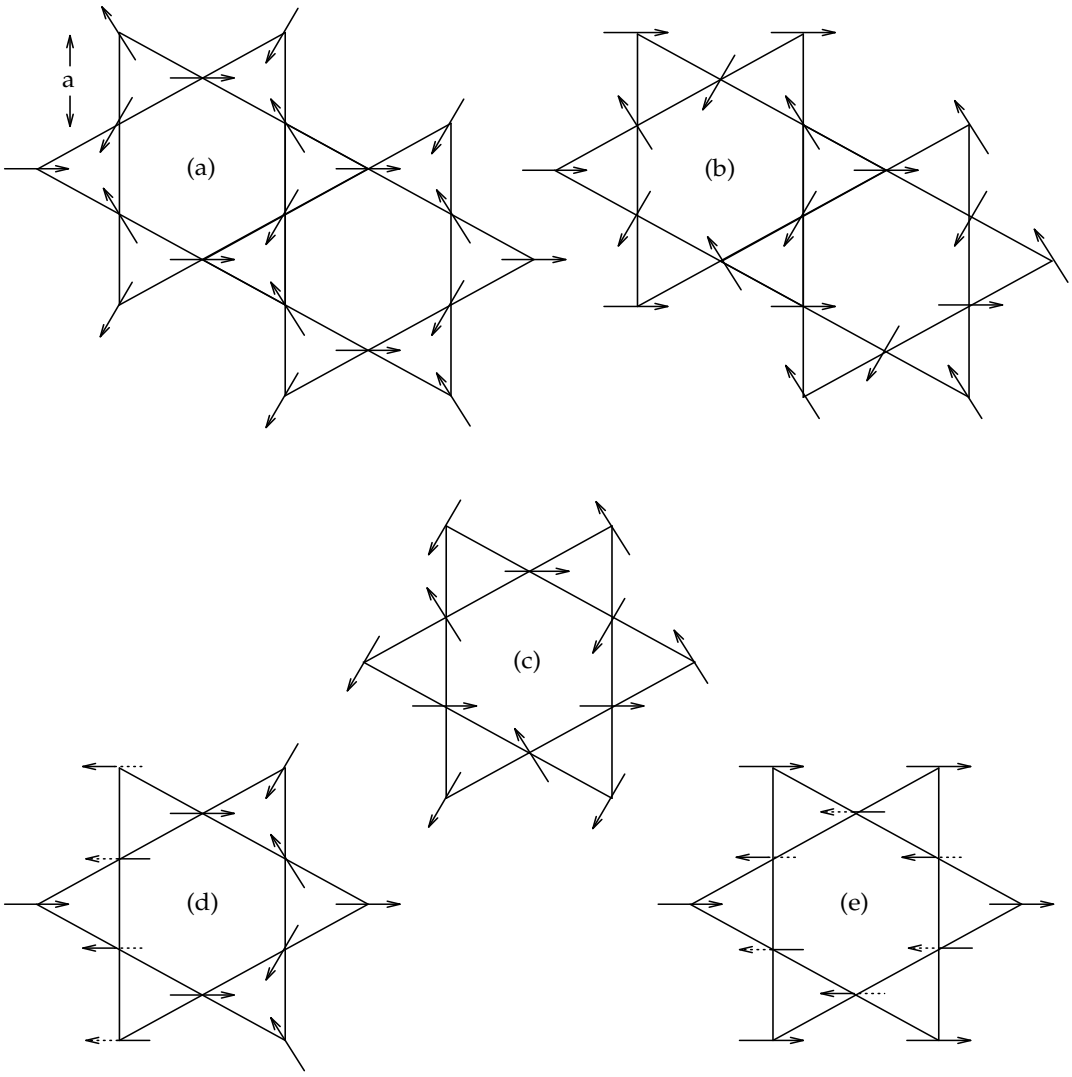

Figure 1.2 (a) is the "q=0" state. (b) is the "$\sqrt{3}\times\sqrt{3}$" state. Both of them are coplanar states. (c) is an example of a disordered coplanar state. The triangular Bravais lattice has lattice constant "2a". (d) is similar to the "q=0" state, except one column of spins are rotated by 90° clockwise in spin space with the spins pointing to the right as rotation axis. (The dotted lines indicate portion of spin behind the plane of the paper. The rotated spins are *not* drawn to scale.) (e) is similar to the "$\sqrt{3}\times\sqrt{3}$" state, except spins around the hexagon is rotated by 90° clockwise in spin space with the spins pointing to the right as rotation axis. (d) and (e) are examples of non-coplanar ground states.

pointing within the 2-dimensional plane of the kagomé lattice. See Figure 1.2.) Less conclusive is the determination of whether one particular coplanar state is selected to be the thermodynamic state, although it is generally believed that the most likely candidate is the "$\sqrt{3} \times \sqrt{3}$" state shown in Figure 1.2. It was found that the anharmonicity of the potential well governing the fluctuations must be taken into account in order to delineate this latter "in-plane" selection.

The case of quantum fluctuations is more complicated. The extreme quantum limit where $S = \frac{1}{2}$ requires special treatment, since spinwave theory is believed to fail here. The techniques used range from various field-theoretic methods such as large-N expansion [12, 13] to exact diagonalizations [14, 15, 16]. The focus has been on the possible existence of spin- Peierls order, as well as other spin-dimerized states which break translational symmetry[17]. These theoretical studies are relevant to understanding the magnetic properties of experiments done on second layer ^{3}He adsorbed on graphite surface [18].

The focus of our research is the semi-classical regime where S is large but not infinite. Several authors have studied this regime previously [5, 19,13, 20], as it is believed to be relevant to the experiments on the layered alloy $SrCr_{8-x}Ga4 + xO_{19}$ (abbreviated as SCGO(x))[21, 22, 23]. The Cr^{3+} ions of this alloy has $S = \frac{3}{2}$. They interact antiferromagnetically and form alternating planes of triangular and kagomé lattices. The interplane coupling between these ions is weaker than the intraplane coupling. Also, the interaction between ions within the kagomé planes is stronger that that within the triangular planes. Therefore, any magnetic ordering that this system exhibits is attributed to the kagomé planes. Neutron scattering experiments on this alloy shows that there is some short range spin-ordering present, which is consistent with the "$\sqrt{3} \times \sqrt{3}$" state.

Similar to the thermal case, theoretical work on this semi-classical system also indicated that the manifold of coplanar states is selected. Within this coplanar manifold, there are again inconclusive evidence to show which particular state is selected by quantum fluctuations. Based on large-N expansion of the symplectic group, Sachdev [13] argued that the "$\sqrt{3} \times \sqrt{3}$" state indeed has the lowest energy among a hundred or so coplanar states in a finite system. We present in this work a method of selecting among the infinite set of coplanar states.

1.3 Outline of Paper

As we saw, there is a lot of previous work done on the kagomé quantum antiferromagnet. We summarize the qualitative picture that emerges from these works in Chapter 2.

The first step in analyzing the kagomé antiferromagnet is to identify all the possible classical ground states (Section[2.1]). For a subset of these states, we show how one may continuously transform one ground state to another without at any point leaving the ground state manifold.

In order to justify our focusing attention on only the coplanar ground states, we show in Section[2.2] how the coplanar state is selected by including harmonic quantum fluctuations. Here we discover a peculiar feature of the coplanar state: one branch of harmonic spinwave spectrum is identically zero throughout the Brillouin zone. We call these excitations "zero modes". We explain (Section[2.3]) the origins of the zero modes by showing that they can be expressed as a linear combination of a complete but non-orthogonal set of zero-frequency modes in real space. These are the "hexagon modes".

Adding anharmonic flutuations to the systems has drastic effects on the zero modes (Section[2.4]). They acquire stiffness and turn into "soft modes". However, the zero modes of different coplanar states acquire different stiffness. This form the basis for selection among different coplanar states: what we call "in-plane" selection.

The detailed calculation of the quantum zero point energy of each coplanar state is presented in Chapter 3 . We construct a spinwave Hamiltonian for the states in the coplanar manifold (Section[3.1]). The spinwave Hamiltonian is simply the quantum Heisenberg Hamiltonian expanded in terms of small deviations from the classical spin directions. If one performs this expansion up to quartic order in the spin deviation variables, it becomes manifest that only the cubic terms depend on the particular Potts configuration. The quartic terms are essential for stabilizing the system against fluctuations; however, they play no role in in-plane selection.

The ground state energy of this spinwave Hamiltonian is estimated by means of a variational wavefunction approach (Section[3.2]). It is essential that such a wavefunction captures the contribution of cubic terms. We employ the low energy eigenstates of a harmonic Hamiltonian to serve as the basis functions of the variational wavefunction subspace. (We call this Hamiltonian the renormalized harmonic Hamiltonian $\tilde{\mathcal{H}}$). We include its ground state (Section[3.3]), which is of course a gaussian, as well as its excited states (Section[3.4]) with one and three magnons as our basis. This basis is the bare minimum necessary for in-plane selection.

In principle, we can take this variational wavefunction and calculate the expectation of the spinwave Hamiltonian for each coplanar state (Section[3.5

]). However, this procedure would allow us to check only a very small number of such states. We find that we can, at the price of treating the cubic spinwave Hamiltonian as a perturbation (Section[3.6]. The nature of our perturbation theory is compared to the conventional reciprocal space perturbation in Section[3.8].), express the zero point energies of *all* the coplanar states in the form of an Ising Hamiltonian,

$$E_g = \text{const.} + \sum_{\alpha\beta} \mathcal{J}_{\alpha\beta}\eta_\alpha\eta_\beta,$$

with the *chiralities* η_α of the triangles serving as the Ising variables (Section[3.7]). The chirality of a triangle in the kagomé spin system has been defined before [9,10]. Each coplanar state can be mapped to a unique set of chirality variables defined on the triangles. The coupling constants $\mathcal{J}_{\alpha\beta}$ can be calculated in terms of the spin-spin correlation functions within just the gaussian part of the variational subspace. Once the $\mathcal{J}_{\alpha\beta}$'s are determined, finding the lowest energy coplanar state becomes the much easier problem of finding the ground state of an Ising model. We find that this corresponds to the "$\sqrt{3}\times\sqrt{3}$" configuration (Section[3.9.1]. We show in Section[3.9.2] that the not-explicitly-Ising terms have no in-plane selection effects.).

There is one technical issue involved in this variational minimization scheme: the variational energy has a minimum only if we artificially decrease the magnitude of the cubic spinwave Hamiltonian (Section[3.9.3] and Section[3.9.4]). This raises some questions concerning the validity of the perturbation approximation which we and Chubukov both depend on. This issue will be discussed in Section[3.10.1]. Possible errors in our in-plane selection result due to the approximations involved are discussed in Section[3.10.2]. We conclude in Section[4].

Chapter 2
Review of Kagomé Peculiarities

2.1 Classical Ground States

The kagoḿe lattice is a triangular lattice with lattice constant a, where vacancies have been introduced at all sites of a triangular superlattice, with lattice constant $2a$. (See Figure 1.2.) The Hamiltonian defined on this lattice has Heisenberg interactions with antiferromagnetic nearest-neighbor couplings:

$$\mathcal{H} = J \sum_{\langle ij \rangle} \mathbf{S}_i \cdot \mathbf{S}_j, \tag{2.1}$$

with $J > 0$.

The basic unit of a classical ground state is the triad of spins residing on one triangle of the lattice: obviously, if the energy of each of this triad is minimized, the resulting state is a global ground state. Now if we consider only 3 spins on a triangle, it is clear that the Hamiltonian can be written as $\mathcal{H} \sim \text{const.} - \frac{1}{2}(\mathbf{S}_1 + \mathbf{S}_2 + \mathbf{S}_3)^2$, and the ground state is obtained when $\mathbf{S}_1 + \mathbf{S}_2 + \mathbf{S}_3 = \mathbf{0}$. This means that the triad of spins on one triangle must lie in the same plane in spin-space, and the angle between any pairs of spins must be 120°. Note however that this spin-plane is independent from the lattice plane. A ground state of the full lattice is then formed by fitting all these spin-triads together. We shall enumerate the different possibilities.

It is clear that the Heisenberg Hamiltonian Eq.(2.1) possesses the continuous global rotational symmetry (O(3)). Hence in the enumeration below, we shall

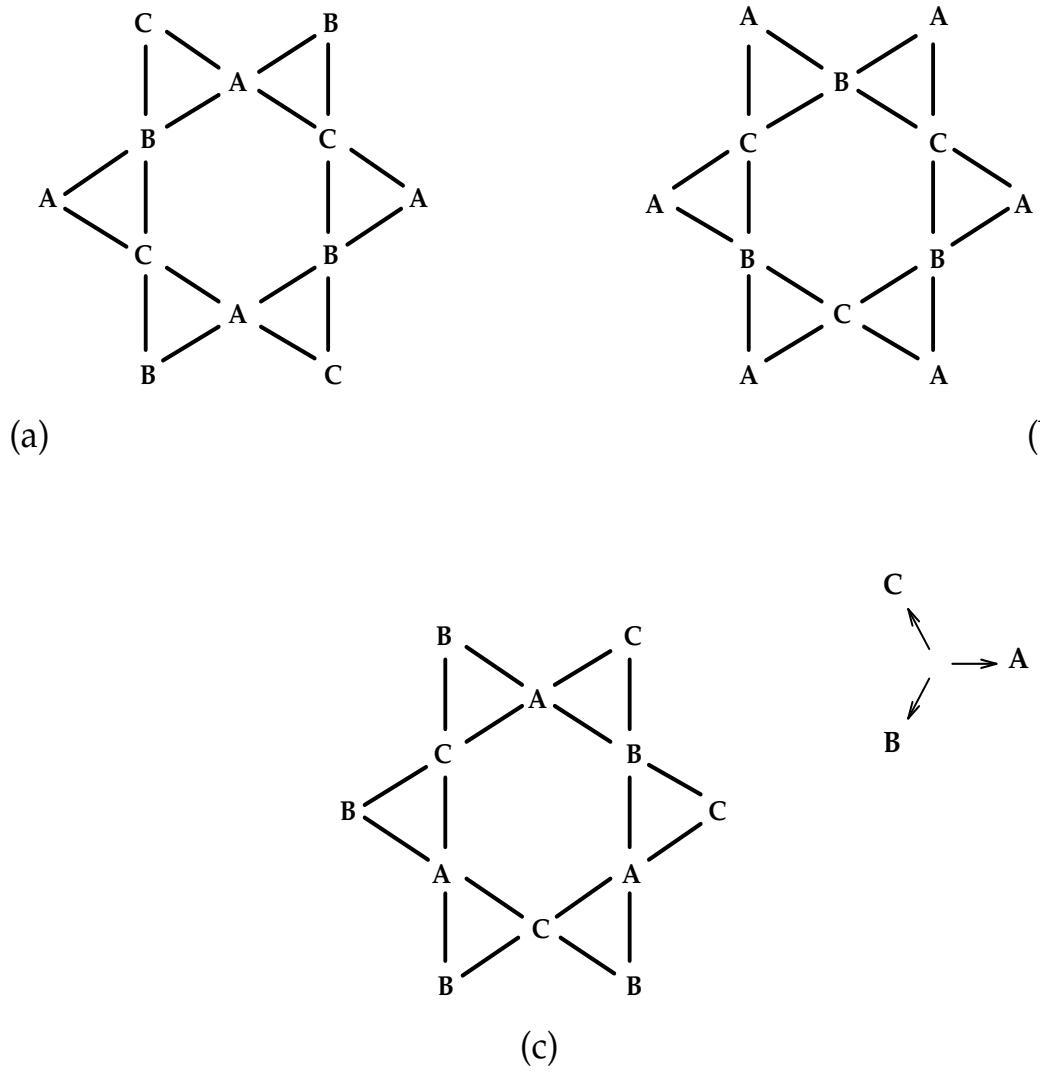

Figure 2.1 Labeling of coplanar states by 3 letters A, B and C, which correspond to the spin directions as shown in the figure. (a), (b) and (c) are the same states as the hexagons marked (a), (b) and (c) respectively in Figure 1.2.

fix the spin-plane formed by one of the spin-triads mentioned above to coincide with the lattice plane to eliminate this trivial degree of freedom.

First, let us restrict to the coplanar manifold, where all the spin-triads are lying on the same spin-plane, which we have fixed to be parallel to the lattice.

If we label the 3 possible spin directions A,B,C, then it is clear that as long as there are 3 different letters on every triangle, it is a classical ground state. (See for example, Figure 2.1). This ensemble of states can clearly be mapped to a 3-state Potts model. In fact, there is a one-to-one correspondence between each classical (coplanar) ground state to each ground state of the antiferromagnetic Potts Hamiltonian; consequently, we call these coplanar states "Potts states". The number of possible Potts states is about $e^{0.126N_s}$, where N_s is the total number of spins[24].

There is one way of describing such Potts states that will prove useful below in understanding the deviations from the Potts configurations. (However, this description is not intended as a convenient way to count all the possible Potts states.) We can identify chains of alternating 2-letter sequence, such as the ABABAB... sequence. The difference between the locations of these chains is a good way to classify the Potts states: once the location of a chain is determined, there remains only the trivial binary degree of freedom for the letters. These chains may be closed or open. For example, for the "$\sqrt{3} \times \sqrt{3}$" state, the AB chains form closed loops around hexagons. For the "q=0" state, they form infinite straight lines.

Now let us consider the non-coplanar ground states. Figure 2.2 shows how one can create a pair of non-coplanar spin-triads from an originally coplanar pair. The trick is to match all the different rotated spin-triads together to form a ground state. One way to do this is to consider the AB-chains that we described above. If we fix the neighboring C spins and rotate all these AB's about the C-axis, we have obtained a non-coplanar ground state. We have illustrated this in Figure 1.2 for the "$\sqrt{3} \times \sqrt{3}$" and the "q=0" states. For "$\sqrt{3} \times \sqrt{3}$" state, spins on each of these hexagons with the AB-chains can be rotated independently

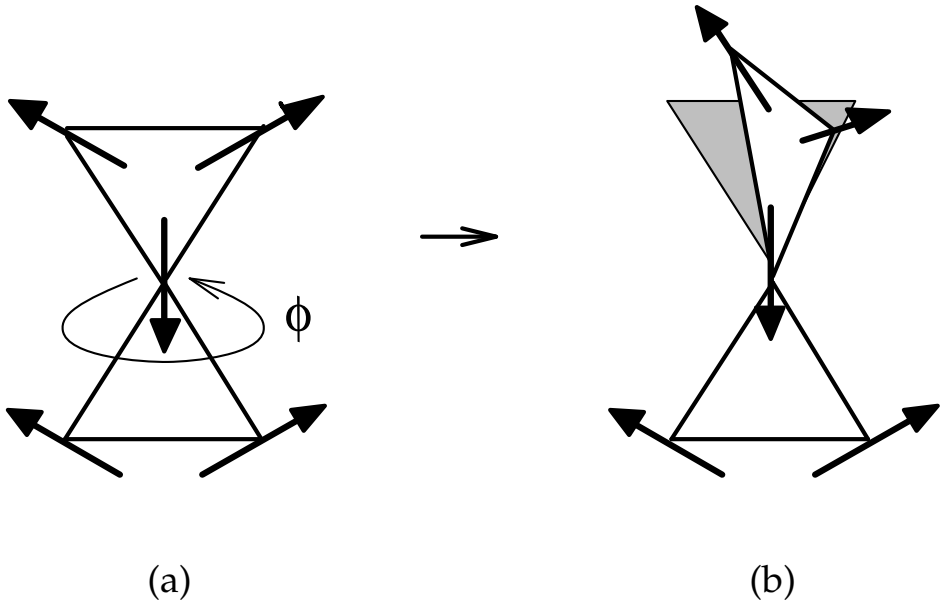

Figure 2.2 Creating a non-coplanar state by rotating the spin-plane of a coplanar state. (a) shows the original coplanar state. If we rotate the upper triangle in *spin* space about the vertical axis by ϕ, we obtain a non-coplanar state which remains a classical ground state.

of others. Since there are $N_s/9$ such independent hexagons, there are at least $N_s/9$ continuous degrees of freedom for such rotations. This particular kind of rotations in the "$\sqrt{3} \times \sqrt{3}$" state is called a "weathervane defect". (If fix the angles of rotations to be the same for every AB-chain, this is just the global rotation of the whole system about the C-axis, an obvious symmetry of the Hamiltonian.)

2.2 Coplanar Selection

We have argued above that one can continuously rotate groups of spins from any coplanar state to a non-coplanar state without any cost in classical energy. However, if we now add fluctuations to the system, the situation will be entirely different for the coplanar and the non- coplanar state. The effects of fluctuations about a classical ground state can be calculated by spinwave theory, which is essentially a Taylor-series expansion of the Hamiltonian for small deviations from the classical ground state. (It will be given explicitly in Section[3.1].) If the expansion is only to quadratic order in spin deviations, the resulting excitation spectrum is called the *harmonic* spinwave spectrum.

If we imagine creating a non-coplanar state by rotating the spins in, say, all AB-chains by an angle ϕ, we will get a spinwave spectrum depicted in Figure 2.3(b), (assuming that the AB-chains are periodic in real space and all of them rotate by the same angle). The total quantum zero point energy for the fluctuations about this noncoplanar state is obtained by summing over all the spinwave frequencies, $E_g = 1/2 \sum_k \hbar\omega(k)$. It is found to be $E_g(\phi) \sim SL|J\sin\phi|$, where L is the total length of all the rotated spin-chains [5, 25]. Since this effective potential $E_g(\phi)$ has a minimum at $\phi = 0$, it may seem sufficient proof that the coplanar state is selected to be the quantum ground state. However, this formula is actually valid only for large ϕ, i.e. ϕ larger than the rms fluctuations $\sqrt{\langle\phi^2\rangle}$ about $\phi = 0$. For smaller ϕ, it is no longer distinguishable from the zero point fluctuations about $\phi = 0$ and cannot be set to a fixed value.

It is unclear from the above arguments whether the coplanar state with all $\phi = 0$ is indeed stable against small fluctuations. In fact, if we now look at the harmonic spinwave spectrum (as calculated, for e.g., in Section[3.3]) for the

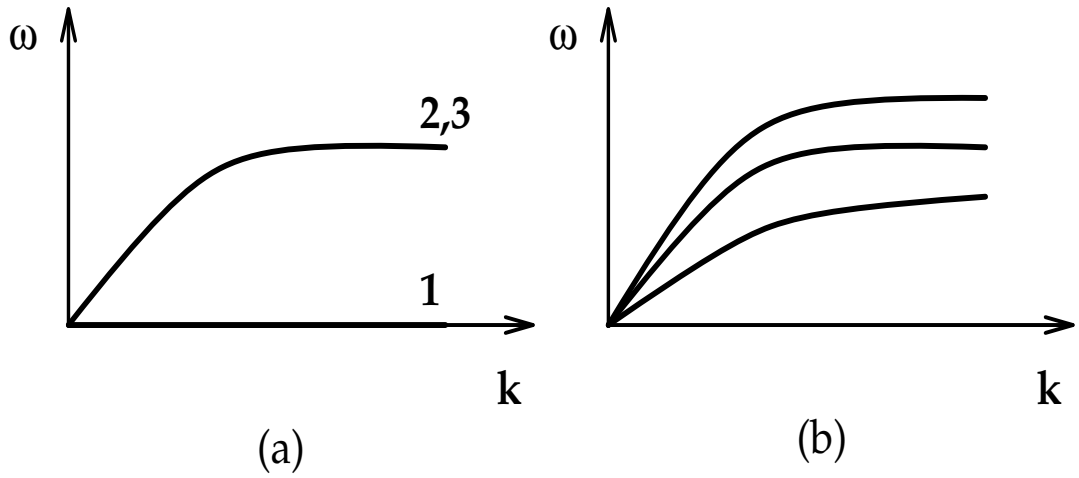

Figure 2.3 Schematic harmonic spinwave spectrum of (a): a coplanar state, and (b): a non-coplanar state along some typical direction in the Brillouin zone. Note that in (a), there is a branch (1) which has $\omega = 0$ for the entire Brillouin zone. These modes are called the "zero modes". Also, the other two branches (the "ordinary modes" 2,3) are degenerate. The calculation of these spectra will be discussed in Sections 3.1 , 3.3 and Appendix B .

coplanar states, a peculiar feature emerges: there is a branch of the spectrum which is zero for the entire Brillouin zone. (See Figure 2.3(a).) This means that there is no stiffness against this mode of fluctuations and the system is unstable. (Another curious feature is that the spinwave spectrums are identical for all Potts states: if we are defining the spin deviations with respect to local coordinate axes. This point will be explained in Section[3.1]. The sameness of spinwave spectrums implies that the same zero modes exist around every Potts states.)

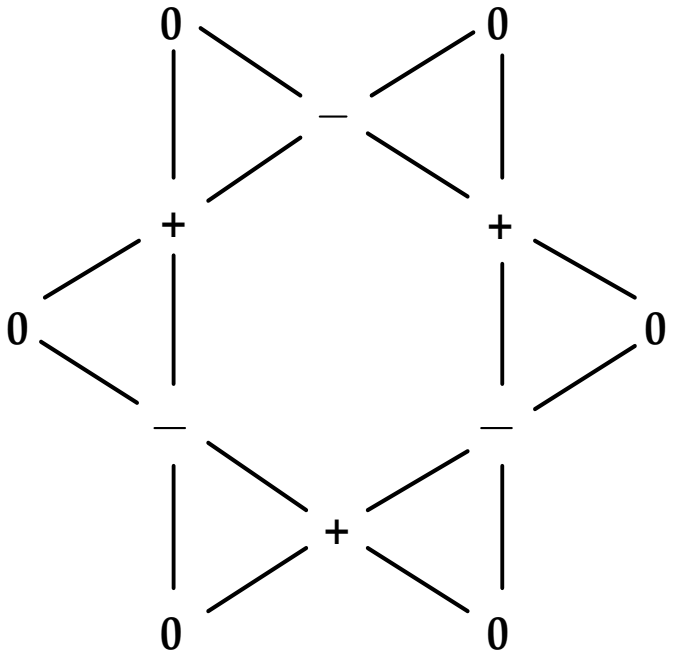

Figure 2.4 The hexagon mode. Spins around a hexagon are deviating vertically up (+) or down (−) with respect to the spin plane (in the harmonic approximation). The surrounding spins have zero deviation.

2.3 Zero Modes

The excitation modes corresponding to the zero branch mentioned in Section[2.2] are called "zero modes", meaning they cost no energy. They can be thought of as linear superpositions of "hexagon modes". A "hexagon mode" is the harmonic analogue of the "weathervane defect" described in Section[2.1]. Instead of rotating the spins on a hexagon by a large, finite angle, a hexagon mode has these spins deviating vertically up or down by an infinitesimal amount in the pattern (+,−,+,−,+,−) with respect to the common spin-plane of the coplanar state. The surrounding spins are fixed to have zero deviation. (See Figure 2.4.)

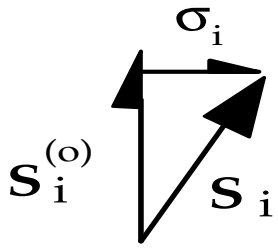

Figure 2.5 Definition of the spin deviation vector $\boldsymbol{\sigma}_i$. $\mathbf{S}_i^{(0)}$ is the spin in classical ground state direction, $\mathbf{S}_i$ is the instantaneous direction of the spin, and $\boldsymbol{\sigma}_i$ is the component of $\mathbf{S}_i$ which is orthogonal to $\mathbf{S}_i^{(0)}$.

We can show easily that this deviation costs no energy to harmonic order, if we allow ourselves to think of the deviating spins as classical vectors for the moment. Define the axis normal to the lattice $\hat{\mathbf{y}}$. Let the spin deviation vector for spin i be $\boldsymbol{\sigma}_i$. The spin deviation vector is defined as $\boldsymbol{\sigma}= \mathbf{S}_i - (\mathbf{S}_i \cdot \mathbf{S}_i^{(0)}/|\mathbf{S}_i^{(0)}|^2)\mathbf{S}_i^{(0)}$, where the $\mathbf{S}^{(0)}$'s are the classical ground state spin directions (Figure 2.5). By construction, $\boldsymbol{\sigma}$ have only x and y components. Since the spins are deviating up or down relative to the spin-plane in the hexagon mode, we have $\boldsymbol{\sigma}_i = \sigma_{iy}\hat{\mathbf{y}}$, where $\sigma_{iy} \propto \pm 1$. For the surrounding spins, $\sigma_{iy} = 0$. Now consider any triangle surrounding the hexagon. Up to harmonic order in σ_{iy}, the energy of spins on each of them is zero: $E \sim -(\mathbf{S}_1 + \mathbf{S}_2 + \mathbf{S}_3)^2 = -(\mathbf{S}_1^0 + \mathbf{S}_2^0 + \mathbf{S}_3^0 + (\sigma_{1y} + \sigma_{2y} + \sigma_{3y})\hat{\mathbf{y}} + \mathcal{O}(\sigma_{iy}^2\hat{\mathbf{z}}))^2 \approx 0$. The $\mathbf{S}^{(0)}$'s are the ground state spin directions, and they add up to zero around a triangle. The σ_y's also add up to zero for the hexagon mode. Hence the energy is zero up to quartic order in σ_{iy}.

One can also verify that the hexagon mode on one hexagon does not intereact with nearby hexagon modes: to harmonic order, the total energy of 2 neigh-

boring hexagon modes is simply the sum of energies of each isolated mode. Say one hexagon has fluctuations $\sigma_y = A_0(+1,-1,+1,-1,+1,-1)$ and its neighbor has fluctuations $\sigma_y = A_1(+1,-1,+1,-1,+1,-1)$. The two hexagons intersect at two triangles. But if we add up the fluctuations on these triangles, we find that they still cost zero energy. Thus any linear combination of these hexagon modes is a zero mode. There are $N_s/3$ such hexagons, and therefore $N_s/3$ independent (but non-orthogonal) zero modes, just enough to form one of the three branches of the spinwave spectrum [9].

2.4 Effects of Anharmonicity

The degeneracy with respect to hexagon mode fluctuations is eliminated once quartic order in σ_y is included. Neighboring hexagon modes now start to interact, and so almost all linear combinations of hexagon modes now cost energy.

There were two calculations done previously to calculate quantitatively the effects of the anharmonicity. The first one, by Chubukov [20], assumes that the spinwave spectrum is renormalized by the anharmonicity and acquires the form given by a harmonic Hamiltonian with next-nearest-neighbor coupling J_3. J_3 is calculated self-consistently through a second-order perturbation theory. In the second calculation, von Delft and Henley [25] use a self-consistent approach in real space. It focuses on the stiffening of the hexagon mode due to the hexagon mode fluctuation of its neighbor. Since the magnitude of fluctuation is related to the amount of stiffening, it can be calculated self-consistently. The effective potential against out-of-plane fluctuations $E_g(\sigma_y)$ at small σ_y is shown to go as $\sim \sigma_y^2$, instead of σ_y if self-consistent stiffening were not taken into account.

Both of these calculations show that the zero modes now acquire a spinwave frequency proportional to $S^{2/3}$, as opposed to S for the other two branches. Thus they are called "soft modes", while the other two branches are called the "ordinary" modes. The coefficient in front of $S^{2/3}$ depends on the particular classical ground state (and on the wave-vector $\mathbf{k}$). In-plane selection is a result of this dependence.

In the calculation of Chubukov, self-consistency is used to calculate the small-k (where $\mathbf{k} = \mathbf{0}$ is the Goldstone mode) part of the soft branch of the spinwave spectrums of the two symmetric states: the "$\sqrt{3}\times\sqrt{3}$" and the "q=0" states. The frequency for the "$\sqrt{3}\times\sqrt{3}$" state is found to be smaller than that of the "q=0" state. However, the spectrum for larger k's is not explicitly calculated, but is merely assumed to have the same form as that of a next-nearest-neighbor harmonic Hamiltonian. Therefore, it is unclear whether this method will give an accurate comparison of the total zero point energies between two states. Furthermore, one would like to find a method that can tell us which state has the lowest energies among *all* coplanar states.

The calculation of von Delft and Henley, on the other hand, suffers from the fact that it is not very systematic in a variety of ways. In particular, it does not take into account $\mathcal{H}_3$, which (as we shall see) largely cancels the stiffening effects of $\mathcal{H}_4$.

As an aside, we mention here an intuitive argument which purports to show that among all coplanar states, the "$\sqrt{3}\times\sqrt{3}$" state has the lowest quantum energy. Consider again rotations of the spins in the spin-chains mentioned in Section[2.1] which cost zero energy. For the "$\sqrt{3}\times\sqrt{3}$" state, we counted $N_s/9$ independent degrees of freedom for this rotation. All the other coplanar states

have fewer degrees of freedom that correspond to the zero modes. For instance, the "q=0" state can have only $O(\sqrt{N_s})$ such degrees of freedom. So in some sense the stiffness against fluctuations for the "$\sqrt{3} \times \sqrt{3}$" state is the smallest of all, and should have the lowest zero point energy. We believe this intuitive argument is inadequate, since it does not take into account the (nonlinear) interactions among these zero modes. As we mentioned in the previous subsection, when only harmonic terms are taken into account, *all* the coplanar states have equal number of zero modes. When anharmonic terms are introduced, almost all zero modes, including the rotation of spin-chains, are stiffened, and it is not clear *a priori* whether the spin-chain around a hexagon should be stiffened less than the others.

Chapter 3
Calculation of In-plane Selection

3.1 Spinwave Hamiltonian

We derive here the spinwave expansion around a Potts state. Starting with the Heisenberg antiferromagnet Hamiltonian in Eq.(2.1), we write the spins in component forms with respect to a set of local coordinate axes (see Figure 3.1) such that $\hat{\mathbf{z}}_i$ points in the same direction as spin i in the classical ground state, $\hat{\mathbf{y}}_i$ is normal to the spin plane (assuming a coplanar ground state) and $\hat{\mathbf{x}}_i$ forms the third direction in the right-handed orthonormal triad,

$$\mathbf{S}_i = S_{ix}\hat{\mathbf{x}}_i + S_{iy}\hat{\mathbf{y}}_i + S_{iz}\hat{\mathbf{z}}_i. \tag{3.1}$$

This set of local axes is the same as the one used by Chalker *et al* [9]. The advantage of using local axes instead of global Cartesian axes is that the quadratic (and quartic) part of the spinwave Hamiltonian will be manifestly identical for all coplanar states, as we shall explain in more details soon. Noting that for any coplanar ground state and nearest-neighbor (i,j), $\hat{\mathbf{x}}_i \cdot \hat{\mathbf{x}}_j = -\frac{1}{2}$, $\hat{\mathbf{y}}_i \cdot \hat{\mathbf{y}}_j = 1$, $\hat{\mathbf{z}}_i \cdot \hat{\mathbf{z}}_j = -\frac{1}{2}$, $\hat{\mathbf{x}}_i \cdot \hat{\mathbf{z}}_j = -\hat{\mathbf{x}}_j \cdot \hat{\mathbf{z}}_i = \pm\frac{\sqrt{3}}{2}$ and $\hat{\mathbf{x}}_i \cdot \hat{\mathbf{y}}_j = \hat{\mathbf{z}}_i \cdot \hat{\mathbf{y}}_j = 0$, the Hamiltonian becomes

$$\mathcal{H} = J \sum_{\langle ij \rangle} -\frac{1}{2} S_{ix}S_{jx} + S_{iy}S_{jy} - \frac{1}{2} S_{iz}S_{jz} + S_{ix}S_{jz}\hat{\mathbf{x}}_i \cdot \hat{\mathbf{z}}_j + S_{iz}S_{jx}\hat{\mathbf{z}}_i \cdot \hat{\mathbf{x}}_j. \tag{3.2}$$

We use the Holstein-Primakoff transformation [26] to perform spinwave expansion about the classical ground state directions,

$$S_{iz} = S - a_i^\dagger a_i,$$

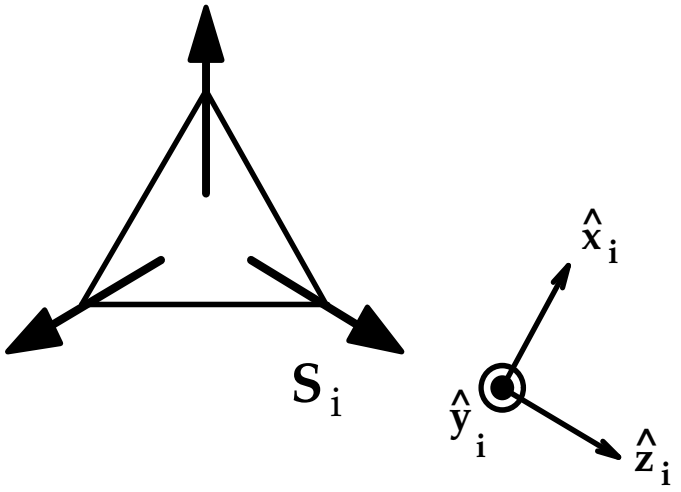

Figure 3.1 Definition of the local coordinate axes $\hat{\mathbf{x}}_i$, $\hat{\mathbf{y}}_i$, and $\hat{\mathbf{z}}_i$ for spin i. $\hat{\mathbf{y}}_i$ points out of the plane.

$$S_{i-} = a_i^\dagger \sqrt{2S - a_i^\dagger a_i},$$
$$S_{i+} = \sqrt{2S - a_i^\dagger a_i}\, a_i, \tag{3.3}$$

with

$$[a_i, a_i^\dagger] = 1.$$

This transformation maps the spins to a set of bosons, which can be thought of as quantum excitations about the classical spins. The $a_i^\dagger$ and a_i are the creation and annihilation operators for boson excitations on spin i, and they are related linearly to the spin deviation operators [27] through a canonical transformation,

$$\sigma_{ix} = \sqrt{\frac{S}{2}}(a_i + a_i^\dagger),$$
$$\sigma_{iy} = -i\sqrt{\frac{S}{2}}(a_i - a_i^\dagger). \tag{3.4}$$

Spin deviation operators are quantum analogues of the classical spin deviation vector mentioned in Section[2.3]. These operators are canonically conjugate

operators and they obey commutation relations similar to the usual position and momentum operators. The only non-zero commutator is

$$[\sigma_{ix}, \sigma_{jy}] = i\, S\, \delta_{ij}. \tag{3.5}$$

The square roots involved in Eq.(3.3) arise from the fixed-length constraint on spins. They are the origins of the (anharmonicity) in the system. Expanding the S-operators up to $O(\sigma^3)$ allow us to write down the quantum Hamiltonian accurate to quartic order in the σ's,

$$\begin{aligned} S_{iz} &= S - \frac{1}{2S}(\sigma_{ix}^2 + \sigma_{iy}^2 - S), \\ S_{ix} &= \sigma_{ix} - \frac{1}{8S^2}(\sigma_{ix}^3 - 2S\sigma_{ix} + \sigma_{iy}\sigma_{ix}\sigma_{iy}), \\ S_{iy} &= \sigma_{iy} - \frac{1}{8S^2}(\sigma_{iy}^3 - 2S\sigma_{iy} + \sigma_{ix}\sigma_{iy}\sigma_{ix}). \end{aligned} \tag{3.6}$$

Substituting Eq.(3.6) into the original Hamiltonian Eq.(3.2) gives us $\mathcal{H} = E_{classical} + \mathcal{H}_0 + \mathcal{H}_2 + \mathcal{H}_3 + \mathcal{H}_4 + \cdots$, where

$$\begin{aligned} E_{classical} &= -N_s J S^2, \\ \mathcal{H}_0 &= -N_s J S, \\ \mathcal{H}_2/J^* &= \sum_{\langle ij \rangle} \sigma_{iy}\sigma_{jy} + \sum_i \sigma_{iy}^2 + \sum_{\langle ij \rangle} \frac{1}{4}(\sigma_{ix} - \sigma_{jx})^2, \\ \mathcal{H}_3/J^* &= \frac{1}{S}\sum_{\langle ij \rangle} [\, -\frac{1}{2}(\sigma_{ix}\sigma_{jy}^2 - \sigma_{iy}^2\sigma_{jx}) - \frac{1}{6}(\sigma_{ix} - \sigma_{jx})^3]\hat{\mathbf{x}}_i \cdot \hat{\mathbf{z}}_j, \\ \mathcal{H}_4/J^* &= \frac{1}{S^2}\sum_{\langle ij \rangle} \frac{1}{16}(\sigma_{ix}\sigma_{jx}^3 - 2\sigma_{ix}^2\sigma_{jx}^2 + \sigma_{ix}^3\sigma_{jx}) - \frac{1}{8}(\sigma_{iy}\sigma_{jy}^3 + \sigma_{iy}^2\sigma_{jy}^2 + \sigma_{iy}^3\sigma_{jy}) \\ &\quad + \frac{1}{16}(\sigma_{ix}\sigma_{jx}\sigma_{jy}^2 + \sigma_{ix}\sigma_{jx}\sigma_{iy}^2 - 2\sigma_{iy}\sigma_{jy}\sigma_{jx}^2 - 2\sigma_{iy}\sigma_{jy}\sigma_{ix}^2 \\ &\quad - 2\sigma_{ix}^2\sigma_{jy}^2 - 2\sigma_{jx}^2\sigma_{iy}^2). \end{aligned} \tag{3.7}$$

N_s here is the number of spins and $J^* = J\sqrt{S(S+1)}/S$. $E_{classical}$ is of course the classical energy of any classical ground state. The constant $\mathcal{H}_0$ term is

typical in spinwave expansion of antiferrogmagnet: its presence implies that the quantum correction to the classical energy of an antiferromagnet is always negative.

In $\mathcal{H}_3$ above we have omitted some terms of $O(\sigma^3)$. But these have prefactors $1/S^2$ (and higher powers) instead of $1/S$. These extra terms would not arise if we use the expansion parameter $\sqrt{S(S+1)}$, which is the magnitude of the total angular momentum, instead of S. However, if S is large, these extra terms will always be small compared with the terms that are included and so can legitimately be omitted. Similar omissions occur in $\mathcal{H}_4$.

Since some of the spin deviation operators do not commute, the $\mathcal{H}_3$ and $\mathcal{H}_4$ parts of the spinwave Hamiltonian Eq.(3.7) may appear non-Hermitian. Actually, $\mathcal{H}_3$ is Hermitian because sites i and j are never identical and the spin operators σ_{ix} and σ_{iy} on different sites do commute. As for $\mathcal{H}_4$, we note that if two operators are switched in this quartic expression, quadratic terms that are prefactored by $1/S$ will be created. These of course scale with a smaller power of S than the quadratic terms already shown in Eq.(3.7). So while strictly speaking $\mathcal{H}_4$ should have been written in a symmetrized form to be Hermitian, the difference between the two forms are negligible in the large S limit.

A generic classical coplanar ground state does not possess translational symmetry, and hence the spinwave Hamiltonian is also disordered. However, because the spin deviation operators are defined with respect to the local axes, which are twisting and turning in space to coincide with the randomly varying classical spin directions, one is able to transform away the disorder in $\mathcal{H}_2$ and $\mathcal{H}_4$, as is apparent from Eq.(3.7). (This is reminiscent of the Mattis spin glass [28], where disorder in the Hamiltonian can also be transformed away by re-

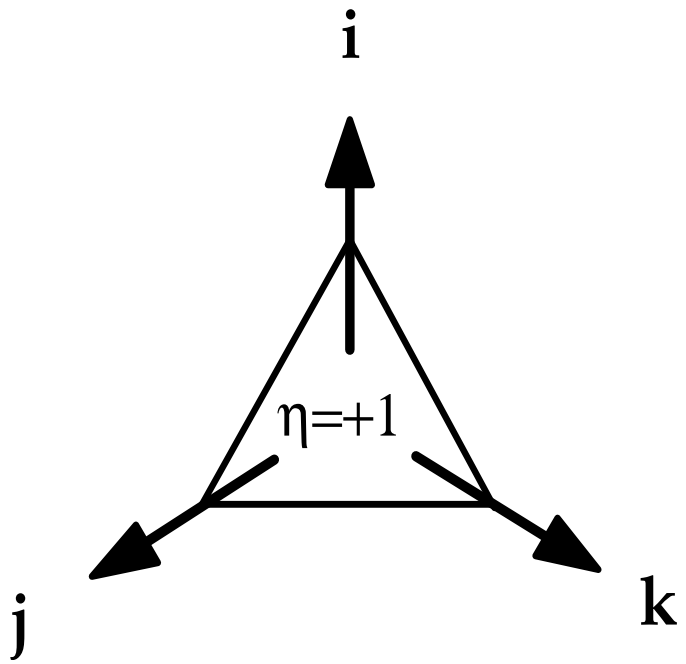

Figure 3.2 A triangle of spins defined to have positive chirality. (i,j,k) goes around the triangle counter-clockwise. They also rotate counter-clockwise in increments of 120°.

defining local spin axes.) Note that this is possible because $\hat{\mathbf{x}}_i \cdot \hat{\mathbf{x}}_j = \hat{\mathbf{z}}_i \cdot \hat{\mathbf{z}}_j = -\frac{1}{2}$ for all i,j. Such factors appeared in $\mathcal{H}_2$ and $\mathcal{H}_4$ but they become constants. In other similar systems, such as the pyrochlore antiferromagnet [29], $\hat{\mathbf{x}}_i \cdot \hat{\mathbf{x}}_j \neq$ const, hence $\mathcal{H}_2$ and $\mathcal{H}_4$ does depend on the ground state. The possibility of transforming away the disorder has the important implication that if we truncate the spinwave expansion up to quadratic order only, *all* the classical ground states will have identical spinwave spectrums and ground state energies. Selection among the coplanar states are due entirely to the cubic terms $\mathcal{H}_3$. (The quartic terms also have no selection effect, but they are necessary to stabilize the coplanar states against out-of-plane fluctuations.)

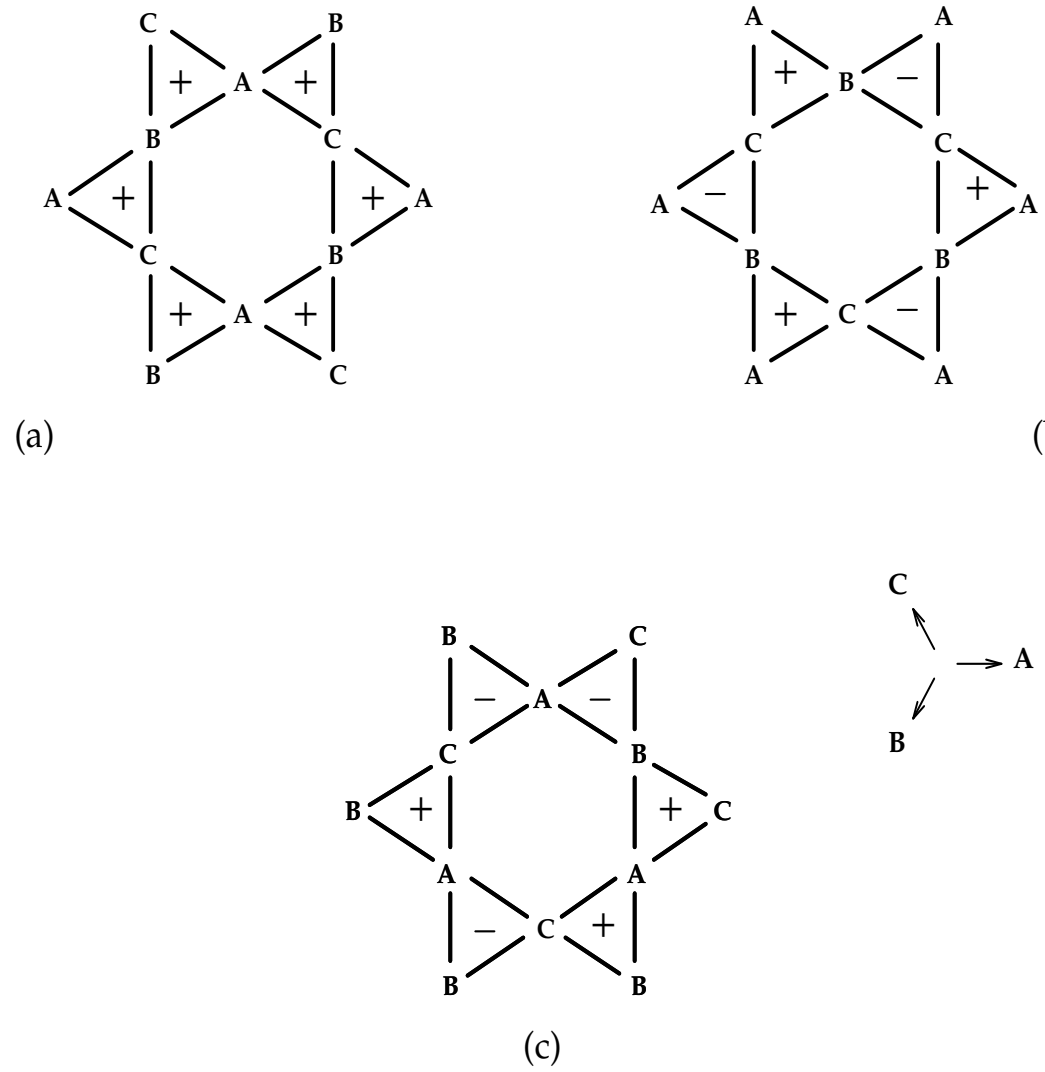

Figure 3.3 Mapping the Potts states in Figure 2.1 to a set of Ising variables η_α defined in Figure 3.2.

There is a way of writing $\mathcal{H}_3$ which will prove to be of considerable conceptual value. For abbreviation, first define $\mathcal{H}_{3\,ij}$ by

$$\mathcal{H}_3 = \sum_{<ij>} \mathcal{H}_{3\,ij} \hat{\mathbf{x}}_i \cdot \hat{\mathbf{z}}_j, \tag{3.8}$$

where $\mathcal{H}_{3\,ij}$ does not depend on the Potts state. If we define an azimuthal angle θ_i specifying the spin directions on the plane, the factor $\hat{\mathbf{x}}_i \cdot \hat{\mathbf{z}}_j$ is simply

$\sin(\theta_j - \theta_i) = \pm\frac{\sqrt{3}}{2}$. We can group three pairs of spins on a triangle together first before summing over all the triangles on the kagomé lattice. If one goes around the triangle, say, in a counter-clockwise direction $(i \rightarrow j \rightarrow k)$, it is easy to convince oneself that $\sin(\theta_j - \theta_i)$ must all be of the same value $\pm\frac{\sqrt{3}}{2}$. (It is positive if the spins also rotate counter-clockwise in increments of 120° as one goes around the triangle, see Figure 3.2.) We can factor out this sign and write it as $\eta_\alpha(= \pm 1)$, where α is the index for the triangle in question. (We use Greek indices to denote triangles throughout.) Thus

$$\mathcal{H}_3 = \sum_\alpha \eta_\alpha \mathcal{H}_\alpha, \tag{3.9}$$

where

$$\mathcal{H}_\alpha \equiv \frac{\sqrt{3}}{2}(\mathcal{H}_{3\,ij} + \mathcal{H}_{3\,jk} + \mathcal{H}_{3\,ki}). \tag{3.10}$$

The set of η_α are called the "chiralities" of the triangles[9,10]. They are a set of Ising variables defined on a honeycomb lattice, since the centers of the kagomé triangles form a honeycomb lattice. Every Potts state maps uniquely onto one set of chiralities, but not every arbitrary set of chiralities map onto a Potts ground state. (See Figure 3.3 for the application of this mapping to several Potts states.)

The presence of zero modes in $\mathcal{H}_2$ can be revealed most clearly by rearranging the terms of $\mathcal{H}_2/J^*$ in Eq.(3.7) involving σ_{iy} into sums over triangles of spins, $\frac{1}{2}\sum_\alpha(\sigma_{1y} + \sigma_{2y} + \sigma_{3y})^2$. It is then obvious that as long as σ_{iy} adds up to zero within a triangle, there will be zero cost in energy for such out-of-plane fluctuations. A few of these modes are genuine Goldstone modes, but most of them are zero modes here only because we ignored higher powers of spin deviations and because of the peculiar lattice structure.

One may question whether this truncation of the Hamiltonian at the quartic terms would alter some essential physics of the system. Indeed, we find that $\mathcal{H}_3$ and $\mathcal{H}_4$ here separately do not preserve rotational symmetry in spin space. However, Chubukov [20] showed by perturbation theory that if we combine the first order contribution of $\mathcal{H}_4$ and the second order contribution of $\mathcal{H}_3$, the spin wave spectrum does have Goldstone modes, up to an energy of order $S^{2/3}$. In order to demonstrate the preservation of Goldstone modes for smaller powers of S, it is necessary to go beyond the quartic terms in the Hamiltonian. But since we anticipate that in-plane selection occur at order $S^{2/3}$, we do not pursue such higher terms.

3.2 Variational Wavefunction

We will now calculate the ground state energy of the spinwave Hamiltonian Eq.(3.7), for each of the Potts state, in order to select the one with the lowest quantum energy. While there is an easy procedure for analytically diagonalizing a quadratic, translationally invariant Hamiltonian via Fourier transform, there is no such procedure for an anharmonic, disordered Hamiltonian. There is, however, a variety of approximation schemes available. The most common are perturbation theory and variational wavefunction. Perturbation approach has been used by Chubukov [20] to renormalize the small-k part of the spinwave spectrum of this system. As we mentioned in Section[2.4], renormalization of the small-k spectrum is not sufficient to determine in-plane selection. We detail below a variational wavefunction approach which is designed to do that. The form of this wavefunction is actually motivated by perturbation theory. How-

ever, once we define the wavefunction rigorously, one can regard this definition as logically independent of the perturbation theory.

The simplest variational ground state wavefunction for $\mathcal{H}$ would have been Gaussian. However, since a gaussian is an even function of the spin deviation operators, the expectation value of $\mathcal{H}_3$ with respect to this wavefunction must be zero. The in-plane selection effect would have vanished altogether. A more detailed symmetry argument in Appendix[A] shows that no appropriate gaussian wavefunction could be found that could in principle distinguish between the "q=0" and "$\sqrt{3}\times\sqrt{3}$" states. A gaussian wavefunction is therefore inadequate for selection purposes.

A gaussian variational wavefunction can be written schematically in the form

$$|\Psi_0\rangle \sim \exp[\sum_i g_i(a_i^\dagger + a_i)^2]|0\rangle, \tag{3.11}$$

where $|0\rangle$ is the ground state of $\mathcal{H}_2$. The expansion of Eq.(3.11) has non-zero coefficients for all possible *even* number of magnons. The exponential operator in Eq.(3.11) simply changes the width of the bare gaussian wavefunction $|0\rangle$. We argued above that this is inadequate: we must include all *odd* number of magnon excitations also (except 1 magnon excitation[3]), in the schematic form

$$|\Psi\rangle \sim \exp[\sum_i g_i(a_i^\dagger + a_i)^2 + h_i(a_i^\dagger + a_i)^3]|0\rangle. \tag{3.12}$$

However, this kind of wavefunction is too complicated for practical variational optimization, and some truncation is necessary. Conventional (as opposed to "many-body") perturbation theory provides guidance on how to truncate this

[3] We do not include a linear polynomial in $a_i^\dagger$ because this is equivalent to applying a constant offset in spin deviation to the gaussian $|0\rangle$. We explain in Appendix[A] why we exclude this from consideration.

wavefunction. Generally speaking, conventional perturbation theory would be valid if the density of the localized excitations $(a_i^\dagger + a_i)^3|0\rangle$ is small. (This density is some increasing function of the h_i's.) In such a situation, we can approximate the wavefunction as

$$|\Psi\rangle \sim [1 + \sum_i h_i (a_i^\dagger + a_i)^3]|\Psi_0\rangle. \tag{3.13}$$

The magnitude of the perturbation matrix element $\langle\Psi|V|\Psi_0\rangle$ is proportional to $h_i N_s$ while the energy gap between the ground state and the excited state is proportional to just N_s. If we fix N_s and choose S to be large, the h_i's will become correspondingly small (as they must in order to obtain the limit $|\Psi\rangle \to |0\rangle$ when $S \to \infty$.) In other words, the size of the system must satisfy the inequality

$$1 \ll N_s \ll N_{max}(S), \tag{3.14}$$

where $N_{max}(S)$ is an increasing function of S. Conventional perturbation theory would be in general valid in such a limit, barring certain detailed considerations which we will discuss in Section[3.4.1] and Appendix[C].

We now proceed to determine the exact form of the variational wavefunction suggested by conventional ("Rayleigh-Schrödinger") perturbation theory. Suppose we divide $\mathcal{H}$ into an unperturbed Hamiltonian $\tilde{\mathcal{H}}$ and a perturbation V,

$$\mathcal{H} = \tilde{\mathcal{H}} + V. \tag{3.15}$$

$\tilde{\mathcal{H}}$ is some harmonic Hamiltonian, not necessarily equal to $\mathcal{H}_2$. We can in principle compute exactly the ground state wavefunction Ψ_0 and all the other eigenstates of $\tilde{\mathcal{H}}$: they are just spinwave states. Now if we choose $\tilde{\mathcal{H}}$ judiciously, the contribution of V will hopefully be small compared to that of $\tilde{\mathcal{H}}$. We can

therefore calculate the ground state wavefunction via conventional perturbation theory,

$$|\Psi\rangle = |\Psi_0\rangle + \frac{1}{E_0 - \tilde{\mathcal{H}}} P_0 V |\Psi_0\rangle + \mathcal{O}(V^2|\Psi_0\rangle), \tag{3.16}$$

where

$$E_0 = \langle\Psi_0|\tilde{\mathcal{H}}|\Psi_0\rangle, \tag{3.17}$$

and P_0 is the complementary projection operator that projects onto all states except Ψ_0,

$$P_0 = 1 - |\Psi_0\rangle\langle\Psi_0|. \tag{3.18}$$

The approximate ground state energy is the familiar

$$E_g = \langle\Psi|\mathcal{H}|\Psi\rangle = E_0 + \langle\Psi_0|V|\Psi_0\rangle + \langle\Psi_0|V P_0 \frac{1}{E_0 - \tilde{\mathcal{H}}} P_0 V|\Psi_0\rangle + \cdots, \tag{3.19}$$

One can ask why we do not use $\mathcal{H}_2$ to be the unperturbed Hamiltonian and treat the anharmonic terms $\mathcal{H}_3 + \mathcal{H}_4$ as perturbation. The reason is that since there is a whole Brillouin-zone- full of zero modes with unbounded fluctuations, the unperturbed wavefunction $|0\rangle$ would be pathological, and the (bare) propagator $(E_0 - \mathcal{H}_2)^{-1}$ would be highly singular. It is necessary to use a renormalized propagator as the starting point for the perturbation theory. Hence before we go on to the perturbative part of the wavefunction, we first discuss how one can derive the properties of this renormalized gaussian wavefunction qualitatively.

3.3 Renormalized Gaussian Wavefunction

We will specify the renormalized Gaussian wavefunction Ψ_0 precisely in Appendix[B]. Here we want to look at some qualitative properties which is independent of the detailed form of this wavefunction.

The way we define Ψ_0 is by first constructing the harmonic Hamiltonian $\tilde{\mathcal{H}}$, of which Ψ_0 is the ground state wavefunction. Once we specify $\tilde{\mathcal{H}}$, we can identify the quantities corresponding to the "mass" and "spring constant" of the system. As we know from the quantum mechanics of 1-dimensional harmonic oscillator, the width of the gaussian ground state wavefunction is determined by the mass and the spring constant.

Schematically, we can write $\mathcal{H}_2$ in its Fourier-space representation as

$$\mathcal{H}_2 \sim \frac{J^*}{2} \sum_{\mathbf{k}} \mathcal{K}_b(\mathbf{k}) \sigma_x(\mathbf{k})^2 + \mathcal{M}_b(\mathbf{k})^{-1} \sigma_y(\mathbf{k})^2. \tag{3.20}$$

Since σ_x and σ_y are analogous to position and momentum operators respectively, we can think of this Hamiltonian as a system of uncoupled harmonic oscillators with "mass" $\mathcal{M}_b(\mathbf{k})$ and "spring constant" $\mathcal{K}_b(\mathbf{k})$. (The subscripts "b" designate these as *bare* mass and spring constants.) The ground state fluctuations in the dynamical variables can be calculated in the same way as a 1-D harmonic oscillator, with some modifications due to the commutator Eq.(3.5). To wit,

$$\begin{aligned} \langle \sigma_x^2 \rangle &\sim S \sqrt{1/\mathcal{K}_b \mathcal{M}_b}, \\ \langle \sigma_y^2 \rangle &\sim S \sqrt{\mathcal{K}_b \mathcal{M}_b}. \end{aligned} \tag{3.21}$$

The spinwave frequencies are

$$\omega \sim S \sqrt{\frac{\mathcal{K}_b}{\mathcal{M}_b}}. \tag{3.22}$$

Since $\mathcal{H}_2$ retains the full symmetry of the atomic lattice which has a basis of 3 sites per primitive unit cell, the spinwave spectrum has 3 branches. The first branch consists of zero modes, and the second and the third the ordinary modes. The coupling constants $\mathcal{K}_b$ and $\mathcal{M}_b^{-1}$ are different for each kind of modes. For the zero modes $\mathcal{K}_b^{(s)}$ is $\mathcal{O}(1)$ and $\mathcal{M}_b^{(s)-1}$ is zero, whereas for the ordinary modes, $\mathcal{K}_b^{(o)}$ and $\mathcal{M}_b^{(o)-1}$ are of $\mathcal{O}(1)$.

In order to create a renormalized Ψ_0 that is non-singular, it is necessary to remove the zero modes in $\mathcal{H}_2$. We need to add terms, especially those that are of the form $\sum_i \sigma_{iy}^2$, to $\mathcal{H}_2$. There are many ways to do this, but written in reciprocal space, they all have the same effect of renormalizing the coupling constants $\mathcal{K}_b$ and $\mathcal{M}_b^{-1}$ to create the renormalized harmonic Hamiltonian $\tilde{\mathcal{H}}$. Furthermore, we choose $\tilde{\mathcal{H}}$ to be translational invariant, and identical for all Potts states, so as to separate the problem of making the fluctuations finite, from that of the "in-plane selection". This separation is useful for writing the quantum energy as an Ising Hamitonian for in-plane selection, a topic we will pursue in Section[3.7]. The $\tilde{\mathcal{H}}$ we choose to use is a harmonic Hamiltonian with next-nearest-neighbor couplings

$$\tilde{\mathcal{H}}/J^* = \mathcal{H}_2/J^* + J_3 \sum_{[ij]} -\frac{1}{2}\{(\sigma_{iy} - \sigma_{jy})^2 + (\sigma_{ix} - \sigma_{jx})^2\}, \tag{3.23}$$

where the $[ij]$ couples spins that are two lattice constants apart, but excluding those that are diagonal across a hexagon. (Note that $J_3 < 0$ is dimensionless.) The reason for choosing this will be discussed in Appendix[B]. Note that we have chosen an overall energy scale for $\tilde{\mathcal{H}}$ in Eq.(3.23) such that $\tilde{\mathcal{H}}$ coincides with $\mathcal{H}_2$ when $J_3 \to 0$. This choice is consistent with our desire to minimize the perturbative contributions of $(\mathcal{H}_2 + \mathcal{H}_4 - \tilde{\mathcal{H}})$. If we imagine letting $\mathcal{H}_4$ goes

to zero, then surely we must have $\tilde{\mathcal{H}} \to \mathcal{H}_2$. It turns out that this $\tilde{\mathcal{H}}$ will have real spinwave spectrum only if $J_3 < 0$, as Harris *et al* have found [8].

The effect of adding the J_3 on the ordinary modes is negligible; the renormalized $\mathcal{K}^{(o)}$ and $\mathcal{M}^{(o)-1}$ are still of $\mathcal{O}(1)$. The effect on the zero modes is more drastic. While we still have[4]

$$\begin{aligned} \mathcal{K}^{(s)} &\sim \mathcal{K}_b^{(s)} - J_3 \\ &\sim \mathcal{K}_b^{(s)} \sim \mathcal{O}(1), \end{aligned} \tag{3.24}$$

the $\mathcal{M}$'s now acquire a non-zero value,

$$\begin{aligned} \mathcal{M}^{(s)-1} &\sim \mathcal{M}_b^{(s)-1} - J_3 \\ &\sim -J_3. \end{aligned} \tag{3.25}$$

Combining these equations with Eq.(3.21) (with the bare quantities replaced by the renormalized ones there) gives us

$$\begin{aligned} \langle \sigma_y^{(s)2} \rangle_0 &\sim S\sqrt{\mathcal{K}^{(s)}\mathcal{M}^{(s)}} \\ &\sim S/\sqrt{|J_3|}. \end{aligned} \tag{3.26}$$

Similarly, we can obtain

$$\langle \sigma_x^{(s)2} \rangle_0 \sim S\sqrt{|J_3|}. \tag{3.27}$$

Note that the subscript "0" means that the expectation is taken with respect to the "renormalized" gaussian wavefunction Ψ_0 which is the ground state of $\tilde{\mathcal{H}}$. The renormalized spinwave frequencies can be obtained through Eq.(3.22) (again replacing the bare coupling constants with the "renormalized" ones), giving

$$\omega^{(s)} \sim J^* S\sqrt{|J_3|}. \tag{3.28}$$

[4] The minus sign in front of J_3 turns out to be necessary to ensure a real eigenvalue for $\mathcal{K}$ and $\mathcal{M}$ to have real spectrums.

Both the ordinary mode fluctuations and frequencies scale with S, and the corresponding numerical prefactors are unaffected by "renormalization" to lowest order of S.

The magnitude of J_3 should be determined by variational minimization of the quantum energy with respect to the full wavefunction, something that we cannot do yet without defining the non-gaussian part of the wavefunction. However, we can estimate J_3 by variationally minimizing the energy with respect to only the gaussian part of the wavefunction, assuming the non- gaussian part is zero. This is, as we argued, equivalent to leaving out $\mathcal{H}_3$ in Eq.(3.7). This variational minimization is much easier than minimizing with respect to the complete wavefunction because Wick's theorem can be applied when the wavefunction is gaussian. The variational energy is

$$\begin{aligned} E_g(J_3) &\sim \langle \mathcal{H}_2 \rangle_0 + \langle \mathcal{H}_4 \rangle_0 \\ &\sim N_s J^* \langle \sigma_x^2 + \sigma_y^2 \rangle_0 + N_s \frac{J^*}{S^2} \langle \sigma_x^4 + \sigma_y^4 \rangle_0. \end{aligned} \tag{3.29}$$

To evaluate the expression Eq.(3.29), we have to anticipate the result that J_3 will turn out to be much smaller than unity for large S. (This is not surprising because the terms in $\mathcal{H}_4$ are all scaled by $1/S^2$, so the "renormalizing" effects of $\mathcal{H}_4$ will no doubt decrease as S increases.) This implies that $\langle \sigma_x^2 \rangle_0$ is dominated by $\langle \sigma_x^{(o)2} \rangle_0$ and $\langle \sigma_y^2 \rangle_0$ is dominated by $\langle \sigma_y^{(s)2} \rangle_0$. However, the $\sigma_y^{(s)}$ terms in $\mathcal{H}_2$ add up to zero as before, because otherwise, the soft branch of the spinwave spectrum would scale with a larger power of S than the ordinary branches at large S. This would have disagreed with the large S limit of the system: that total harmonic spinwave energy should scale with S.

We can now utilize these results, together with Eq.(3.26) and Eq.(3.27), to write down the scaling with J_3 of the various terms in Eq.(3.29) (up to the first

non-zero power of J_3):

$$E_g(J_3)/N_s \sim J^*(S + S\sqrt{-J_3}) + \frac{J^*}{S^2}\frac{S^2}{(-J_3)}$$
$$= b_0 S + b_1 S|J_3|^{1/2} + b_2|J_3|^{-1}, \tag{3.30}$$

where the b_i's are constants. Minimizing $E_g(J_3)$ with respect to $|J_3|$ gives the equation

$$b_1 S|J_3|^{-1/2} - b_2|J_3|^{-2} = 0, \tag{3.31}$$

which produces the result

$$|J_3| \sim (\frac{b_1}{b_2}S)^{-2/3}. \tag{3.32}$$

Substituting this into Eq.(3.28) produces

$$\omega^{(s)} \sim J^* S^{2/3}. \tag{3.33}$$

These scalings with S are the same as the ones obtained in Ref.[20], even though we have ignored the cubic ($\mathcal{H}_3$) terms so far.

The reason why including the effects of $\mathcal{H}_3$ will not alter the scaling with S is that $\mathcal{H}_3$ also contributes an energy of $\mathcal{O}(J^* J_3^{-1})$ to E_g, the same power of J_3 as the $\mathcal{H}_4$ terms, as we saw in Eq.(3.30). Hence the form of Eq.(3.30) remains unchanged. This scaling of the $\mathcal{H}_3$ with J_3 is dealt with in Appendix[C.2]. The method used there is similar to the one used here: it is based on the fluctuation magnitudes Eq.(3.26) and Eq.(3.27). However, since the contribution of $\mathcal{H}_3$ to E_g is in the form of a second-order perturbation (see Section[3.4]), it is a *negative* contribution. If we trace the calculations Eq.(3.30) through Eq.(3.33), we will find that a negative contribution results in a *smaller* (possibly even negative) b_2 and therefore a smaller numerical prefactor for J_3 and $\omega^{(s)}$, although they still scale with $S^{-2/3}$ and $S^{2/3}$ respectively. We shall return to this point in Section[3.9.3]

3.4 Non-gaussian Part of Wavefunction

Now we want to understand the nature of the perturbative, non- Gaussian part of the wavefunction in Eq.(3.16). V in our case equals $\mathcal{H}_3 + (\mathcal{H}_2 + \mathcal{H}_4 - \tilde{\mathcal{H}})$. This perturbation acting once excites up to 4 magnons out of the harmonic vacuum Ψ_0. We want to obtain a qualitative estimate of the magnitude of the various perturbative terms. This serves two purposes: it validates the use of perturbation theory as a guide to the construction of our wavefunction; and it shows us what kind of excited states are more important. This estimate is based on the fluctuation magnitude for the various modes given in the previous section, assuming that Eq.(3.32) and Eq.(3.33) are correct. The details of the derivation is given in Appendix[C].

The first order perturbation scales with $S^{2/3}$. Proceeding to the higher order terms, we should distinguish between the contributions of the $\mathcal{H}_3$ part of V and the $(\mathcal{H}_2 + \mathcal{H}_4 - \tilde{\mathcal{H}})$ part.

For the $\mathcal{H}_3$ part, there are 2 kinds of intermediate excited states that dominate the perturbative energy. The first one consists purely of soft magnons, the other kind is a mixture of soft and ordinary magnons. We find that for the mixed state, each higher even-order perturbation of $\mathcal{H}_3$ is down by a factor of $S^{1/3}$ compared with the preceding order. Thus cutting off the perturbation at second order is well-justified for the mixed state. However, for the purely soft state, all orders of perturbation of $\mathcal{H}_3$ scale with the same power of S. Whether the perturbation series converges depend on the precise numerical coefficients of the terms. For both the mixed and the purely soft intermediate states, the second-order perturbative energy scales with $S^{2/3}$.

The same situation happens with the $(\mathcal{H}_2+\mathcal{H}_4-\tilde{\mathcal{H}})$ part. The perturbative terms of all orders scale with $S^{2/3}$, and convergence depends on numerical values of the prefactors.

In conclusion, ignoring higher order terms involving the soft modes may introduce significant errors into the energy estimate. (Note that Chubukov's calculation[20] is based on the assumption that these higher order terms cancel each other. This assumption is supported by prior work on antiferromagnetic spinwave expansion[30].) However, we emphasize again that our primary interest is which Potts state has the lowest energy if quantum corrections are included. The exact energies of the states are not significant for our purposes. Excluding the higher-than-second order perturbations of $\mathcal{H}_3$ and the higher-than-first order perturbations of $\mathcal{H}_2+\mathcal{H}_4-\tilde{\mathcal{H}}$ will merely change the optimal J_3. We shall see (Section[3.7]) that in-plane selection depends on the *relative* magnitudes of various spin-spin correlation functions . For large S, these relative magnitudes are insensitive to J_3. Anticipating this numerical fact, we summarily exclude the higher order perturbative terms in the following calculations.

3.4.1 Kinds of Excited States to be Included

The excitations that $V \sim \mathcal{H}_3$ creates are linear combinations of localized excited states $\mathcal{H}_\alpha|\Psi_0\rangle$ (see Eq.(3.10)). Each of these excited states is localized to spins around one triangle. Each of them is composed of a linear mixture of one- and three-magnon states which are the eigenstates of $\tilde{\mathcal{H}}$. (These one- and three-magnon states are labeled by the wavevector $\mathbf{k}$.) Since the localized

excited states live within the one- and three-magnon subspace, the action of $1/(E_0 - \tilde{\mathcal{H}})$ is to simply transform them within this subspace. However, after the transformation, the excitations are no longer localized to a triangle. Nevertheless, we believe that the localized excitations are the ones important to the selection energy (i.e. the energy difference between two coplanar states.) Just as in the case of coplanar selection (in the kagomé system) where it was shown that a calculation based on localized fluctuations [25] gives the same qualitative effect as one based in reciprocal space [20], here we conjecture that a variational wavefunction with only localized excitations will give the same selection effect as a more general nonlocal wavefunction. This local viewpoint is derived from the belief that the renormalized zero modes form the most important contributions to the selection energy. Since the hexagon modes form a complete basis for the zero modes, and since the hexagon modes are local, we believe that all important physics can be derived locally. This qualitative idea can be expressed mathematically by means of a locator expansion, commonly used in the theory of electronic bands in disordered media [31].

Locator expansion is a way of expressing the Green's function $1/(E_0 - \tilde{\mathcal{H}})$ in a series such that the first term is diagonal in real space, the second term only couples sites close together (nearest-neighbor triangles in the kagomé case), the third term can "hop" twice as far, and so on. In real space, the $\tilde{\mathcal{H}}$ in $1/(E_0 - \tilde{\mathcal{H}})$ can be divided into a diagonal part $\tilde{\mathcal{H}}_D$ and a non-diagonal part $\tilde{\mathcal{H}}_{hop}$,

$$\tilde{\mathcal{H}} = \tilde{\mathcal{H}}_D + \tilde{\mathcal{H}}_{hop}. \tag{3.34}$$

The expansion of the Green's function is a Taylor-series expansion assuming that $\tilde{\mathcal{H}}_{hop}$ is a small quantity. Since $\tilde{\mathcal{H}}$ is translationally invariant, the diagonal elements are in fact all equal to some constant $(1/\overline{g})$. Hence we can approximate

the non-Gaussian (perturbative) part of the wavefunction from Eq.(3.16) as

$$|\Psi\rangle - |\Psi_0\rangle \sim \overline{g}\,\mathcal{H}_3|\Psi_0\rangle + \overline{g}^2\overline{t}\mathcal{H}_3|\Psi_0\rangle + \cdots, \tag{3.35}$$

where $\overline{g}$ is a constant, $\overline{t}$ is a "hopping operator" which has only off-diagonal elements and mixes states that are close together in real space. This locator expansion will be derived in Section[3.6].

3.4.2 Definition of Non-gaussian Wavefunction

We now attempt to design the non-gaussian part of the variational wavefunction that will resemble the perturbative wavefunction discussed above, but greatly simplified to include only the most important excitations. Although this construction is motivated by the arguments in Section[3.4.1], it is logically independent of perturbation theory.

We begin our construction of the variational wavefunction by creating a set of excited states $\{\Psi_\alpha|\alpha = 1, ..., N_\alpha\}$. (Together with the ground state Ψ_0, they form what we called the variational subspace Ξ.) N_α is the number of triangles on the kagomé lattice,

$$N_\alpha = (2/3)N_s. \tag{3.36}$$

These excited states are created by some operators (which are cubic polynomials of spin operators) $\mathcal{Q}_\alpha$ acting on the gaussian ground state. The spin operators in each $\mathcal{Q}_\alpha$ are those of a set (α) of spins localized to nearby lattice sites. Thus we have a linearly-independent but non-orthogonal (and incomplete, with respect to the 3-magnon subspace) set of states

$$\begin{aligned}\Psi_\alpha^{(s)} &= c^{(s)}\mathcal{Q}_\alpha^{(s)}\Psi_0,\\ \Psi_\alpha^{(o)} &= c^{(o)}\mathcal{Q}_\alpha^{(o)}\Psi_0.\end{aligned} \tag{3.37}$$

These excited states can be thought of as "local atomic orbitals", in the language of electronic band theory. Appropriate linear combinations of them can form Bloch states. The $\mathcal{Q}$'s are Hermitian operators which are designed to have a similar structure to $\mathcal{H}_\alpha$ in Eq.(3.9),

$$\begin{aligned}\mathcal{Q}_\alpha^{(s)} &= \sum \frac{1}{2}[(\sigma_{ix}^{(s)}\sigma_{jy}^{(s)2} - \sigma_{iy}^{(s)2}\sigma_{jx}^{(s)}) + h.c.], \\ \mathcal{Q}_\alpha^{(o)} &= \sum (\sigma_{ix}^{(o)}\sigma_{jy}^{(s)2} - \sigma_{iy}^{(s)2}\sigma_{jx}^{(o)}),\end{aligned} \tag{3.38}$$

where the sums are over the three pairs of (i,j)'s around a triangle α. The order of summing (whether the pair of spins going clockwise or counter-clockwise) is not important, as long as it is the same for all the triangles. The superscripts s or o on the σ's indicate that we include only soft or ordinary modes in the fluctuations, as explained in Section[3.3]. Note that since

$$[\sigma_{ix}^{(s)}, \sigma_{jy}^{(s)}] \neq 0 \tag{3.39}$$

even though $[\sigma_{ix}, \sigma_{jy}] = 0$ for $i \neq j$, we must the symmetrization in $\mathcal{Q}_\alpha^{(s)}$ to make it Hermitian. Since the soft and ordinary operators commute, $\mathcal{Q}_\alpha^{(o)}$ is Hermitian without symmetrization. The c's in Eq.(3.37) are the normalization constants,

$$c^{(m)} = \langle \Psi_0 | \mathcal{Q}_\alpha^{(m)2} | \Psi_0 \rangle^{-1/2}, \tag{3.40}$$

where we have used the generic superscript (m) to represent either (s) or (o) modes.

Comparing with Eq.(3.35), it may appear that mainly terms in the first part $\mathcal{H}_3|\Psi_0\rangle$, and only a small subset[5] of terms in the second part $\overline{t}\mathcal{H}_3|\Psi_0\rangle$, are

[5] The terms in the $\overline{t}\mathcal{H}_3|\Psi_0\rangle$ part that are represented by our basis are of the form $(\sigma_i\sigma_j)(\sigma_i^2\sigma_j)$, where the first parenthesis contains terms from the nearest-neighbor, off-diagonal part of $\tilde{\mathcal{H}}$, and the second parenthesis contains terms from $\mathcal{H}_3$. This set of apparently quintic operators actually create a state with only three magnons because $\tilde{\mathcal{H}}$ certainly does not change the number of magnons when it operates on a state.

represented by the basis states defined in Eq.(3.38). We are indeed ignoring nonlocal states that involve excitations with a form $\sigma_i\sigma_j\sigma_k|\Psi_0\rangle$, where i and k are further neighbors. This is consistent with our intention stated in Section[3.4.1] of including only the most local excitations necessary for in-plane selection. Furthermore, one may notice that $\mathcal{Q}_\alpha$ only contains half the terms in $\mathcal{H}_3$ as shown in Eq.(3.7). We can show that the other part of $\mathcal{H}_3$ creates excitations that scale with smaller powers of S (see Appendix[E]).

We can see immediately that the definitions Eq.(3.38) ensure that $\Psi_\alpha^{(s)}$ and $\Psi_\beta^{(o)}$ are orthogonal to each other. This can be shown quite easily using Wick's theorem and the fact that the ordinary and the soft modes are orthogonal eigenstates of the renormalized quadratic Hamiltonian $\tilde{\mathcal{H}}$. However, $\Psi_\alpha^{(s)}$ is only approximately orthogonal to $\Psi_\beta^{(s)}$ if $\alpha \neq \beta$, and the same holds for the o states. To orthogonalize them, as is necessary for subsequent diagonalization purposes, we can transform to a new set of *orthonormal* states $\{|\alpha^{(m)}\rangle\}$,

$$|\alpha^{(m)}\rangle = \sum_\beta \mathcal{L}_{\alpha\beta}^{(m)-1/2}|\Psi_\beta^{(m)}\rangle, \tag{3.41}$$

where $\mathcal{L}^{(m)}$ is the overlap matrix

$$\mathcal{L}_{\alpha\beta}^{(m)} = \langle\Psi_\alpha^{(m)}|\Psi_\beta^{(m)}\rangle. \tag{3.42}$$

The overlap $\langle\Psi_\alpha^{(m)}|\Psi_\beta^{(m)}\rangle$ has a power-law decay with distance between α and β (for large distances). The largest off-diagonal matrix elements of $\mathcal{L}^{(m)}$ are of $\mathcal{O}(10^{-2})$ as found from our later numerical calculations (See Table 3.2 . The largest off- diagonal matrix elements are $\mathcal{L}_{\alpha\beta}^{(s)}$ for nearest-neighbor α,β).

Again in the language of electron band theory, these $|\alpha^{(m)}\rangle$ are "Wannier states" [32]. Our complete variational wavefunction is then

$$|\Psi\rangle = a_0|\Psi_0\rangle + \sum_\alpha (a_\alpha^{(s)}|\alpha^{(s)}\rangle + a_\alpha^{(o)}|\alpha^{(o)}\rangle). \tag{3.43}$$

3.5 Partial Optimization of Wavefunction

To find the ground state energy E_g, we have to optimize the width of Gaussian Ψ_0 (controlled by J_3) s well as the $a_\alpha^{(m)}$ coefficients in Eq.(3.43) (subjected to normalization). Since E_g depends on the $a_\alpha^{(m)}$'s quadratically, optimizing with respect to the a's is equivalent to diagonalizing the Hamiltonian $\mathcal{H}$ in the $(2N_\alpha+1)$-dimensional subspace Ξ spanned by $\{|\Psi_0\rangle, |\alpha^{(s)}\rangle, |\alpha^{(o)}\rangle\}$, and picking the lowest eigenvalue. That is to say, we would like to diagonalize $P^{-1}\mathcal{H}P$, where P is the projection operator onto Ξ. This can of course be expressed as a $(2N_\alpha+1)\times(2N_\alpha+1)$ matrix. This matrix has the form

$$P^{-1}\mathcal{H}P = \begin{pmatrix} \langle \mathcal{H}_2+\mathcal{H}_4\rangle_0 & V_\alpha^{(s)} & \cdots & V_\alpha^{(o)} & \cdots \\ & \langle\alpha^{(s)}|\mathcal{H}_2+\mathcal{H}_4|\alpha^{(s)}\rangle & & & \\ & & \ddots & & \\ & & & \langle\alpha^{(o)}|\mathcal{H}_2+\mathcal{H}_4|\alpha^{(o)}\rangle & \\ & & & & \ddots \end{pmatrix}, \tag{3.44}$$

where

$$V_\alpha^{(m)} = \langle\Psi_0|\mathcal{H}_3|\alpha^{(m)}\rangle. \tag{3.45}$$

Note that none of the matrix elements in Eq.(3.44) are zero: we do not display some of them simply because they are not important to our calculations.

One can numerically diagonalize this matrix, but that would mean that we have to do this diagonalization for each iteration of the minimization over J_3, and for each of the infinite number of Potts states! Clearly, our program to achieve ground state selection is not feasible unless we can find an analytical expression (in terms of the chiralities) for the lowest eigenvalue of matrix Eq.(3.44). One can use perturbation theory to do this (see Appendix[J] for a demonstration). This perturbation theory is essentially the same as the second order perturbation theory that motivated our wavefunction originally. The

importance of restricting to the subspace Ξ is that this makes formal our approximation that we include only $\mathcal{H}_3$ as the perturbation Hamiltonian for the second order term, with $\tilde{\mathcal{H}}$ as the bare Hamiltonian. We can display this perturbation in matrix form as

$$P^{-1}\mathcal{H}P = \begin{pmatrix} E_0 & 0 & \cdots \\ & \begin{bmatrix} E_\alpha^{(s)} & \\ & \ddots \end{bmatrix} & 0 \\ & & \begin{bmatrix} E_\alpha^{(o)} & \\ & \ddots \end{bmatrix} \end{pmatrix} + \begin{pmatrix} V_0 & V_\alpha^{(s)} & \cdots & V_\alpha^{(o)} & \cdots \\ & & \cdots & & \\ & & \cdots & & \end{pmatrix}, \tag{3.46}$$

where $E_0 = \langle\Psi_0|\tilde{\mathcal{H}}|\Psi_0\rangle$, $E_\alpha^{(m)} = \langle\alpha^{(m)}|\tilde{\mathcal{H}}|\alpha^{(m)}\rangle$, and $V_0 = \langle\Psi_0|\mathcal{H}_2+\mathcal{H}_4-\tilde{\mathcal{H}}|\Psi_0\rangle$ The matrix on the left is the bare Hamiltonian $P^{-1}\tilde{\mathcal{H}}P$. There are no off-diagonal elements connecting the upper-left and lower-right submatrices which we have blocked off: $P^{-1}\tilde{\mathcal{H}}P$ is block- diagonal[6]. In the perturbation matrix on the right, we have only displayed the top row, because these elements (together with the left column, of course) are the only important ones for the second-order perturbation expansion of the ground state energy. (The undisplayed diagonal elements of the perturbation matrix are $\langle\alpha^{(m)}|\mathcal{H}_2 + \mathcal{H}_4 - \tilde{\mathcal{H}}|\alpha^{(m)}\rangle$.) Note that for the off-diagonal part of these displayed elements, only $\mathcal{H}_3$ appears. So we can essentially regard $\mathcal{H}_3$ as the only perturbation. Also note that although the excited states of $P^{-1}\tilde{\mathcal{H}}P$ are degenerate, the ground state is unique, so we do *not* run into complications with degenerate perturbation if we are only interested in the ground state energy (to second order).

[6] The reason why the $\{\Psi_\alpha^{(s)}\}$ and $\{\Psi_\alpha^{(o)}\}$ subspaces are orthogonal invariant subspaces with respect to $\tilde{\mathcal{H}}$ is because $\sigma_x^{(s)}$ and $\sigma_x^{(o)}$ are *defined* to be orthogonal by virtue of the diagonalization of $\tilde{\mathcal{H}}$.

3.6 Perturbation Theory in the Subspace Ξ

We now carry out the perturbation calculation of the lowest eigenvalue of the Hamiltonian in the subspace Ξ spanned by Ψ_0 and the localized cubic excitations. Inserting a complete set of states in Ξ into the perturbation formula Eq.(3.19) gives us

$$E_g = \langle \mathcal{H}_2 + \mathcal{H}_4 \rangle_0 + \sum_{\alpha,\beta,m} \langle \Psi_0 | \mathcal{H}_3 | \alpha^{(m)} \rangle \langle \alpha^{(m)} | \frac{1}{E_0 - \tilde{\mathcal{H}}} | \beta^{(m)} \rangle \langle \beta^{(m)} | \mathcal{H}_3 | \Psi_0 \rangle. \tag{3.47}$$

This is different from conventional formula of second order perturbation where the intermediate states $|\alpha^{(m)}\rangle$ are eigenstates of $\tilde{\mathcal{H}}$. However, this restriction is not really necessary in principle. We saw in Eq.(3.19) that it is possible to write the second-order perturbation formula in a basis-invariant form. The apparent disappearance of the unperturbed Hamiltonian $\langle \tilde{\mathcal{H}} \rangle_0$ is because the first two terms in Eq.(3.19) add up to nothing but $\langle \mathcal{H}_2 + \mathcal{H}_4 \rangle_0$. This perturbation formula Eq.(3.47) can be written in matrix form as

$$E_g = \langle \mathcal{H}_2 + \mathcal{H}_4 \rangle_0 + \sum_{\alpha,\beta,m} V_\alpha^{(m)} G_{\alpha\beta}^{(m)} V_\beta^{(m)}, \tag{3.48}$$

where the transition matrix elements $V_\alpha^{(m)}$ are defined in Eq.(3.45) and the Green's function[7] is

$$G_{\alpha\beta}^{(m)} \equiv \langle \alpha^{(m)} | \frac{-1}{\tilde{\mathcal{H}} - E_0} | \beta^{(m)} \rangle. \tag{3.49}$$

Now, in order to actually compute these matrix elements, it is necessary to transform back to the $\Psi_\alpha^{(m)}$ basis. This is because only the $\Psi_\alpha^{(m)}$ are directly

[7] Since $\tilde{\mathcal{H}} - E_0$ is block-diagonal in the subspace spanned by $\{|\alpha^{(s)}\rangle, |\alpha^{(o)}\rangle\}$, the inverse of $\tilde{\mathcal{H}} - E_0$ in the same subspace is no doubt also block-diagonal. The Green's matrix therefore does not have cross- terms between the (s) and (o) states.

defined in terms of the spin deviation operators σ_i's, whose fluctuation magnitudes we can calculate using the recipe described in Appendix[B]. We employ Eq.(3.41) to write these matrix elements in the Ψ_α basis,

$$\begin{aligned}
\overline{V}^{(m)}_{\alpha} &\equiv \langle\Psi_0|\mathcal{H}_3|\Psi^{(m)}_{\alpha}\rangle = \sum_{\alpha'} \mathcal{L}^{(m)1/2}_{\alpha\alpha'} V^{(m)}_{\alpha'}, \\
\overline{G}^{(m)}_{\alpha\beta} &\equiv \langle\Psi^{(m)}_{\alpha}|\frac{-1}{\tilde{\mathcal{H}} - E_0}|\Psi^{(m)}_{\beta}\rangle = \sum_{\alpha'\beta'} \mathcal{L}^{(m)1/2}_{\alpha\alpha'} \mathcal{L}^{(m)1/2}_{\beta\beta'} G^{(m)}_{\alpha'\beta'}
\end{aligned} \tag{3.50}$$

From hereon we use the convention that the overline denotes a matrix in the Ψ_α basis. Furthermore, if we now use a matrix notation for $V^{(m)}$ and $G^{(m)}_{\alpha\beta}$ and the the notation $V^{(m)} \cdot G^{(m)} \cdot V^{(m)}$ for the contraction $\sum_{\alpha\beta} V^{(m)}_{\alpha} G^{(m)}_{\alpha\beta} V^{(m)}_{\beta}$ in Eq.(3.48), we see immediately that the change of basis leaves the form of this scalar quantity invariant:

$$\sum_m V^{(m)} \cdot G^{(m)} \cdot V^{(m)} = \sum_m \overline{V}^{(m)} \cdot \overline{G}^{(m)} \cdot \overline{V}^{(m)}. \tag{3.51}$$

Instead of numerically inverting the matrix $\tilde{\mathcal{H}} - E_0$ to get $\overline{G}^{(m)}$, we can perturbatively expand $\overline{G}^{(m)}$ around its diagonal elements. This is justified because as we can check from Table 3.2 , the diagonal matrix elements $\langle\Psi^{(m)}_{\alpha}|\tilde{\mathcal{H}} - E_0|\Psi^{(m)}_{\alpha}\rangle$ are always larger (by an order of magnitude) than the off-diagonal elements. This is the locator expansion alluded to in Section[3.4.1]. Defining

$$\begin{aligned}
\overline{E}^{(m)} &\equiv \langle\Psi^{(m)}_{\alpha}|\tilde{\mathcal{H}}|\Psi^{(m)}_{\alpha}\rangle, \\
\overline{g}^{(m)} &\equiv -(\overline{E}^{(m)} - E_0)^{-1} \\
\overline{t}^{(m)}_{\alpha\beta} &\equiv \begin{cases} \langle\Psi^{(m)}_{\alpha}|\tilde{\mathcal{H}} - E_0|\Psi^{(m)}_{\beta}\rangle, & \alpha \neq \beta \\ 0, & \alpha = \beta \end{cases}
\end{aligned} \tag{3.52}$$

$\overline{t}^{(m)}$ is the off-diagonal part of $\langle\Psi^{(m)}_{\alpha}|\tilde{\mathcal{H}} - E_0|\Psi^{(m)}_{\beta}\rangle$. Since α and β are site indices, we can interpret $\overline{g}^{(m)}$ as a "locator", while $\overline{t}^{(m)}$ is a "hopping" matrix element (which can "hop" further than nearest-neighbors), consistent with the

usage in the electronic literature. (Because of translational invariance, $\overline{E}^{(m)}$ or $\overline{g}^{(m)}$ are the same for all sites and we can dispense with site indices.) We find numerically that the largest matrix elements in $(\overline{t}^{(m)}\overline{g}^{(m)})$ are of $\mathcal{O}(10^{-1})$, similar to the magnitude of the corresponding (off-diagonal) matrix elements in of $\mathcal{L}^{(m)}$.(See Table 3.2 . The largest matrix elements are $\overline{t}^{(s)}_{\alpha\beta}\overline{g}^{(s)}$ for nearest-neighbor α,β). Expanding $\overline{G}^{(m)}$ around $\overline{g}^{(m)}$, we find

$$\overline{G}^{(m)} = \overline{g}^{(m)} + \overline{g}^{(m)}\overline{t}^{(m)}\overline{g}^{(m)} + \mathcal{O}(\overline{g}(\overline{t}\overline{g})^2). \tag{3.53}$$

Note that $\overline{t}^{(m)}_{\alpha\beta}$ decays algebraically with $|\mathbf{r}_\alpha - \mathbf{r}_\beta|$. Thus it is plausible that keeping $\overline{t}^{(m)}_{\alpha\beta}$ for farther neighbors (α,β) is more important than $\mathcal{O}(\overline{t}^2)$ terms, which connect to the same farther neighbors but decay exponentially. (See similar comments in Footnote[8].) Putting this expansion into Eq.(3.51) and then Eq.(3.48), we get

$$E_g = \langle \mathcal{H}_2 + \mathcal{H}_4 \rangle_0 + \sum_m [\overline{g}^{(m)}\overline{V}^{(m)} \cdot \overline{V}^{(m)} + \overline{g}^{(m)2}\overline{V}^{(m)} \cdot \overline{t}^{(m)} \cdot \overline{V}^{(m)}] \tag{3.54}$$

3.7 Effective Ising Hamiltonian

We shall now rewrite parts of Eq.(3.54) in the form of an Ising Hamiltonian with the chiralities as Ising variables. The coupling constants of this effective Ising Hamiltonian will be expressed in terms of correlation functions in the form $\langle \mathcal{Q}_\alpha \mathcal{Q}_\beta \rangle_0$ or $\langle \mathcal{Q}_\alpha (\tilde{\mathcal{H}} - E_0) \mathcal{Q}_\beta \rangle_0$. We call them "triangle" correlations. As we shall see later in Figure 3.10 , these triangle correlations decay rapidly with distance, making it reasonable to truncate the Ising coupling constants at short distance. This truncation facilitates the easy evaluation of the ground state

energy of *any* spin configuration and the determination of the lowest energy Potts configuration.

Employing Eq.(3.9), Eq.(3.37) and Eq.(3.45), we can write

$$\begin{aligned}\overline{V}^{(m)} \cdot \overline{V}^{(m)} &= c^{(m)2} \sum_{\alpha\beta\gamma} \langle \mathcal{H}_\beta \mathcal{Q}_\alpha^{(m)} \rangle_0 \langle \mathcal{H}_\gamma \mathcal{Q}_\alpha^{(m)} \rangle_0 \eta_\beta \, \eta_\gamma \\ &= c^{(m)2} N_\alpha \langle \mathcal{H}_\alpha \mathcal{Q}_\alpha^{(m)} \rangle_0^2 + 2c^{(m)2} \langle \mathcal{H}_\alpha \mathcal{Q}_\alpha^{(m)} \rangle_0 \sum_{(\alpha,\beta)} \langle \mathcal{H}_\beta \mathcal{Q}_\alpha^{(m)} \rangle_0 \eta_\alpha \, \eta_\beta \\ &\quad + \ldots, \end{aligned} \tag{3.55}$$

where (α, β) in the second line indicates the sum is over all pairs of nearest-neighbor, second-nearest- neighbor, third-nearest neighbors, . . . , triangles. (Each pair will be counted twice in the sum in the second line of Eq.(3.55).) The terms that follow the last displayed terms in Eq.(3.55) involve a product

$$\langle \mathcal{H}_\beta \mathcal{Q}_\alpha^{(m)} \rangle_0 \langle \mathcal{H}_\gamma \mathcal{Q}_\alpha^{(m)} \rangle_0$$

, where each of the pairs (α, β) and (α, γ) are at least the nearest-neighbor kind (if not farther). Therefore, the coupling of two triangles by these omitted terms is necessarily smaller than the coupling generated by the last displayed term in Eq.(3.55), which just involves one triangle correlation function[8]. This omission amounts to a very analogous approximation that was made in the locator expansion Eq(3.53). Similarly, we write

$$\overline{V}^{(m)} \cdot \overline{t}^{(m)} \cdot \overline{V}^{(m)} = c^{(m)4} \langle \mathcal{H}_\alpha \mathcal{Q}_\alpha^{(m)} \rangle_0^2 \sum_{(\alpha,\beta)} \langle \mathcal{Q}_\alpha^{(m)} (\tilde{\mathcal{H}} - E_0) \mathcal{Q}_\beta^{(m)} \rangle_0 \eta_\alpha \eta_\beta + \ldots . \tag{3.56}$$

[8] Consider the coupling of two triangles α and β that are distance $2r$ apart. We can couple these two triangles by $\mathcal{H}(0)\mathcal{Q}(2r)$, or a product of two $\mathcal{H}(0)\mathcal{Q}(r)$ (as well as other intermediate cases). We shall see below that triangle correlations decay as a power law: $\langle \mathcal{H}(0)\mathcal{Q}(r) \rangle \sim 1/r^\zeta$. Therefore, the first kind of coupling is of order $1/(2r)^\zeta$, whereas the second kind is of order $1/r^{2\zeta}$. The latter is obviously much smaller. In this argument, we have not taken into account the fact that there can be many paths that correspond to the second kind of coupling. But we don't expect the number of paths to increase exponentially in a 2- dimensional lattice.

Before we collect the various terms together, we can simplify Eq.(3.56) somewhat by showing that $\langle \mathcal{H}_\alpha \mathcal{Q}_\beta^{(m)} \rangle_0$ is proportional to $-\langle \mathcal{Q}_\alpha^{(m)} \mathcal{Q}_\beta^{(m)} \rangle_0$ to leading order of S, provided we are using the form of $\mathcal{Q}_\alpha^{(m)}$ defined in Eq.(3.38). We show this in Appendix[D]. The result is

$$\langle \mathcal{H}_\alpha \mathcal{Q}_\beta^{(m)} \rangle_0 \approx \langle \mathcal{H}_\alpha^{(m)} \mathcal{Q}_\beta^{(m)} \rangle_0 = -\frac{\sqrt{3}}{4S} J^* \langle \mathcal{Q}_\alpha^{(m)} \mathcal{Q}_\beta^{(m)} \rangle_0. \tag{3.57}$$

Finally, if we collect the results of Eq.(3.40), Eq.(3.55), Eq.(3.56) and Eq.(3.57) and substitute them into Eq.(3.54), we obtain an effective Ising Hamiltonian with $\{\eta_\alpha\}$ as the Ising variables,

$$E_g = \langle \mathcal{H}_2 + \mathcal{H}_4 \rangle_0 + (\frac{\sqrt{3}J^*}{4S})^2 N_\alpha \sum_{m=o,s} \overline{g}^{(m)} \langle \mathcal{Q}_\alpha^{(m)2} \rangle_0 - \sum_{m=o,s} \sum_{(\alpha,\beta)} \mathcal{J}_{\alpha\beta}^{(m)} \eta_\alpha \, \eta_\beta, \tag{3.58}$$

where the coupling constants are

$$\mathcal{J}_{\alpha\beta}^{(m)} = -\overline{g}^{(m)} (\frac{\sqrt{3}J^*}{4S})^2 [2\langle \mathcal{Q}_\alpha^{(m)} \mathcal{Q}_\beta^{(m)} \rangle_0 + \overline{g}^{(m)} \langle \mathcal{Q}_\alpha^{(m)} (\tilde{\mathcal{H}} - E_0) \mathcal{Q}_\beta^{(m)} \rangle_0]. \tag{3.59}$$

These coupling constants determine the selection energy. We can show that[9] for both $\mathcal{J}_{\alpha\beta}^{(s)}$ and $\mathcal{J}_{\alpha\beta}^{(o)}$,

$$\mathcal{J}_{\alpha\beta}^{(m)} \propto J^* \frac{|J_3|^{-1}}{r_{\alpha\beta}^{\zeta^{(m)}}}, \tag{3.60}$$

where $r_{\alpha\beta}$ is the distance between α and β, and[10]

$$\zeta^{(s)} = 5,$$

$$\zeta^{(o)} = 3. \tag{3.61}$$

---

[9] This scaling of $\mathcal{J}_{\alpha\beta}$ with J_3 is valid for large S or small $|J_3|$. There are corrections that scale with a smaller power of S or a larger power of $|J_3|$.

[10] The exponent $\zeta^{(m)}$ can be derived using the r-exponent of the pair correlations worked out in Appendix[B.3]. As far as r-dependence is concerned, $\mathcal{J}_{\alpha\beta}^{(m)} \sim \langle \mathcal{Q}_\alpha^{(m)} \mathcal{Q}_\beta^{(m)} \rangle_0 \sim \langle \sigma_x^{(m)}(0) \sigma_x^{(m)}(r_{\alpha\beta}) \rangle_0 \langle \sigma_y^{(m)}(0) \sigma_y^{(m)}(r_{\alpha\beta}) \rangle_0^2$. Note that the $\sigma_y^{(m)}$- pairings cannot be $\langle \sigma_y^{(m)2}(0) \rangle_0 \langle \sigma_y^{(m)2}(r_{\alpha\beta}) \rangle_0$ instead, because such terms cancel each other.

If we use the variational estimate Eq.(3.32) for J_3, then

$$\mathcal{J}^{(m)}_{\alpha\beta} \propto J^* \frac{S^{2/3}}{r^{\zeta^{(m)}}_{\alpha\beta}}. \tag{3.62}$$

The power of $S^{2/3}$ is consistent with Chubukov's [20] calculation.

We summarize here the scaling of the other terms in Eq.(3.58) with S and J_3. Based on Eq.(3.30), we have $\langle \mathcal{H}_2 \rangle_0 \sim J^* S$, $\langle \mathcal{H}_4 \rangle_0 \sim J^* S |J_3|^{1/2}$. Now from the scaling results in Appendix[G], we find that the third term in Eq.(3.58) scales with $J^*|J_3|^{-1}$, just like the $\mathcal{J}_{\alpha,\beta}$'s. (The terms in Eq.(3.58) are Section[3.9.3].)

3.8 Relation to Reciprocal Space Perturbation

We now comment on the form of the second-order perturbative energy, given as the third and fourth terms in Eq.(3.58). We shall denote this second-order energy by E_2. We focus on the non-Ising part of E_2 (the third term in Eq.(3.58)), because it dominates[11] the total E_2.

As discussed in Section[3.4], our perturbative energy is calculated in the subspace Ξ – the subspace wherein the excited states are localized. As given in the third term of Eq.(3.58), it has the form

$$E_2 \sim -\sum_{m,\alpha} \frac{\langle \Psi_0 | \mathcal{H}_3 | \Psi^{(m)}_\alpha \rangle \langle \Psi^{(m)}_\alpha | \mathcal{H}_3 | \Psi_0 \rangle}{\overline{E}^{(m)} - E_0}. \tag{3.63}$$

This is to be compared with the reciprocal space perturbative energy E_2', which is computed in a subspace that includes *all* possible 1- and 3-magnon states,

[11] From Table 3.2 , Table 3.3 and Table 3.1 , it can be estimated that the non-Ising part forms about 80 percent of the total second-order perturbative energy E_2.

not just the localized ones[12],

$$E_2' = -\sum_{p_1\mathbf{k}_1} \frac{\langle\Psi_0|\mathcal{H}_3|p_1\mathbf{k}_1\rangle\langle p_1\mathbf{k}_1|\mathcal{H}_3|\Psi_0\rangle}{\hbar\omega^{(p_1)}(\mathbf{k}_1)} - \sum_{\substack{p_1p_2p_3\\ \mathbf{k}_1\mathbf{k}_2\mathbf{k}_3}} \frac{\langle\Psi_0|\mathcal{H}_3|p_1\mathbf{k}_1p_2\mathbf{k}_2p_3\mathbf{k}_3\rangle\langle p_1\mathbf{k}_1p_2\mathbf{k}_2p_3\mathbf{k}_3|\mathcal{H}_3|\Psi_0\rangle}{\hbar(\omega^{(p_1)}(\mathbf{k}_1)+\omega^{(p_2)}(\mathbf{k}_2)+\omega^{(p_3)}(\mathbf{k}_3))}. \quad (3.64)$$

(The p's are the polarization indices, consistent with our usage in Appendix[B].)

By comparing Eq.(3.63) and Eq.(3.64), we can see clearly the approximations involved in making the locator expansion. As far as the numerators are concerned, we have clearly a far smaller number of intermediate excited states in Eq.(3.63) than in Eq.(3.64). In particular, we have combined the 2 different ordinary branches ($p = 2, 3$) to one coherent mixtures of ordinary modes denoted by $m = o$. This would tend to make our estimate of the second-order energy smaller in absolute magnitude than the exact second-order energy.

Turning our attention to the denominators, note that we have approximated the $\mathbf{k}$-dependent energy denominator in Eq.(3.64) with a constant $\overline{E}^{(m)} - E_0$ in Eq.(3.63): in fact, we use the same constant as energy denominator for both the 1-magnon and the 3-magnon excited states. The error $(E_2' - E_2)$ in second order energy that this approximation introduces depends on the way in which the numerator and denominator are correlated in Eq.(3.64).

[12] States in this larger subspace is what Chubukov implicitly used as excited states in his second-order term.

3.9 Results

3.9.1 In-plane Selection

Formula (3.58) is all we need to determine ground state selection. Because of the rapid decay in absolute magnitudes of these coupling constants with distance, we only need to compute a few of them. The Ising ground state corresponding to these coupling constants is usually quite trivial to find. The problem of determining which Potts state corresponds to the Ising ground state requires more thought, because although there is a unique mapping between the Potts states and the Ising states, there are some Ising states that do not map to any Potts state. Fortunately, we shall see that we don't run into such difficulties for our Ising ground state.

The Ising coupling constants are composed of different multiple spin- spin correlation functions computed with the Ψ_0 wavefunction. These correlation functions can be written as sums of products of all possible pair correlations using Wick's theorem. The calculational algorithm for performing Wick's theorem with the help of a symbolic manipulation program is given in Appendix[I]. These pair correlations can be computed as described in Section[3.3], but more formally treated in Appendix[B]. The algorithm for using the pair correlations to obtain Eq.(3.58) will be discussed in Appendix[H]. All these quantities are in general functions of J_3: the J_3 variable cannot be optimized analytically in the same way as the coefficients $a_\alpha^{(s)}$ and $a_\alpha^{(o)}$ (which was done using the perturbation theory discussed in Section[3.5].) We must optimize J_3 numerically.

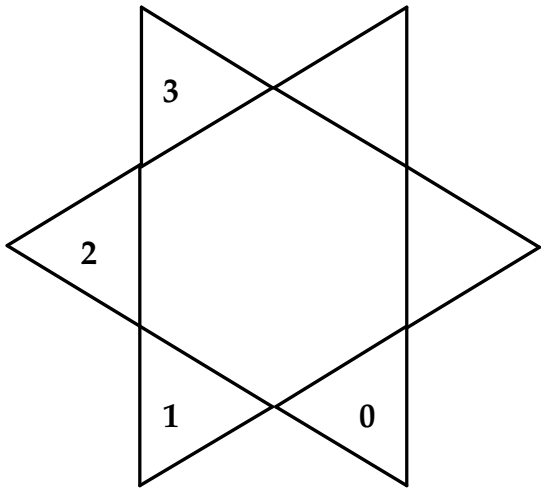

Figure 3.4 The labelling of triangles used in all the Tables and Figures of this section.

We will postpone discussion of this numerical optimization until Section[3.9.3], because we shall see in the following paragraph that we can determine the ground state without performing this optimization.

We have calculated $\mathcal{J}_{\alpha\beta}$ for different S's and lattice sizes with periodic boundary conditions. We have plotted the dependence of the couplings $\mathcal{J}_{\alpha\beta}$ on $|J_3|$ for a $L = 16$ system in Figure 3.5. In these and other similar diagrams, J_3 on the x-axis is expressed as sub-multiples of $J_3(f = 0)$. This $J_3(f = 0)$ is the value of J_3 which optimizes the variational energy of $\mathcal{H}$ when $\mathcal{H}_3$ is set to zero. (We shall discuss $J_3(f = 0)$ in more details in Section[3.9.4], where it is found that $J_3(f = 0) = a(S)S^{-2/3}$, with $a(S)$ going to a constant as $S \to \infty$.) This kind of scaling by $J_3(f = 0)$ is useful because, by the arguments of Section[3.3], the optimal J_3 resulting from a variational minimization of the expectation value of the complete $\mathcal{H}$ (including $\mathcal{H}_3$) is certainly smaller (in

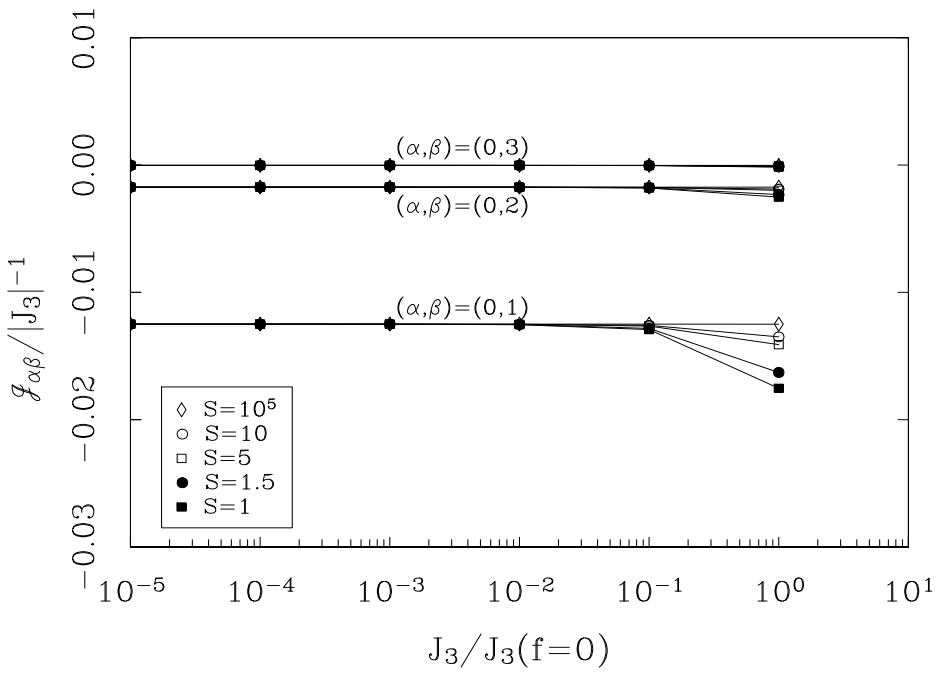

Figure 3.5 The three short-range Ising coupling constants, as a function of variational parameter J_3. They all scale with $|J_3|^{-1}$ at large S or small $|J_3|$. All data are for $L = 16$. The y-intercepts are the sums of the soft and ordinary components listed in Table 3.1 . J_3 is written here as sub-multiples of $J_3(f = 0)$ which minimizes the variational energy with the $\mathcal{H}_3$ term set to zero. See Eq.(3.75). The values of $J_3(f = 0)$ for various S are listed in Table 3.4 .

absolute magnitude) than $J_3(f = 0)$. Thus we are only interested in values of $|J_3|$ which are sub-multiples of $|J_3(f = 0)|$.

For each lattice size, we take the value of $\mathcal{J}_{\alpha\beta}$ at $S = 10^5$ and $J_3 = 10^{-5}J_3(f = 0)$ to be the large S and small $|J_3|$ limit. These limiting values of $\mathcal{J}_{\alpha\beta}$ for several different L's are then plotted versus $1/L$. (See Figure 3.6.) The resulting curves are then fitted empirically to a quadratic functions $\mathcal{J}_{\alpha\beta}(L) = c_0 + c_1(1/L) + c_2(1/L)^2$. The resulting extrapolated values at

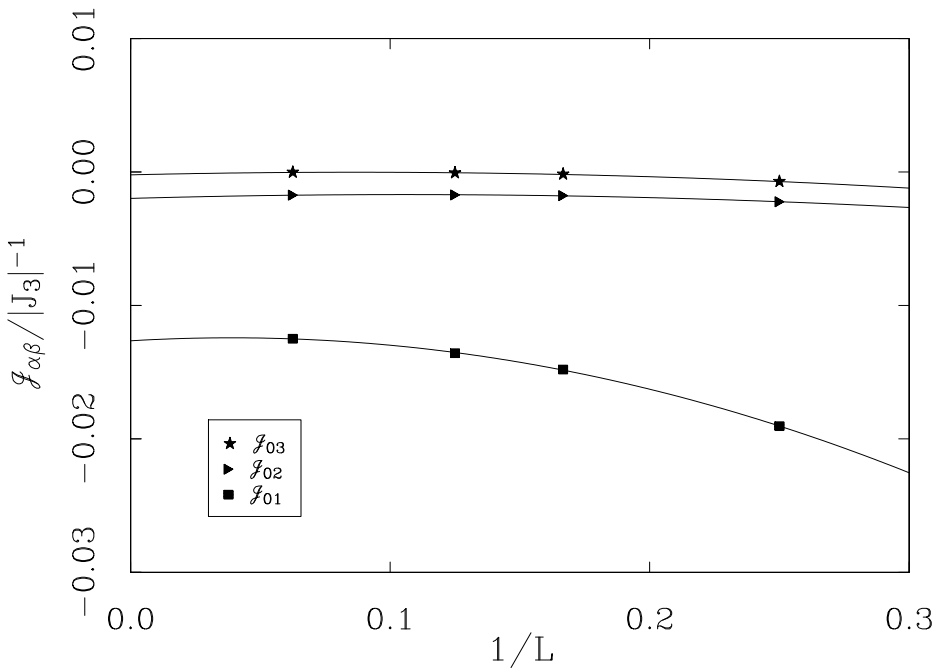

Figure 3.6 This is the finite-size extrapolation plot for Figure 3.5. The four lattice sizes are $L = 4, 6, 8, 16$. The data points come from the intercepts in Figure 3.5 (i.e. they are the extrapolated results at $S \to \infty$ and $J_3 \to 0$.) The curves are fitted by quadratic functions of $1/L$. The intercepts at $L = \infty$ are listed in Eq.(3.65).

$L = \infty$ are

$$\begin{aligned} \mathcal{J}_{\alpha\beta} &\equiv \mathcal{J}^{(s)}_{\alpha\beta} + \mathcal{J}^{(o)}_{\alpha\beta} \\ &= \begin{cases} -1.265 \times 10^{-2} J^* |J_3|^{-1}, & \text{for } (\alpha,\beta) = (0,1) \\ -1.979 \times 10^{-3} J^* |J_3|^{-1}, & \text{for } (0,2) \\ -2.135 \times 10^{-4} J^* |J_3|^{-1}, & \text{for } (0,3), \end{cases} \end{aligned} \tag{3.65}$$

where $(0,1)$ refer to nearest-neighbor triangles, $(0,2)$ to next- nearest-neighbors etc. (The labeling of the triangles α, β is defined in Figure 3.4.) The contributions due to the soft and ordinary modes separately are listed in Table 3.1 . We cut off the interaction at the third-nearest-neighbor distance because as we have noted in Eq.(3.60), the $\mathcal{J}_{\alpha\beta}$ decays rapidly with distance. The third-

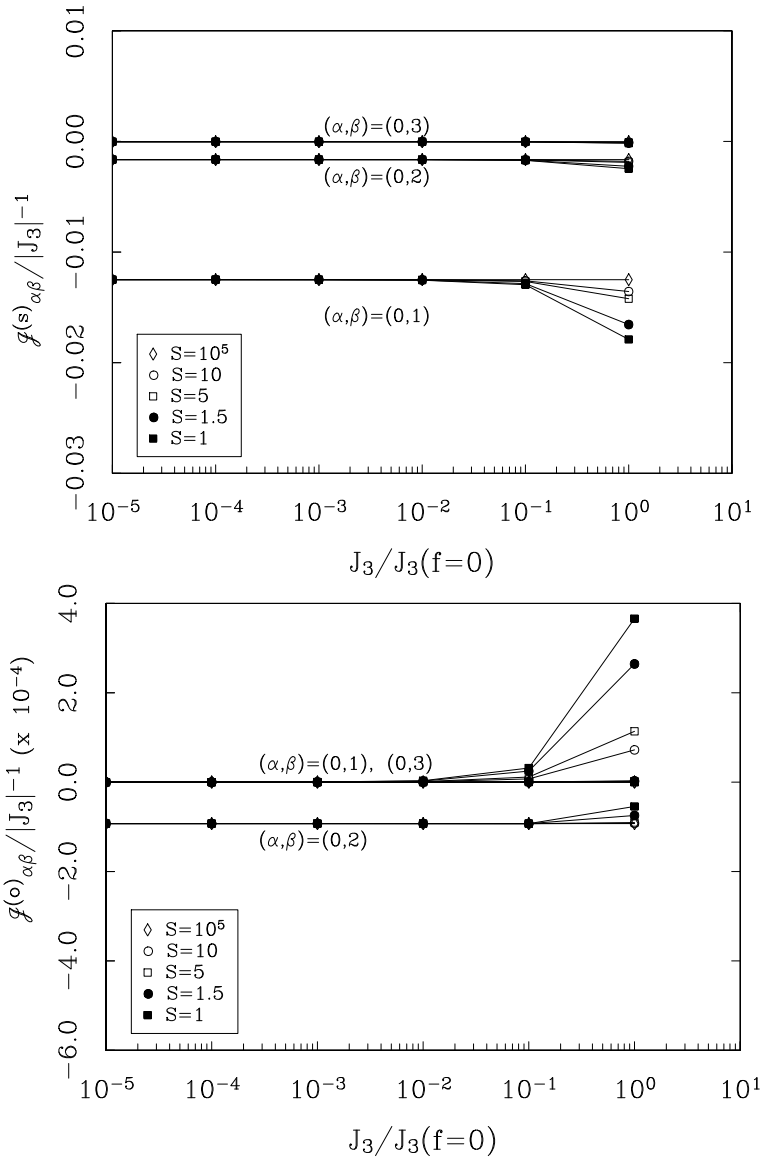

Figure 3.7 Similar to Figure 3.5, but for $\mathcal{J}^{(s)}_{\alpha\beta}$ and $\mathcal{J}^{(o)}_{\alpha\beta}$. The y-intercepts are listed in Table 3.1 .

nearest- neighbor Ising coupling is already so weak that it does not affect in-plane selection.

To determine the Ising ground state resulting from this set of Ising couplings, first note that not all Ising ground states correspond to allowed Potts

Table 3.1 Soft and Ordinary Modes Contributions to $\mathcal{J}_{\alpha\beta}$. The numbers quoted are for a $L = 16$ lattice, with $S = 10^5$ and $J_3 = 10^{-5} \times J_3(f = 0)$. These numbers are derived from the y-intercepts of Figure 3.7 .

Ising Couplings	Scaling with S and J_3	Prefactor ($\times 10^{-4}$) for Triangles (α, β)		
		(0,1)	(0,2)	(0,3)
$\mathcal{J}^{(s)}_{\alpha\beta}$	$J^*\|J_3\|^{-1}$	-125	-16.43	-0.2837
$\mathcal{J}^{(o)}_{\alpha\beta}$	$J^*\|J_3\|^{-1}$	0	-0.9277	0

ground states. So we need only focus on a small set of Ising states which do have Potts counterparts. The condition for an allowed Ising state is that each hexagon is surrounded by either all $\eta = +1$ triangles, or half $\eta = +1$ and half $\eta = -1$ triangles [33]. It is easy to see that there are only 4 such kinds of hexagons. The numerical values[13] of our Ising coupling constants dictate that we must (if possible) have hexagons where the $\eta = +1$ triangles alternates with the $\eta = -1$ triangles. This is nothing but the "$\sqrt{3} \times \sqrt{3}$" state.

We have plotted the dependence of the couplings $\mathcal{J}_{\alpha\beta}$ on $|J_3|$ in Figure 3.5. In these and other similar diagrams, J_3 on the x-axis is expressed as sub-multiples of $J_3(f = 0)$. This $J_3(f = 0)$ is the value of J_3 which optimizes the variational energy of $\mathcal{H}$ when $\mathcal{H}_3$ is set to zero. (We shall discuss $J_3(f = 0)$ in more details in Section[3.9.4], where it is found that $J_3(f = 0) = a(S)S^{-2/3}$, with $a(S)$ going to a constant as $S \to \infty$.) This kind of scaling by $J_3(f = 0)$ is useful because, by the arguments of Section[3.3], the optimal J_3 resulting from

[13] Note that if $|\mathcal{J}_{01}/\mathcal{J}_{02}| < 4$, then the Potts ground state would have been different.

a variational minimization of the expectation value of the complete $\mathcal{H}$ (including $\mathcal{H}_3$) is certainly smaller (in absolute magnitude) than $J_3(f=0)$. Thus we are only interested in values of $|J_3|$ which are sub-multiples of $|J_3(f=0)|$.

3.9.2 Implicit Contributions to Selection Energy

We have written Eq.(3.58) in such a way that the dependence on the Potts state appears only in the last term, the "Ising Hamiltonian". In reality, however, *all* the terms depend implicitly on the Potts state through their dependence on J_3. Spinwave expansion around different Potts states will result in different variationally optimal J_3's. Does this render the whole effective Ising Hamiltonian formalism useless? The answer is no, as we can demonstrate as follows.

Let us assume that the dependence on the Potts state can be characterized by a single[14] continuous parameter κ, which is the averaged nearest- neighbor chirality correlation:

$$\kappa \equiv \langle \eta_\alpha \eta_\beta \rangle, \tag{3.66}$$

where the average is over all possible nearest-neighbor pairs of triangles, α and β. Obviously, $\kappa = 1$ for the "q=0" state, $\kappa = -1$ for the "$\sqrt{3} \times \sqrt{3}$" state, and κ acquires an intermediate value for all other Potts states. Now we can rewrite the variational energy Eq.(3.58) in the form

$$E_g(J_3, \kappa) \equiv \mathcal{F}(J_3) - \mathcal{J}(J_3)\kappa, \tag{3.67}$$

[14] In general, we should have a set of parameters $\kappa_1, \kappa_2, \ldots$ corresponding to chirality correlations between nearest-neighbors, next-nearest-neighbors, etc. However, the basic argument remains the same as the case where there is only one parameter.

where $\mathcal{F}$ represents all the non-Ising terms of Eq.(3.58), and $\mathcal{J}$ equals $\mathcal{J}_{01}$ times twice the number of pairs of nearest-neighbor triangles. Now we have to minimize $E_g(J_3)$ with respect to J_3 to obtain the ground state energy for each Potts state,

$$E_g(\kappa) = \min_{J_3} \{\mathcal{F}(J_3) - \mathcal{J}(J_3)\kappa\}. \tag{3.68}$$

If we Taylor-expand $E_g(\kappa)$ in powers of κ about $\kappa = 0$, we get

$$E_g(\kappa) = const. - \mathcal{G}\kappa + \ldots, \tag{3.69}$$

where $\mathcal{G}$ is a constant. We can see that Eq.(3.69) defines $\mathcal{G}$ to be the true Ising coupling constant. We can express $\mathcal{G}$ in terms of $\mathcal{F}$ and $\mathcal{J}$:

$$\begin{aligned} \mathcal{G} &= -\frac{dE_g(\kappa)}{d\kappa} \\ &= -(\frac{d\mathcal{F}}{dJ_3} - \kappa\frac{d\mathcal{J}}{dJ_3})\frac{dJ_3}{d\kappa} + \mathcal{J}(J_3). \end{aligned} \tag{3.70}$$

Since we are evaluating this expression at the optimal value of J_3, the parenthesis in Eq.(3.70) vanishes, by virtue of Eq.(3.68). Thus

$$\mathcal{J} = \mathcal{G}, \tag{3.71}$$

the Ising coupling constants in Eq.(3.65) is indeed the true Ising coupling constant. We can safely ignore the selection effects of the terms that do not depend explicitly on η_α's.

We also see that the optimal value of J_3 depends somewhat on κ; however, as we remarked in Footnote[11], $\mathcal{J} \ll \mathcal{F}$ and so $\frac{d\mathcal{F}}{dJ_3} = \kappa\frac{d\mathcal{J}}{dJ_3}$ gives a value of J_3 that is only a little different from what $\frac{d\mathcal{F}}{dJ_3} = 0$ would give. This means we can ignore the explicitly Ising terms in Eq.(3.58) during variational minimization.

3.9.3 Failure of Optimization

These seemingly clearcut results mask a problem with the above calculation. Since this is a variational wavefunction calculation, one must ask what the optimal J_3 is for a given Potts state. If we do in fact attempt this optimization, we find that the minimum in variational energy does not exist: the system is unstable.

To understand this instability, we display Eq.(3.58) again, this time writing the various terms as functions of J_3 and S (similar to Eq.(3.30):

$$E_g/N_s = b_0 S + b_1 S|J_3|^{1/2} + (b_2 - b_3)|J_3|^{-1}, \tag{3.72}$$

where $b_0 = 0.5608$ comes from $\langle \mathcal{H}_2^{(s)} \rangle_0$, $b_1 = 0.2565$ is from $\langle \mathcal{H}_2^{(o)} \rangle_0$, $b_2 = 0.01326$ is from $\langle \mathcal{H}_4^{(s)} \rangle_0$ and finally $b_3 = 0.06491$ is from second-order perturbation of $\mathcal{H}_3$– the third term[15] in Eq.(3.58). (All these values, which are the $S \to \infty$ limits, can be read off from Table 3.2 and Table 3.3 .) It is clear that this instability comes from the fact that the second-order perturbation term is bigger in absolute magnitude than the first-order perturbation term $\langle \mathcal{H}_4 \rangle_0$, although they are both proportional to $|J_3|$, making $b_2 - b_3 < 0$.

(The various terms in Eq.(3.58) as functions of J_3 and S are plotted in Figure 3.8, Figure 3.9 and Figure 3.10. Their numerical values at large S are listed in Table 3.2 and Table 3.3 .)

This failure to find a minimum may seem to contradict the previous result of Chubukov [20]. His self-consistent second- order perturbation calculation is mathematically equivalent to using a variational wavefunction whose

[15] At small $|J_3|$, the ratio of the second term ($\langle \mathcal{H}_4 \rangle_0$) to the third (non-Ising) term in Eq.(3.58) is about -0.204. The fourth (Ising) term in Eq.(3.58) is about 5 times smaller in magnitude than the previous two terms, as we commented at Footnote[11]–it has little effect on the variational minimum. Therefore we have omitted the Ising terms in Eq.(3.72).

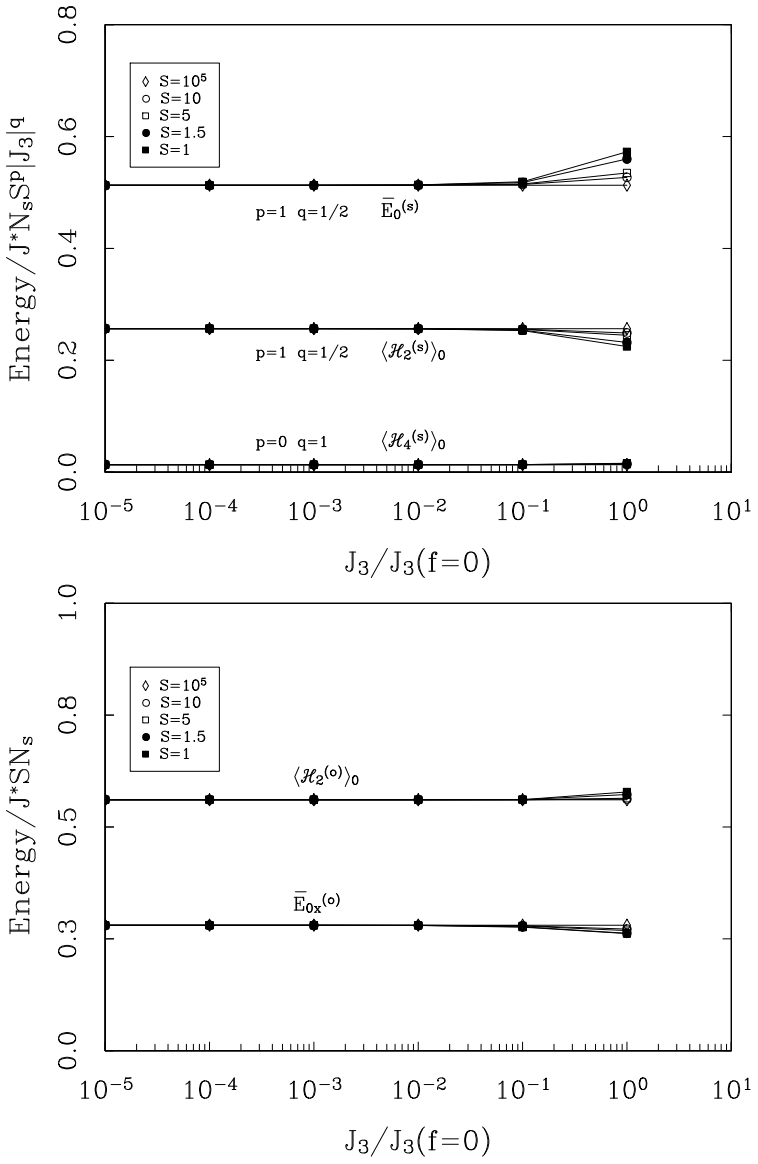

Figure 3.8 Expectation values of various terms of the Hamiltonian $\mathcal{H}$ and $\tilde{\mathcal{H}}$ in the Ψ_0 ground state for a $L = 16$ system. The top figure is for the soft modes while the bottom one is for the ordinary modes. Each component scale differently with S and J_3. The y-intercepts are listed in Table 3.3 . J_3 is written here as sub-multiples of $J_3(f = 0)$ which minimizes the variational energy with the $\mathcal{H}_3$ term set to zero.(See Eq.(3.75).) The values of $J_3(f = 0)$ for various S are listed in Table 3.4 .

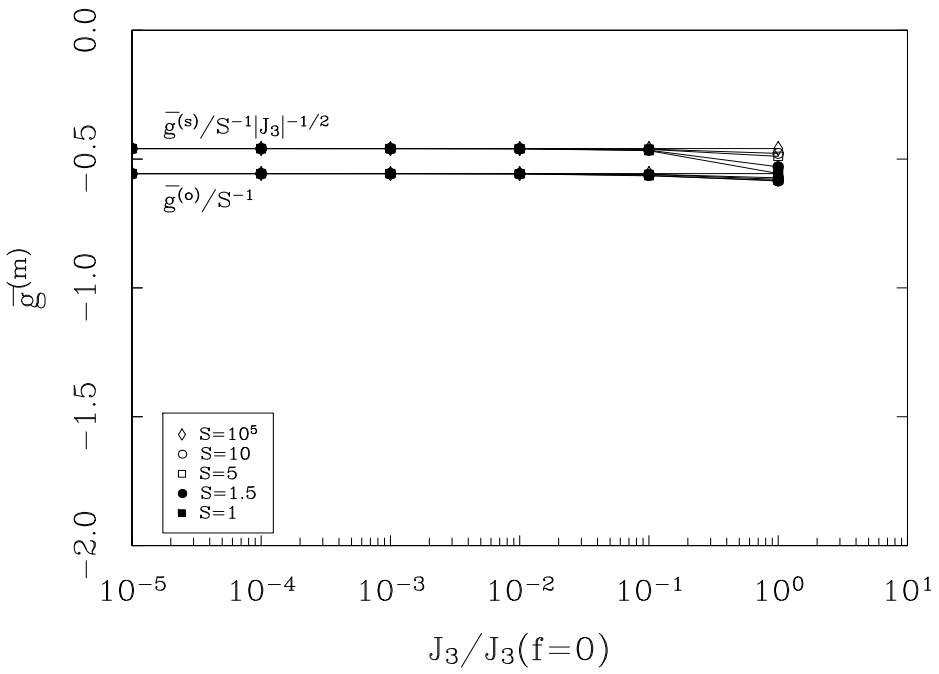

Figure 3.9 The bare propagator $\overline{g}^{(m)}$. $\overline{g}^{(s)}$ scales as $S^{-1}|J_3|^{-1/2}$, and $\overline{g}^{(o)}$ scales as S^{-1}. The y-intercepts are listed in Table 3.3 . J_3 is written here as sub-multiples of $J_3(f=0)$ which minimizes the variational energy with the $\mathcal{H}_3$ term set to zero.(See Eq.(3.75).) The values of $J_3(f=0)$ for various S are listed in Table 3.4 .

non-gaussian part includes multiple excitations of one- and three- magnon states, similar to the wavefunction in Eq.(3.11). Our variational wavefunction Eq.(3.43) captures essentially the same excitations when the density of excitations is low, which is obtained when the spin number S is large (as we mentioned in Section[3.2]). Since he has found a finite self-consistent solution (albeit for $k \to 0$ only), there seems to be no possibility that we could find no minimum. The only place this could have gone wrong is the perturbation theory we used in subspace Ξ to find the *approximate* variational minimum energy. This perturbation theory breaks down when the magnitude of the perturbation $\sqrt{\langle V_\alpha^2 \rangle_0}$ is bigger than the magnitude of the energy denominator ΔE.

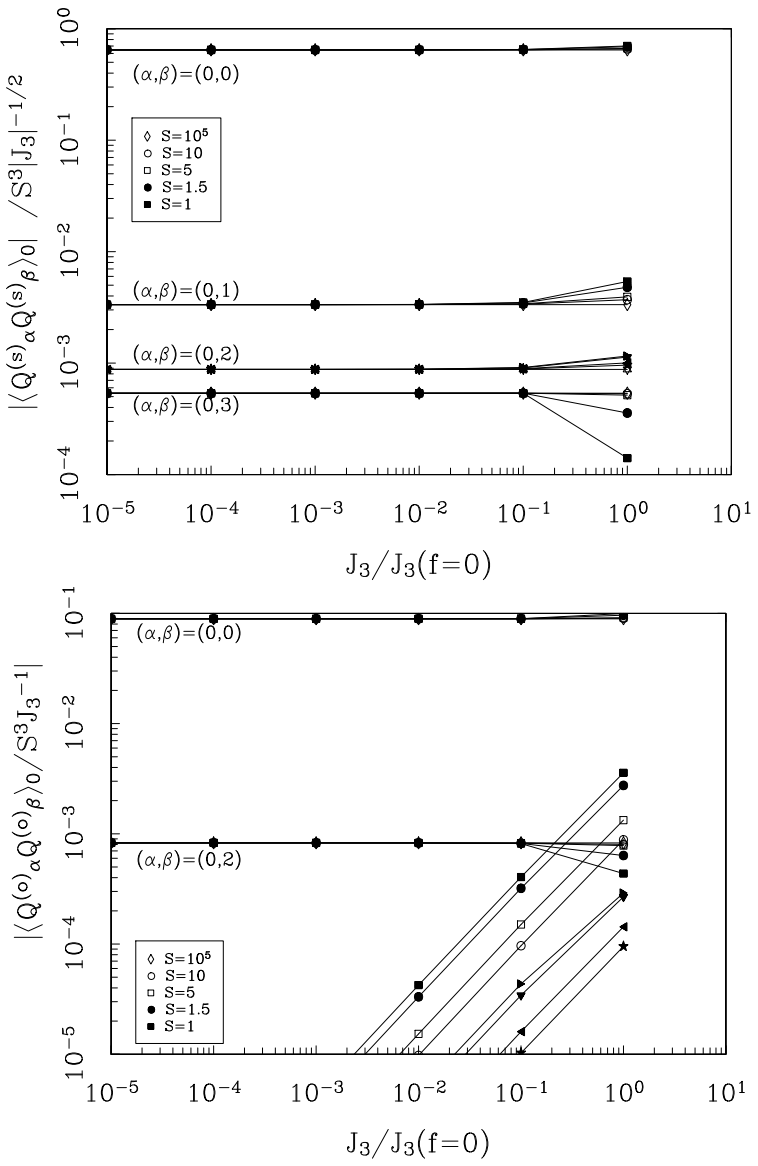

Figure 3.10 $\langle \mathcal{Q}^{(o)}_\alpha \mathcal{Q}^{(o)}_\beta\rangle_0$ and $\langle \mathcal{Q}^{(s)}_\alpha \mathcal{Q}^{(s)}_\beta\rangle_0$ as functions of J_3 for a $L = 16$ system. The top figure is for the soft modes while the bottom one is for the ordinary modes. All the soft correlations scale with $S^3|J_3|^{-1/2}$ for large S or small J_3, while the ordinary correlations scale with $S^3 J_3^{-1}$ in the same regime. In the bottom figure, the slanted lines at the lower right belong to $(\alpha,\beta) = (0,1)$ and $(0,2)$, where the values of $\langle \mathcal{Q}^{(o)}_\alpha \mathcal{Q}^{(o)}_\beta\rangle_0$ extrapolate to 0 at small $|J_3|$. The y-intercepts are listed in Table 3.2 . J_3 is written here as sub-multiples of $J_3(f = 0)$ which minimizes the variational energy with the $\mathcal{H}_3$ term set to zero.(See Eq.(3.75).) The values of $J_3(f = 0)$ for various S are listed in Table 3.4 .

Table 3.2 Numerical values of the various triangle correlation functions for a $L = 16$ lattice at $S = 10^5$ and $J_3 = 10^{-5} \times J_3(f = 0)$. (These are accurate upto at least 3 significant digits.) See Figures 3.10 and 3.11 . The method for calculating $\langle \mathcal{Q}^{(m)}(\tilde{\mathcal{H}} - E_0)\mathcal{Q}^{(m)}\rangle_0$ is detailed in Appendix[H].

Triangle Correlations	Scaling with S and J_3	Numerical Prefactor ($\times 10^{-2}$) for Triangle Pairs (α, β)			
		(0,0)	(0,1)	(0,2)	(0,3)
$\langle\langle \mathcal{Q}^{(s)}_\alpha \mathcal{Q}^{(s)}_\beta \rangle\rangle_0$	$S^3\|J_3\|^{-1/2}$	64.56	-0.3346	0.05364	-0.08774
$\langle \mathcal{Q}^{(o)}_\alpha \mathcal{Q}^{(o)}_\beta \rangle_0$	$S^3\|J_3\|^{-1}$	8.92	0	-0.08272	0
$\langle \mathcal{Q}^{(s)}_\alpha (\tilde{\mathcal{H}} - E_0)\mathcal{Q}^{(s)}_\beta \rangle_0$	$J^* S^4$	140.6	30.14	4.387	-0.3103
$\langle \mathcal{Q}^{(o)}_\alpha (\tilde{\mathcal{H}} - E_0)\mathcal{Q}^{(o)}_\beta \rangle_0$	$J^* S^4\|J_3\|^{-1}$	16.03	0	-0.1375	0

The form of our second-order perturbation energy is given in Eq.(3.63). Hence we can formally define the ratio of the perturbation matrix element to the energy gap to be

$$\begin{aligned} \mathcal{R}^{(m)} &\equiv \frac{[\langle \Psi_0|\mathcal{H}_3|\Psi^{(m)}_\alpha\rangle\langle\Psi^{(m)}_\alpha|\mathcal{H}_3|\Psi_0\rangle]^{1/2}}{\overline{E}^{(m)} - E_0} \\ &= \frac{\sqrt{3}J^*}{4S}\overline{g}^{(m)}\sqrt{\langle \mathcal{Q}^{(m)2}_\alpha\rangle_0}. \end{aligned} \tag{3.73}$$

In Appendix[C], we have inserted the scalings with J_3 and S of the various quantities involved in Eq.(3.73) and have obtained the scaling of $\mathcal{R}^{(m)}$. We find that

$$\begin{aligned} \mathcal{R}^{(s)} &\sim S^{-1/2}|J_3|^{-3/4}, \\ \mathcal{R}^{(o)} &\sim S^{-1/6}. \end{aligned} \tag{3.74}$$

Therefore, for large S, perturbation theory is guaranteed to be valid in the $|\alpha^{(o)}\rangle$ subspace, but it may well fail in the $|\alpha^{(s)}\rangle$ subspace if $|J_3|$ is small enough. As

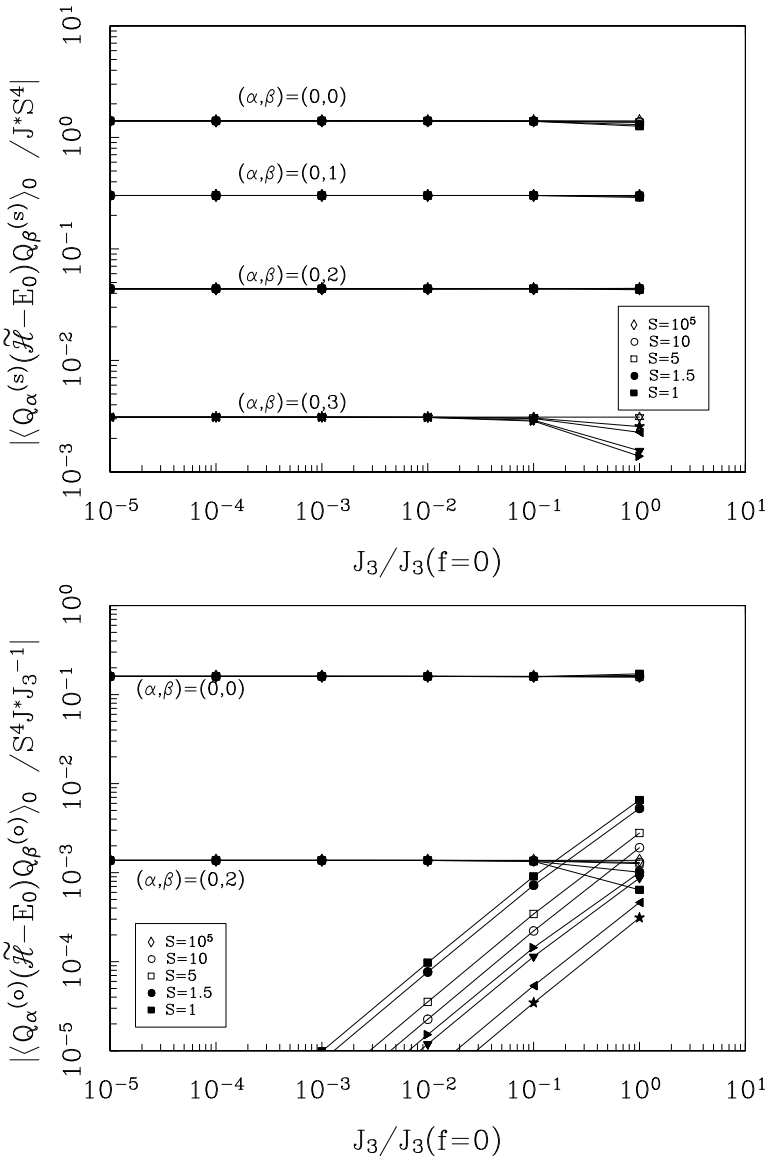

Figure 3.11 $\langle \mathcal{Q}_\alpha^{(m)}(\tilde{\mathcal{H}}-E_0)\mathcal{Q}_\beta^{(m)}\rangle_0$ as function of J_3 for a $L=16$ system, similar to Figure 3.10. The top figure is for the soft modes while the bottom one is for the ordinary modes. All the soft correlations scale with S^4, for large S or small J_3, while the ordinary correlations scale with $S^4J_3^{-1}$ in the same regime. In the bottom figure, the slanted lines at the lower right belong to $(\alpha,\beta)=(0,1)$ and $(0,3)$, where the values of $\langle \mathcal{Q}_\alpha^{(o)}(\tilde{\mathcal{H}}-E_0)\mathcal{Q}_\beta^{(o)}\rangle_0$ extrapolate to 0 at small $|J_3|$. The y-intercepts are listed in Table 3.2 .

Table 3.3 Numerical values of various terms in calculating the ground state energy Eq.(3.58), for a $L = 16$ lattice at $S = 10^5$ and $J_3 = 10^{-5} \times J_3(f = 0)$. See Figure 3.8 and Figure 3.9. For the definitions of $\tilde{\mathcal{H}}^{(s)}$ and $\tilde{\mathcal{H}}_x^{(o)}$, see Appendix[H]. Note also that if we add the $E_{classical}$ and the $\mathcal{H}_0$ terms in Eq.(3.7) to $\langle \mathcal{H}_2^{(s)} \rangle_0$, the sum should equal the value in Eq.(2.30) in Ref.8. The small difference is perhaps due to finite-size effects.

Quantity	Scaling with S and J_3	Numerical Prefactor
$E_0^{(s)} = \langle \tilde{\mathcal{H}}^{(s)} \rangle$	$J^* S \lvert J_3 \rvert^{1/2} N_s$	0.513
$E_{0x}^{(o)} = \langle \tilde{\mathcal{H}}_x^{(o)} \rangle$	$J^* S N_s$	0.2804
$\langle \mathcal{H}_2^{(s)} \rangle$	$J^* S \lvert J_3 \rvert^{1/2} N_s$	0.2565
$\langle \mathcal{H}_2^{(o)} \rangle$	$J^* S N_s$	0.5608
$\langle \mathcal{H}_4^{(s)} \rangle$	$J^* \lvert J_3 \rvert^{-1} N_s$	0.01326
$\overline{g}^{(s)}$	$(J^* S \lvert J_3 \rvert^{1/2})^{-1}$	-0.4593
$\overline{g}^{(o)}$	$(J^* S)^{-1}$	-0.5565

we shall show in the next section, $|J_3|$ may indeed be so small as to render perturbation theory inaccurate.

Note that we have already remarked on the possible inaccuracy in using perturbation theory (both in our restricted subspace Ξ and in the full 1- and 3-magnon subspace) in Section[3.4.1]. Here, we see that this inaccuracy prevents us from obtaining a variational minimum altogether.

3.9.4 Regulated Hamiltonian

We would like to systematically explore what the magnitude of J_3 is in the neighborhood of the true variational minimum. Even without actually finding the optimal value of J_3 for an *exact* variational calculation, we can set an upper bound for $|J_3|$. We do this by artificially multiplying the cubic terms in the spinwave Hamiltonian by a regulating parameter f, thus

$$\mathcal{H} = \mathcal{H}_2 + f\mathcal{H}_3 + \mathcal{H}_4. \tag{3.75}$$

Allowing the spins to fluctuate more will increase the positive contribution of $\mathcal{H}_4$ and the negative contribution of $\mathcal{H}_3$. Thus $\mathcal{H}_3$ is the destabilizing term. If we set $f = 0$, then the system is certainly stable. For this situation, we can find numerically the value of J_3 which minimizes the energy. Here as we have shown using the qualitative arguments in Section[3.3], $J_3 \propto -S^{-2/3}$ for large S, and from Figure 3.12 and Table 3.4 , we get

$$J_3(f = 0) \approx -0.2203S^{2/3}. \tag{3.76}$$

Clearly, $E_g(|J_3|)$ will fail to have a variational minimum when $b_2 - f^2 b_3 \leq 0$, which in our case is obtained when $f \geq 0.4517$.

Now, using Eq.(3.73) and the numerical value $J_3(f = 0)$ obtained in Eq.(3.76), as well as the numerical values listed in Tables 3.2 and 3.3 , we can estimate a lower bound for $\mathcal{R}^{(s)}$. We find that

$$\mathcal{R}^{(s)} > 0.495 \tag{3.77}$$

for the any $|J_3| < |J_3(f = 0)|$. Hence second order perturbation theory may already be inaccurate when $|J_3| = |J_3(f = 0)|$: we probably need to go to

higher order in the perturbation series. Any smaller J_3 would clearly render a perturbation calculation highly questionable.

We think it is not completely unexpected that we have an unstable system here. Chubukov found out that the $\mathcal{O}(\mathcal{H}_4)$ and $\mathcal{O}(\mathcal{H}_3^2)$ contributions to the self-energy $\Sigma(k)$ (correcting a propagator) cancel exactly at the Goldstone limit $\mathbf{k} -> \mathbf{0}$. So it is conceivable that they are close to cancelling here, for $f = 1$, and any approximation we make might push us either way (more or less stable.)

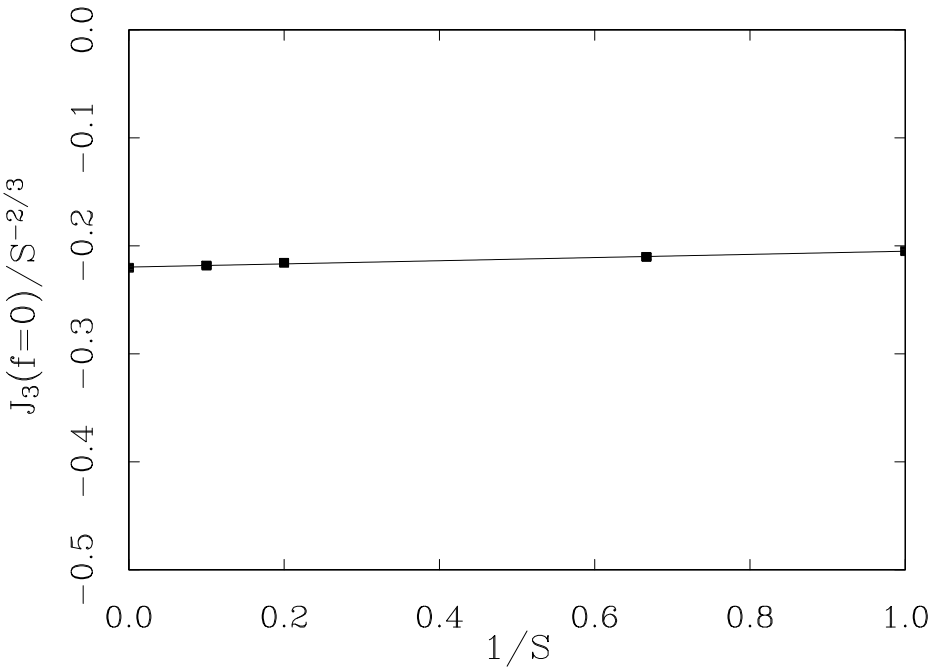

Figure 3.12 The optimal J_3 versus S, when we choose $f = 0$ for the Hamiltonian in Eq.(3.75), for a $L = 16$ system. Obviously, this optimal J_3 scales with $S^{-2/3}$. This data is listed in Table 3.4 also.

Table 3.4 The variational parameter J_3 that minimizes the variational energy at various S when the $\mathcal{H}_3$ term is omitted (*i.e.* $f = 0$).

	S				
	1	1.5	5	10	10^5
$J_3(f=0)/S^{-2/3}$	-0.2049	-0.2102	-0.2157	-0.2183	-0.2203

3.10 Discussion

3.10.1 Implications on Perturbative Approach

Does the breakdown of our perturbation approximation have any implications on the validity of Chubukov's perturbation theory? Although our perturbation theory is in position space, while his theory is in reciprocal space, the basic quantities involved in our respective perturbation are very similar. In particular, our gaussian ground state Ψ_0 is the same, the non-Gaussian part of our wavefunction lies within the subspace of his excited states, and the energy gap between the gaussian ground state and the excited states scales the same way with S in both calculations. So the ratio $\mathcal{R}^{(s)}$ may be close to 1 in Chubukov's calculations also.

Since the details of the calculations are different, and since the perturbation approximation is found to be inaccurate in our case, some numerical constants may well be different. Presumably Chubukov's reciprocal space calculation will give a more accurate estimate of these constants. Because the existence of a

variational minimum depends on the delicate balance between the contributions of $\mathcal{H}_3$ and $\mathcal{H}_4$, it is very sensitive to these numerical constants. Perhaps if we use the constants resulting from a reciprocal space calculation in our variational equation Eq.(3.72), we would have found a minimum. Even so, at that minimum, perturbation treatment may well be inaccurate since $\mathcal{R}^{(s)}$ may still be close to 1.

To illustrate this rather abstruse point, we depict in Figure 3.13 a possible scenario of what might be the case if we do not use perturbation approximation in calculating our variational energy in Section[3.5]. The solid curve is the variational energy as a function of J_3 calculated by, say, a numerical diagonalization of the Hamiltonian matrix in Eq.(3.44), which we never actually attempted. It is depicted having a minimum, as Chubukov's theory suggested. The dotted curve is our perturbation approximation to the variational energy. It agrees very well with the exact variational energy for large $|J_3|$, where $\mathcal{R}$ is very small. However, it starts to deviate from the solid curve near the minimum of the solid curve, and goes off to negative infinity for still smaller $|J_3|$. Thus while perturbation theory may still give a reasonable estimate of the minimum energy, it is giving a bad estimate of the curvature of the curve at that point.

In order to verify whether this scenario is correct, it would be necessary to check directly the numerical values of some of the fluctuation magnitudes from Chubukov's theory, and to calculate the ratio $\mathcal{R}^{(m)}$ in Eq.(3.73) there. If it turns out that these numerical values confirm our results that $\mathcal{R}^{(s)} \sim \mathcal{O}(1)$, one should at least go to higher order perturbation in order to ensure that the variational ground state is indeed stable with respect to fluctuations.

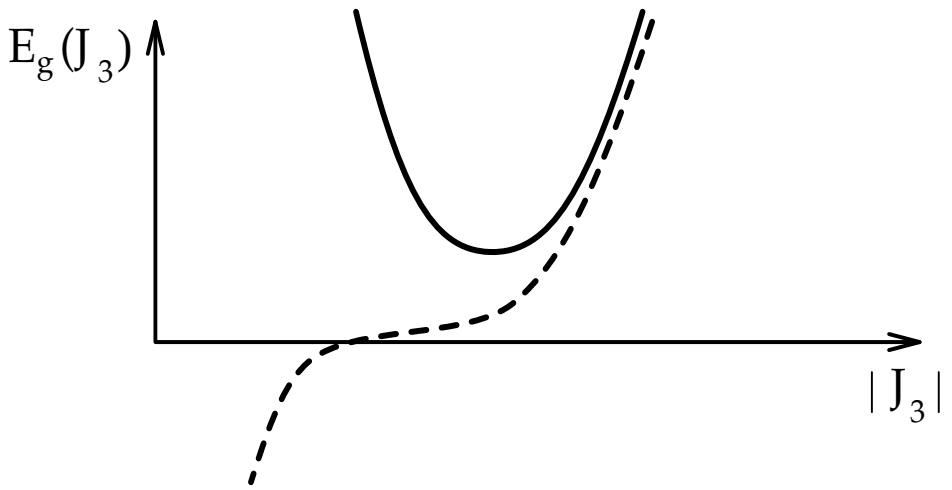

Figure 3.13 Illustration of the difference between an exact variational calculation (solid curve), and one based on a perturbative approximation to the variational calculation (dashed curve). The agreement is good for large $|J_3|$, but at the J_3 which is the minimum of the solid curve, the agreement starts to become so bad that the dashed curve fails to have a minimum.

3.10.2 Possible Error in In-plane Selection?

Inaccuracies in our perturbative approximation may have cost us our minimum in variational energy, as we argued in Section[3.10.1]. However, this should not affect our in-plane selection result because in-plane selection does not depend on the absolute magnitude of the perturbative energy. As we saw in Section[3.9.4], artificially decreasing the magnitude of $\mathcal{H}_3$ by a factor f will stabilize the system, but the same selection result is obtained at any f.

On the other hand, an insufficiently general variational wavefunction may produce a wrong in-plane selection result. There are three possible insufficiencies in our variational wavefunction.

Firstly, we have argued in Appendix[A] that the variational wavefunction for the two symmetric Potts states ("$q = 0$" and "$\sqrt{3} \times \sqrt{3}$" states) should have $\langle \sigma_{ix} \rangle_0 = 0$. Therefore we have constructed a variational wavefunction that does not have this non-zero offset as a variational parameter. However, for other unsymmetric Potts states, they may indeed have non-zero $\langle \sigma_{ix} \rangle_0$'s after quantum fluctuations are introduced. Optimizing the variational energy with respect to such parameters would probably result in additional contributions to the selection energies of the unsymmetric states. In the worst case scenario, this contribution may be larger than that from the explicitly Ising-part of Eq.(3.58).

Secondly, the form of $\tilde{\mathcal{H}}$ derived in Appendix[B] is based on a spinwave expansion around the "$q = 0$" state. What if we use an alternative $\tilde{\mathcal{H}}$ that is based on an expansion around the "$\sqrt{3} \times \sqrt{3}$" state instead? This is another variational subspace which we have not explored. Using a variational wavefunction in this subspace would generate different numerical values for b_1, b_2 and b_3 in the variational energy Eq.(3.72). We should choose the form of $\tilde{\mathcal{H}}$ which gives the lowest variational energy. (We argue in Ref.[34] that expanding around "$q = 0$" state might give the lowest variational energy. However,this argument is not yet checked by numerical computation.) Choosing a different form of $\tilde{\mathcal{H}}$ may conceivably change the sign of $\mathcal{J}_{\alpha\beta}$. In fact, we argue in Ref.[34] that the nearest-neighbor $\mathcal{J}_{\alpha\beta}$ should be ferromagnetic if we use the $\tilde{\mathcal{H}}$ from expansion around the "$q = 0$" state, and antiferromagnetic if the expansion is around the "$\sqrt{3} \times \sqrt{3}$" state, contradicting the numerical result here.

Thirdly, one can wonder, is our localized basis states too restrictive?

Recall that we define the non-gaussian variational wavefunction in a way such that it will be similar to the first term in Eq.(3.35). We are ignoring the

second order (in $\overline{g}$) term,

$$\overline{g}^2\overline{t}\mathcal{H}_3|\Psi_0\rangle, \tag{3.78}$$

in the locator expansion in that equation. On the other hand, in the locator expansion of the Green's function Eq.(3.53), we have to expand up to the second order term, because the first order term will be subsequently cancelled. To be consistent, should we have introduced terms like those in Eq.(3.78) into our variational wavefunction? This would mean including basis states like $\{\tilde{\mathcal{H}}\mathcal{Q}_\alpha|\Psi_0\rangle|\alpha = 1,\ldots,N_\alpha\}$ into the subspace Ξ defined in Section[3.5]. These states involve spin-excitation that are very non- local[16]. However, although these states are certainly linearly independent of the $\mathcal{Q}_\alpha|\Psi_0\rangle$ basis, they are not even approximately orthogonal to our localized basis states. To orthogonalize them is a very tedious procedure. After we orthogonalize them, would it turn out that the $\overline{g}^{(m)2}\overline{V}^{(m)}.\overline{t}^{(m)}.\overline{V}^{(m)}$ terms in Eq.(3.54) be cancelled also? We leave these questions for future work to answer.

[16] $\tilde{\mathcal{H}}\mathcal{Q}_\alpha$ will create excitations of form $(\sigma_l\sigma_m)(\sigma_i^2\sigma_j)$, where l and m are sites that may be arbitrarily far from i and j. To understand why these excited states do not actually contain 5 magnons, see Footnote[5] in Section[3.4.2].

Chapter 4
Conclusion

In this paper we have presented a variational-perturbative method to determine selection of Potts state by quantum fluctuations. In some ways, this work can be thought of as an extension to Chubukov's [20] self-consistent perturbation calculation. The variational wavefunction is designed so as to resemble the wavefunction given by second-order perturbation. The major difference is that the basis functions we use are localized 3-magnon spin excitations. This allows us to write the variational energy in the form of an effective Ising Hamiltonian, at the price of some additional approximations. We found that this Ising Hamiltonian has antiferromagnetic coupling for the nearest neighbors, and the selected Potts state is found to be the "$\sqrt{3} \times \sqrt{3}$" state. (This numerical result is displayed in Eq.(3.65) in Section[3.9.1].) This is consistent with widespread expectation.

We find that the approximate variational energy (Eq.(3.58) in Section[3.7]) that we have calculated does not have a minimum as a function of J_3. Since we believe that there should be a minimum for the exact variational energy (as indicated by Chubukov's work), we attributed the lack of minimum here to the breakdown of our perturbation theory near the optimal J_3 obtained by an exact variational calculation. This breakdown of our perturbation theory may also have implications on the accuracy of Chubukov's result. The only way to confirm these speculations would be to examine carefully the fluctuation magnitudes given in Chubukov's calculation near his self-consistent solution. A more thorough diagrammatic perturbation calculation would also be needed– one that renormalize the spinwave spectrum at *all* frequencies, not just the

Goldstone modes. Furthermore, it may be necessary to extend the perturbation series beyond second order.

While the inaccuracy of our perturbation theory seriously affect the variational energy minimization, they may not affect the selection result. The reason for this is that selection depends only on the signs of the Ising coupling constants. We find that the signs are constant over a wide range of the variational parameter J_3. Even though the absolute magnitude of the energy may be indeterminate, the sign of the energy differences between Potts states is better determined.

What may indeed affect our selection results is the insufficient generality of our variational wavefunction, not the subsequent perturbative estimate of the variational energy. We have discussed this issue in Section[3.10.2]. In writing the gaussian part of the wavefunction, we have not included non-zero mean spin-deviations $\langle \sigma_{ix} \rangle$ as variational parameters. While this would not affect the selection between the "$q = 0$" and "$\sqrt{3} \times \sqrt{3}$" states, it may affect the selection energies of the non-symmetric Potts states.

We also have to consider the effects of using an alternative form of $\tilde{\mathcal{H}}$, such as one based on an expansion around the "$\sqrt{3} \times \sqrt{3}$" state. (Our current expansion is around "$q = 0$" state.) Expansion around the "$\sqrt{3} \times \sqrt{3}$" state may cause the Ising coupling constants to have the opposite signs, possibly changing the selection results.

Finally, there is also the question of whether the localized excited states are sufficient for our selection purpose[17]. It is conceivable that non-local terms of

[17] We emphasize that including non-local excited states will not cure our problem of the lack of energy minimum. Their effects are too small to affect this.

the form $\{\tilde{\mathcal{H}}\mathcal{Q}_\alpha|\Psi_0\rangle|\alpha = 1,\ldots,N_\alpha\}$ will also contribute to the selection energy. The likely effect of this contribution is to modify the numerical magnitudes of the $\mathcal{J}_{\alpha\beta}$'s. Whether this will affect the selection result has to be clarified by future work.

We have considered in this work only zero point fluctuations about a classical ground state in the kagomé system. These are usually regarded as small amplitude motions. There is another effect, that of quantum tunneling, which involves a large change in configuration, that we have not considered. Zero point fluctuations create an effective coplanar potential where the different minima, of different energies, correspond to different Potts states. If the system can easily tunnel from one such minima to another, than the in-plane selection that we and others have predicted will be irrelevant. The effect of quantum tunneling is to ultimately destroy in-plane order when the tunneling amplitude is large enough (as it would be if S is not large enough). Von Delft and Henley[25] estimated the effect of quantum tunneling on one hexagon of spins in the "$\sqrt{3}\times\sqrt{3}$" state, assuming that the surrounding spins remain fixed and approximating effects of interactions of these spins by a "coplanarity" effective potential. They found that the tunneling splitting is proportional to $\exp[-c\sqrt{S}]$, where c is a positive constant. Thus for large S, tunneling between a pair of coplanar states is very small. However, as Shender and Holdsworth [7] pointed out, this may be compensated by the large number of states to which one particular coplanar state can tunnel. A more complete tunneling calculation involving all the spins in the system is called for.

Finally, one can ask whether our calculation has any relevance to the experimental results on SCGO(x) [21,22,23]. Unfortunately, the answer is probably no. As Shender *et al*[6] have shown, 2% vacancies on the kagomé system is

sufficient to remove all spin coplanarity almost completely. The experimental system contains 10% to 20% substitutional impurities[22]. This disorder is probably the main reason why neutron scattering experiments show only short-range order (limited to a few lattice spacings) in the spin orientations. Furthermore, our calculations are valid only in the limit $S \to \infty$. For small S, there are terms with subdominant powers of S which may be important. Since the Cr^{3+} ions in SCGO(x) has only $S = 3/2$, it may be wrong to ignore the subdominant terms. Thus, in order to test the various theoretical calculations, it is necessary to prepare materials of higher purity, and perhaps larger S.

Appendix A
Why a Gaussian Ψ is Inadequate

In this Appendix, we show that a wavefunction gaussian in spin deviations, even when a non-zero mean is allowed, cannot in principle discriminate the energy between the "q=0" and "$\sqrt{3} \times \sqrt{3}$" states. Therefore it is inadequate for our selection purposes. This conclusion leads us to consider a non-gaussian wavefunction in Section[3.2].

A Gaussian wavefunction Ψ_0 that centers at $\sigma_{ix} = 0$ and $\sigma_{iy} = 0$ will give $\langle \mathcal{H}_3 \rangle_0 = 0$, since $\mathcal{H}_3$ is an odd function of the spin deviation operators. Hence this wavefunction will produce no in-plane selection effect. Furthermore, even if we widen the class of Gaussian wavefunctions to include[18] those where $\langle \sigma_{ix} \rangle_0 \neq 0$, the requirement[19] that the wavefunction should have all the symmetries of the Potts state (or equivalently, the spinwave Hamiltonian) in question will nevertheless force all $\langle \sigma_{ix} \rangle_0$ to be zero for both "$q = 0$" and "$\sqrt{3} \times \sqrt{3}$" ground states[20], precluding any energy difference due to $\langle \sigma_{ix} \rangle_0$ terms betweem them. We can demonstrate this as follows.

First, we show that for the "$q = 0$" and "$\sqrt{3} \times \sqrt{3}$" states, any spin can be mapped onto any other spin by symmetry operations; and therefore all of the spins should have the same $\langle \sigma_x \rangle_0$. Consider a triangle in one of the

[18] Recall that σ_y is a deviation out of the spin plane, and σ_x is a deviation within the spin plane. Using our local coordinate axes in Eq.(3.1), σ_x is essentially an angle of rotation within the spin plane.

[19] This requirement is based on the assumption that the symmetry of the Potts state is not broken when fluctuations are introduced. To explore the possibility of such a symmetry-breaking, we would need to construct a variational wavefunction which allows for this possibility. Here we merely wish to demonstrate that *if* the quantum ground states of the two symmetric Potts states preserve the symmetry of their Potts configurations, *then* their $\langle \sigma_{ix} \rangle_0$ must be zero.

[20] It is obvious that symmetry requires $\langle \sigma_y \rangle_0 = 0$ for *any* Potts state.

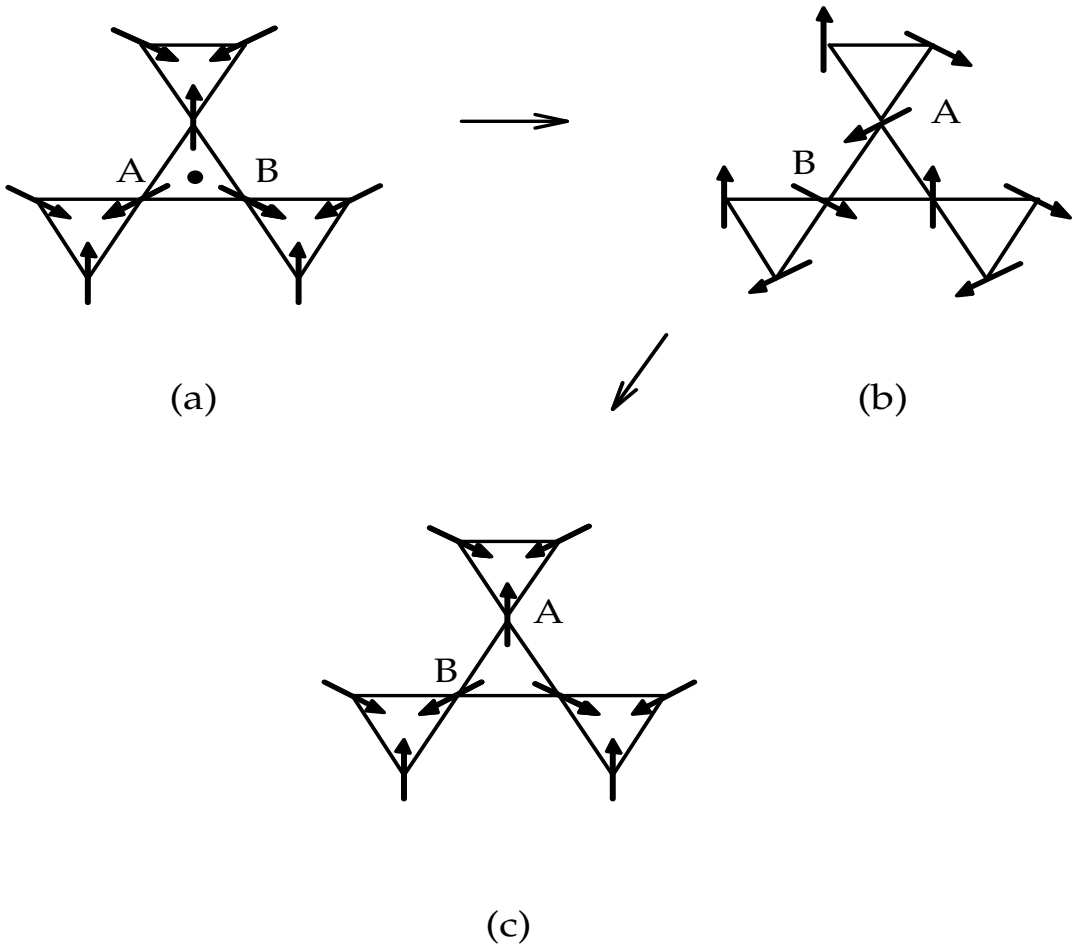

Figure A .1 To show all the spins are equivalent in a symmetric Potts state: they can be mapped onto one another by symmetry operations. We only show the $q = 0$ state because the $\sqrt{3} \times \sqrt{3}$ state follows the same argument. From (a) to (b), we rotate the lattice by 120° clockwise about the center point marked by a dot. From (b) to (c) we rotate the spins in spin space by 120° clockwise. This compound operation leaves the Potts state unchanged, and is therefore a symmetry operation of the spinwave Hamiltonian, since this spinwave Hamiltonian is determined by the Potts state. This operation maps spin B to spin A, and thus they are equivalent. Repeating this process leads to the equivalence of all spins.

symmetric Potts states. (See Figure A .1). Rotate the whole lattice by 120°

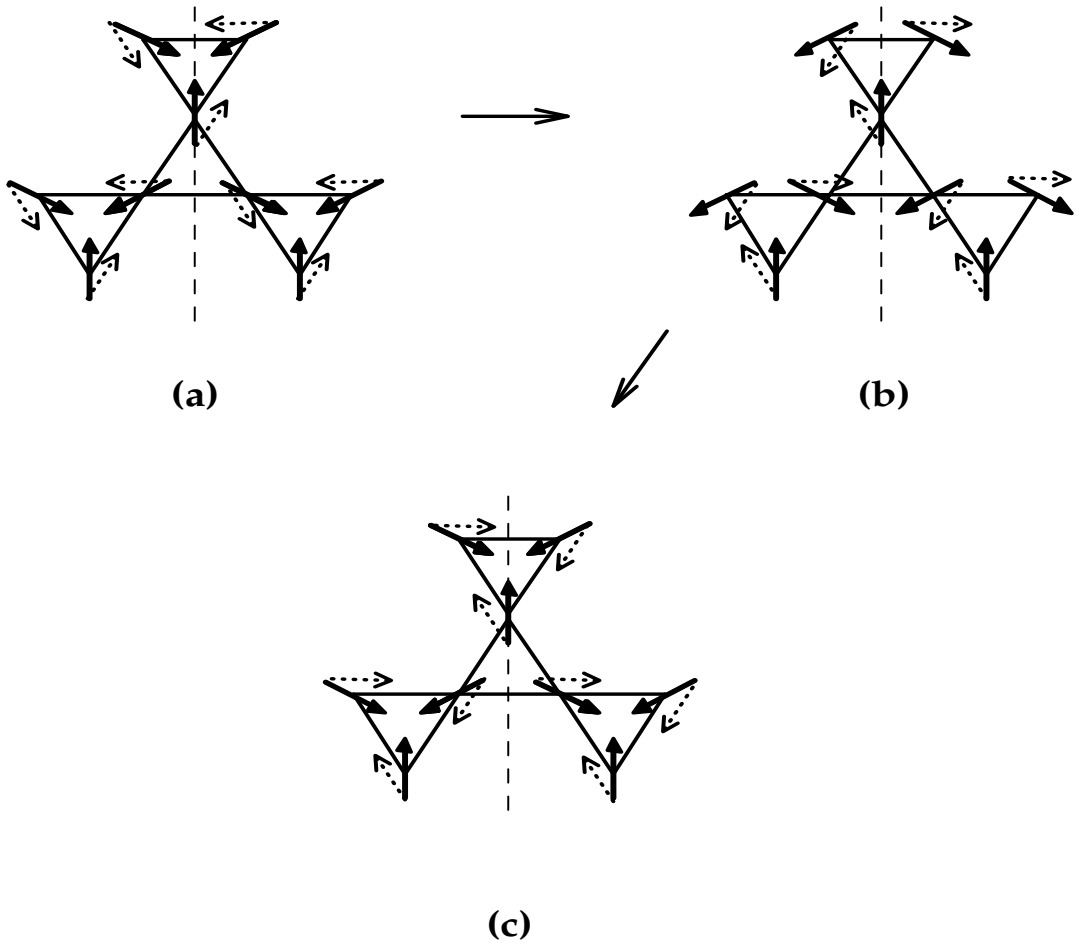

Figure A .2 To show the effect of reflection on a wavefunction with non-zero $\langle\sigma_x\rangle_0$. The solid arrows indicate the spin directions in a "q=0" state. From (a) to (b), we reflect the (solid) spins across the dashed line in real space. From (b) to (c), we reflect the spins across the vertical axis in spin space. This compound operation leaves the Potts state unchanged, and is therefore a symmetry operation of the spinwave Hamiltonian. Now consider adding quantum fluctuations governed by the wavefunction Ψ_0 to the system. Suppose the spins now suffer a uniform rotation $\langle\sigma_x\rangle_0$ under some wavefunction Ψ_0. The dotted arrows indicate the average direction of the spins $\langle\mathbf{S}_i\rangle_0$. Note that applying the compound reflection on the wavefunction changes the direction of the deviation to $-\langle\sigma_x\rangle_0$. This compound reflection is therefore *not* a symmetry of the wavefunction.

clockwise in real space about the center of this triangle, then rotate all the spins by 120° clockwise in spin space. (Note that rotating in spin space by 120° is a discrete symmetry of the Hamiltonian because this preserves the set of chiralities of $\mathcal{H}_3$. Hence even though our spinwave Hamiltonian is truncated at quartic order and does not preserve Goldstone symmetry, this rotation by 120° remains a symmetry.) It is clear that the classical ground state has been mapped onto itself, because both the "$q = 0$" state and the "$\sqrt{3} \times \sqrt{3}$" state have 3-fold symmetry. (This is not true for other disordered or non-symmetric Potts states.) Also, this proves that all the spins in the center triangle are equivalent to each other. Now repeating this operation with other triangles as centers of rotations allows us to map any spin onto any other and therefore shows that all of the spins are equivalent. Since all spins are equivalent, if one of them has a mean deviation $\langle \sigma_{ix} \rangle_0$, all of them must have the same deviation $\langle \sigma_{ix} \rangle_0$.

Second, we want to show that if all the $\langle \sigma_{ix} \rangle_0$ are equal, then they must be zero. Consider again a triangle in one of the symmetric Potts states. Reflect the spins in spin-space about the vertical spin-axis, then reflect the spins in real-space about the same vertical axis (see Figure A .2). Since we have shown previously that all the spins are equivalent, it does not matter which spin we choose to be the vertical spin-axis. Obviously the Potts state has been mapped onto itself: this compound reflection operation is a symmetry of the system. Now consider a Ψ_0 that produces a uniform non-zero $\langle \sigma_x \rangle_0$ on all the spins. Performing the same compound reflection operation on this wavefunction will leave all the spins with a negative deviation, $-\langle \sigma_x \rangle_0$. This means that the wavefunction is *not* invariant with respect to the compound reflection operation.

This contradicts our assumption that Ψ_0 should have all the symmetries of the Potts state. Therefore, $\langle \sigma_{ix} \rangle_0 = 0$.

Appendix B
Renormalized Harmonic Hamiltonian

This Appendix aims to provide some detailed mathematical derivations to supplement the qualitative results in Section[3.3].

In Appendix[B.1] here, we motivate our choice of the renormalized harmonic Hamiltonian $\tilde{\mathcal{H}}$ as written in Eq.(3.23). We show in section[B.2] how the spin fluctuations provided by the gaussian wavefunction can be calculated. The long wavelength behavior of these spin fluctuations is described in Appendix[B.3].

B.1 Definition

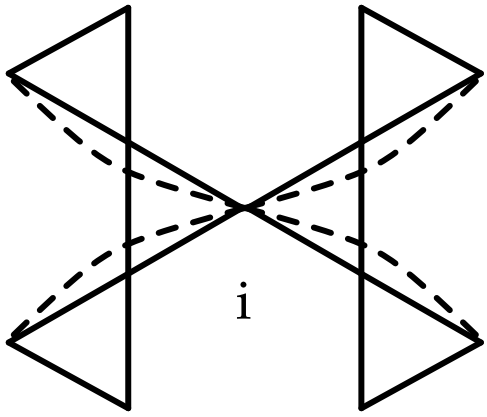

Figure B .1 Dashed curves indicate the couplings J_3 from the center spin i.

We choose our $\tilde{\mathcal{H}}$ to differ as little as possible in form from the "bare" quadratic Hamiltonian $\mathcal{H}_2$. In other words, we want to have as few variational

parameters as possible. But, to obtain finite $\langle\sigma_y^2\rangle_0$ fluctuations, we must remove the zero modes present in the bare $\mathcal{H}_2$. One way to do this is to add a single-ion anisotropic term, $\sim D_y\sigma_y^2$. This has the somewhat undesirable effect of removing the (σ_y) Goldstone modes in Ψ_0 (or equivalently, in $\tilde{\mathcal{H}}$) [21] also.

Next-nearest-neighbor exchange couplings are necessary to simultaneously preserve the Goldstone modes *and* lift the other non-Goldstone zero modes. Here we have a choice of using second nearest-neighbor coupling or third nearest-neighbor coupling. In the following we will use only the third nearest-neighbor coupling, excluding coupling between spins diagonal across a hexagon, in conformity with Harris *et al* [8] and Chubukov's[20] choice (See Figure B .1.) We have checked that choosing the other alternative– second nearest-neighbor coupling– does not affect the stability of the variational energy (i.e. the variational energy still has no minimum. See Section[3.9.2]), nor does it affect the in-plane selection results (Section[3.9.1]). This indifference to whether we use J_2 or J_3 is because the renormalization of the soft modes is sensitive to $J_2 - J_3$ only, as shown in Eq. (2.28a) of Ref.8. (See also the comment on our Figure B 8 .)

Since we are deriving the spinwave Hamiltonian from a Heisenberg Hamiltonian with third neighbor coupling, the form of the spinwave Hamiltonian depends on the Potts state. However, our goal is to choose a $\tilde{\mathcal{H}}$ that has the same form for any Potts state. In principle, we have to expand around the Potts

[21] As we commented in the last paragraph of Section[3.1], Chubukov has shown that Goldstone modes are approximately restored to the truncated spinwave Hamiltonian $\mathcal{H}$ if we include the second-order perturbation of $\mathcal{H}_3$. Hence we desire a variational wavefunction, or a renormalized harmonic Hamiltonian $\tilde{\mathcal{H}}$, which has Goldstone symmetry to leading powers of S. Hopefully, this $\tilde{\mathcal{H}}$ will have a fluctuation spectrum closer to that of $\mathcal{H}$ than a $\tilde{\mathcal{H}}$ without Goldstone modes.

state which results in the lowest variational energy. However, this defeats the purpose of the effective Ising Hamiltonian approach. Hence we simply expand the Heisenberg Hamiltonian around the "$q = 0$" state and use the resulting $\tilde{\mathcal{H}}$ for all other Potts states. (This is equivalent to a restriction of the variational subspace– a familiar if not foolproof procedure. We have remarked in Section[3.10.2] that expanding around the "$\sqrt{3} \times \sqrt{3}$" state might conceivably give a different selection result, but that expanding around the "$q = 0$" state should give the lowest variational energy and is thus the correct choice. In the published version of this paper, we shall include the results of expanding around the "$\sqrt{3} \times \sqrt{3}$" state.)

We can derive this $\tilde{\mathcal{H}}$ in the same way as we derived $\mathcal{H}_2$ in Section[Spinwave Hamiltonian]. We write the third neighbor Hamiltonian as

$$J^* J_3 \sum_{[ij]} \mathbf{S}_i \cdot \mathbf{S}_j. \tag{B1}$$

This is meant to be ferromagnetic, with the dimensionless coupling $J_3 < 0$. Expanding in terms of local axes, keeping in mind that we need only up to quadratic order and assuming the "$q = 0$" state, we get

$$J_3 \sum_{[ij]} S_{ix} S_{jx} + S_{iy} S_{jy} + S_{iz} S_{jz}. \tag{B2}$$

Introducing spin-deviation operators, we finally have

$$\tilde{\mathcal{H}}/J^* = \mathcal{H}_2/J^* + J_3 \sum_{[ij]} -\frac{1}{2}\{(\sigma_{iy} - \sigma_{jy})^2 + (\sigma_{ix} - \sigma_{jx})^2\}. \tag{B3}$$

B.2 Spin-spin correlations

Our next task is to calculate the spin-spin correlations in the gaussian ground state Ψ_0. These are the basic quantities on which all our selection energy formulae (e.g. Eq.(3.58)) depend. The selection energy in Eq.(3.59) is the expectation value of a product of many spin operators taken with respect to the Gaussian Ψ_0 . Clearly we can use Wick's theorem to decompose this into a product of 2-spin correlations such as $\langle\Psi_0|\sigma_{ix}\sigma_{jx}|\Psi_0\rangle$. (This is a very tedious operation when we have a product of many operators, but we can do this using a symbolic manipulation program described in Appendix[I].) Hence we need a method here to obtain such correlations from $\tilde{\mathcal{H}}$. We do this by first diagonalizing $\tilde{\mathcal{H}}$ via the equation of motion approach, *i.e.* $\dot{\sigma}_i = \frac{i}{\hbar}[\tilde{\mathcal{H}}, \sigma_i]$. (We denote a time derivative by a overline dot.) The Heisenberg equations of motion for the spin operators are the following:

$$\begin{aligned}
\dot{\sigma}_{ix} &= \frac{|J^*|S}{\hbar}[2\sigma_{iy} + \sum_{\langle j\rangle_i}\sigma_{jy} + J_3(-4\sigma_{iy} + \sum_{[j]_i}\sigma_{jy})], \\
\dot{\sigma}_{iy} &= -\frac{|J^*|S}{\hbar}[2\sigma_{ix} - \frac{1}{2}\sum_{\langle j\rangle_i}\sigma_{jx} + J_3(-4\sigma_{ix} + \sum_{[j]_i}\sigma_{jx})],
\end{aligned} \tag{B4}$$

where the notation $\langle j\rangle_i$ means summing over all j that are nearest neighbors of i. We need to Fourier-transform to $\mathbf{k}$-space. So define (with $\mathbf{r}_i$ indicating the position vector of the i^{th} spin)

$$\begin{aligned}
\sigma_s(\mathbf{k})_x &= \sum_{i\in s} e^{-i\mathbf{k}\cdot\mathbf{r}_i}\sigma_{ix}, \\
\sigma_s(\mathbf{k})_y &= \sum_{i\in s} e^{i\mathbf{k}\cdot\mathbf{r}_i}\sigma_{iy}.
\end{aligned} \tag{B5}$$

The s here is an index of the three triangular superlattices. The $\sigma_s(\mathbf{k})$'s obey the commutation relations

$$[\sigma_s(\mathbf{k})_x, \sigma_{s'}(\mathbf{k}')_y] = iSN\delta_{\mathbf{k}\mathbf{k}'}\delta_{ss'}, \tag{B6}$$

where N is the number of primitive cells of the triangular lattice.

In reciprocal space the equations of motion become

$$\dot{\sigma}_s(-\mathbf{k})_x = \frac{J^*S}{\hbar}\sum_{s'=1}^{3}\mathcal{M}^{-1}_{ss'}(\mathbf{k})\sigma_{s'}(\mathbf{k})_y,$$
$$\dot{\sigma}_s(-\mathbf{k})_y = -\frac{J^*S}{\hbar}\sum_{s'=1}^{3}\mathcal{K}_{ss'}(\mathbf{k})\sigma_{s'}(\mathbf{k})_x, \tag{B7}$$

where

$$\mathcal{K}(\mathbf{k}) = \begin{pmatrix} d_1(\mathbf{k}) & -\frac{1}{2}(1+e^{-i\mathbf{k}\cdot\mathbf{a}_2}) & -\frac{1}{2}(1+e^{-i\mathbf{k}\cdot\mathbf{a}_1}) \\ -\frac{1}{2}(1+e^{i\mathbf{k}\cdot\mathbf{a}_2}) & d_2(\mathbf{k}) & -\frac{1}{2}(1+e^{i\mathbf{k}\cdot(\mathbf{a}_2-\mathbf{a}_1)}) \\ -\frac{1}{2}(1+e^{i\mathbf{k}\cdot\mathbf{a}_1}) & -\frac{1}{2}(1+e^{-i\mathbf{k}\cdot(\mathbf{a}_2-\mathbf{a}_1)}) & d_3(\mathbf{k}) \end{pmatrix},$$

$$\mathcal{M}^{-1}(-\mathbf{k}) = \begin{pmatrix} d_1(\mathbf{k}) & 1+e^{-i\mathbf{k}\cdot\mathbf{a}_2} & 1+e^{-i\mathbf{k}\cdot\mathbf{a}_1}) \\ 1+e^{i\mathbf{k}\cdot\mathbf{a}_2} & d_2(\mathbf{k}) & 1+e^{i\mathbf{k}\cdot(\mathbf{a}_2-\mathbf{a}_1)} \\ 1+e^{i\mathbf{k}\cdot\mathbf{a}_1} & 1+e^{-i\mathbf{k}\cdot(\mathbf{a}_2-\mathbf{a}_1)} & d_3(\mathbf{k}) \end{pmatrix}, \tag{B8}$$

with

$$d_1(\mathbf{k}) \equiv 2 + J_3\{-4 + 2[\cos(\mathbf{k}\cdot\mathbf{a}_1) + \cos(\mathbf{k}\cdot\mathbf{a}_2)]\}$$
$$d_2(\mathbf{k}) \equiv 2 + J_3\{-4 + 2[\cos(\mathbf{k}\cdot(\mathbf{a}_1-\mathbf{a}_2) + \cos(\mathbf{k}\cdot\mathbf{a}_2)]\}$$
$$d_3(\mathbf{k}) \equiv 2 + J_3\{-4 + 2[\cos(\mathbf{k}\cdot\mathbf{a}_1) + \cos(\mathbf{k}\cdot(\mathbf{a}_1-\mathbf{a}_2))]\}. \tag{B9}$$

The $\mathbf{a}_1$ and $\mathbf{a}_2$ are the primitive vectors of the triangular superlattice as defined in Figure B .2. The notation used is designed to resemble the spring constant $\mathcal{K}$ and mass $\mathcal{M}$ of a one-dimensional harmonic oscillator. Since J_3 couples spins within the same sublattice, it only appears in the diagonal matrix elements.

The Hamiltonian in reciprocal space can be written

$$\tilde{\mathcal{H}} = \frac{J^*}{N}\sum_{\mathbf{k}}(\frac{1}{2}\sigma_s(-\mathbf{k})_x\mathcal{K}_{ss'}(\mathbf{k})\sigma_{s'}(\mathbf{k})_x + \frac{1}{2}\sigma_s(-\mathbf{k})_y\mathcal{M}^{-1}_{ss'}(\mathbf{k})\sigma_{s'}(\mathbf{k})_y). \tag{B10}$$

Now we may diagonalize $\tilde{\mathcal{H}}$ by first finding the transformation matrix that diagonalize $\mathcal{K}$ and $\mathcal{M}^{-1}$. In the limit of $J_3 \to 0$ (all our applications are in this limit), it can be shown that $\mathcal{K}(\mathbf{k})$ and $\mathcal{M}^{-1}(-\mathbf{k})$ commute and that if $T(\mathbf{k})$ diagonalizes $\mathcal{K}(\mathbf{k})$, then the same $T(\mathbf{k})$ diagonalizes $\mathcal{M}^{-1}(-\mathbf{k})$,

$$\begin{aligned} T^{\dagger}(\mathbf{k})\mathcal{K}(\mathbf{k})T(\mathbf{k}) &= \mathcal{K}^{(p)}(\mathbf{k}), \\ T^{\dagger}(\mathbf{k})\mathcal{M}^{-1}(-\mathbf{k})T(\mathbf{k}) &= \mathcal{M}^{(p)-1}(-\mathbf{k}), \end{aligned} \tag{B11}$$

where $\mathcal{K}^{(p)}$ and $\mathcal{M}^{(p)-1}$ are diagonal. Hence we can define the spin deviation operators in the eigenbasis (indexed by "p") via

$$\begin{aligned} \sigma_s(\mathbf{k})_x &= \sum_{p=1}^{3} T_{sp}(\mathbf{k})\sigma^{(p)}(\mathbf{k})_x, \\ \sigma_s(\mathbf{k})_y &= \sum_{p=1}^{3} T_{sp}(-\mathbf{k})\sigma^{(p)}(\mathbf{k})_y. \end{aligned} \tag{B12}$$

(If J_3 is not nearly zero, diagonalization of $\tilde{\mathcal{H}}$ is much more cumbersome. See Ref. 1 for a method.)

In all our numerical calculations, we need real-space spin operators which include only the soft or the ordinary modes, but not both. That is, we would like to define some *projected* spin operators which are the original spin operators σ_x and σ_y projected into the soft ($p = 1$) or ordinary ($p = 2$ and $p = 3$) eigenspaces. We can define these operators by setting the appropriate $\sigma^{(p)}$'s in Eq.(B 12) to zero. For $\sigma^{(s)}$ ("(s)" here means "soft", as distinct from the site index subscript s in Eq.(B 12)), we set the two ordinary modes ($p = 2, 3$) to zero. For $\sigma^{(o)}$, we set the one unique soft mode ($p = 1$) to zero. Thus for either x or y operators,

$$\begin{aligned} \sigma_s^{(s)} &= T_{s1}\sigma^{(p=1)} \\ \sigma_s^{(o)} &= T_{s2}\sigma^{(p=2)} + T_{s3}\sigma^{(p=3)}, \end{aligned} \tag{B13}$$

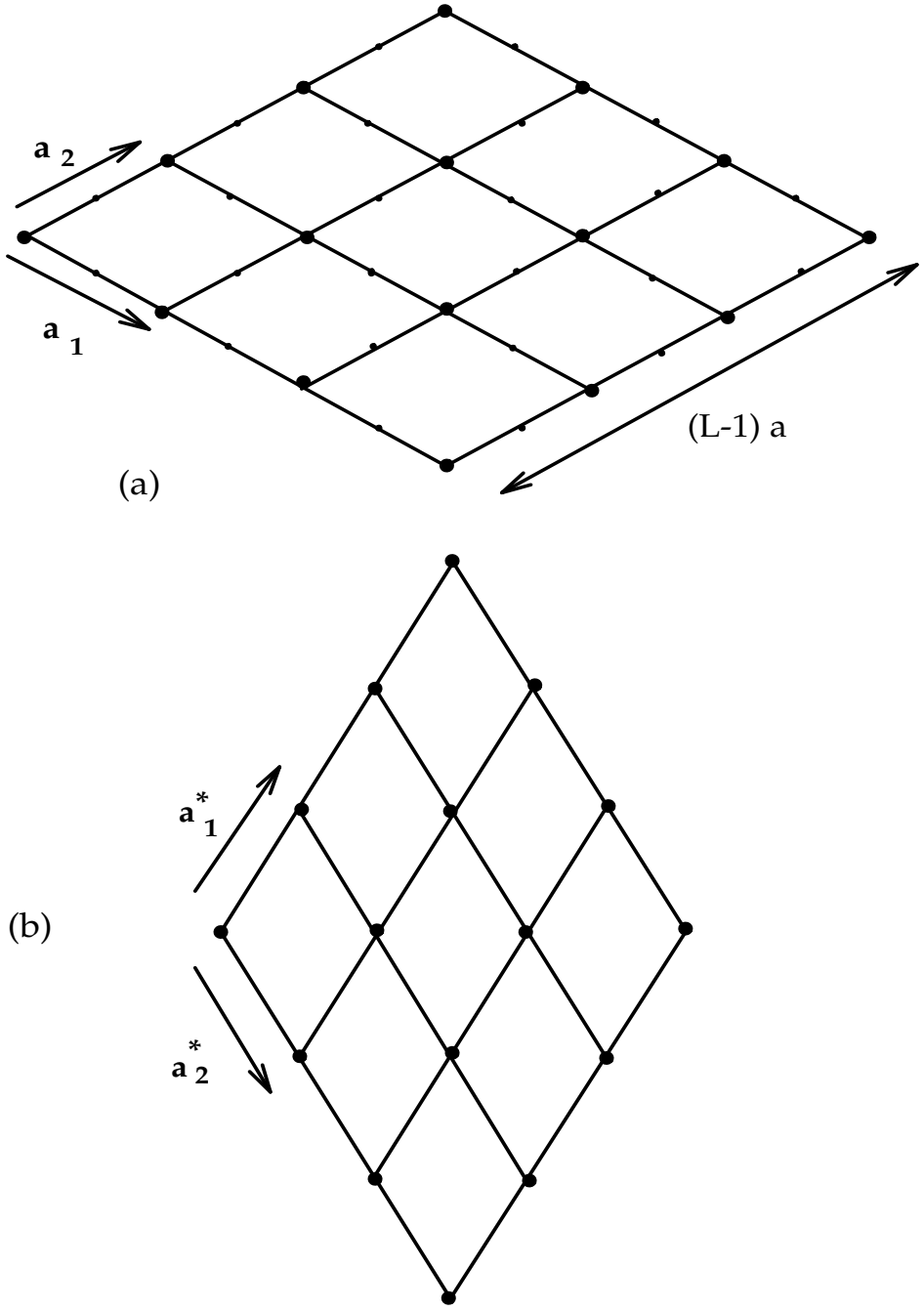

Figure B .2 The shape of the direct (a) and reciprocal (b) lattices that we use in our numerical computation. There are $3L \times L$ lattice points in (a). The big dots are the Bravais lattice points, whereas the small dots are the sublattice sites. $\mathbf{a}_1$ and $\mathbf{a}_2$ are the primitive lattice vectors for the direct lattice, and $\mathbf{a}_1^*$ and $\mathbf{a}_2^*$ are the corresponding ones for the reciprocal lattice.

and we get back the original σ if we add them:

$$\sigma_s = \sigma_s^{(s)} + \sigma_s^{(o)}. \tag{B14}$$

In all operators composed of products and sums of these σ's, we adopt the superscript notation (s) and (o) such that only the corresponding σ operators are used.

Now the Hamiltonian is diagonal in $\mathbf{k}$ and p,

$$\tilde{\mathcal{H}} = \frac{J^*}{N}\sum_{\mathbf{k},p}(\frac{1}{2}\mathcal{K}^{(p)}(\mathbf{k})\sigma^{(p)}(-\mathbf{k})_x\sigma^{(p)}(\mathbf{k})_x + \frac{1}{2}\mathcal{M}^{(p)-1}(\mathbf{k})\sigma^{(p)}(-\mathbf{k})_y\sigma^{(p)}(\mathbf{k})_y). \tag{B15}$$

The ultimate goal is to make this Hamiltonian diagonal in the magnon-number operator. A Bogoliubov transformation will now take us there,

$$\begin{aligned}\sigma^{(p)}(\mathbf{k})_x &= \sqrt{\frac{SN}{2\sqrt{\mathcal{K}^{(p)}\mathcal{M}^{(p)}}}}(A^\dagger_{-\mathbf{k},p} + A_{\mathbf{k},p}),\\ \sigma^{(p)}(\mathbf{k})_y &= i\sqrt{\frac{SN\sqrt{\mathcal{K}^{(p)}\mathcal{M}^{(p)}}}{2}}(A^\dagger_{\mathbf{k},p} - A_{-\mathbf{k},p}).\end{aligned} \tag{B16}$$

The creation and annihilation operators obey the commutation relations

$$[A_{\mathbf{k},p}, A^\dagger_{\mathbf{k}',p'}] = \delta_{\mathbf{k},\mathbf{k}'}\delta_{p,p'}. \tag{B17}$$

The Hamiltonian is finally diagonal,

$$\tilde{\mathcal{H}} = \sum_{\mathbf{k}}\hbar\omega^{(p)}_{\mathbf{k}}(A^\dagger_{\mathbf{k},p}A_{\mathbf{k},p} + \frac{1}{2}), \tag{B18}$$

where the eigenfrequencies are

$$\omega^{(p)}_{\mathbf{k}} = \frac{J^*S}{\hbar}\sqrt{\mathcal{M}^{(p)-1}(\mathbf{k})\mathcal{K}^{(p)}(\mathbf{k})}. \tag{B19}$$

To obtain the fluctuations, we make use of Eq.(B 16) and the fact that $\langle A_{\mathbf{k},p}A^\dagger_{\mathbf{k},p}\rangle_0 = 1$. Thus

$$\langle\sigma^{(p)}(\mathbf{k})_x\sigma^{(p)}(-\mathbf{k})_x\rangle_0 = \frac{SN}{2}\sqrt{\frac{\mathcal{M}^{(p)-1}(\mathbf{k})}{\mathcal{K}^{(p)}(\mathbf{k})}},$$

$$\langle\sigma^{(p)}(\mathbf{k})_x\sigma^{(p)}(\mathbf{k})_y\rangle_0 = -\langle\sigma^{(p)}(\mathbf{k})_y\sigma^{(p)}(\mathbf{k})_x\rangle_0 = i\frac{SN}{2}\,,$$
$$\langle\sigma^{(p)}(\mathbf{k})_y\sigma^{(p)}(-\mathbf{k})_y\rangle_0 = \frac{SN}{2}\sqrt{\frac{\mathcal{K}^{(p)}(\mathbf{k})}{\mathcal{M}^{(p)-1}(\mathbf{k})}}\,. \qquad \text{(B20)}$$

The real space correlations $\langle\sigma^{(m)}_{ix}\sigma^{(m)}_{jx}\rangle_0$, $\langle\sigma^{(m)}_{iy}\sigma^{(m)}_{jy}\rangle_0$ and $\langle\sigma^{(m)}_{ix}\sigma^{(m)}_{jy}\rangle_0$ can be obtained by summing these $\mathbf{k}$-space correlation functions in Eq.(B 20) over the Brillouin zone via Eq.(B 5) and Eq.(B 12),

$$\begin{aligned}
\langle\sigma^{(m)}_{ix}\sigma^{(m)}_{jx}\rangle_0 &= \frac{1}{N^2}\sum_{\mathbf{k}} e^{i\mathbf{k}\cdot(\mathbf{r}_i-\mathbf{r}_j)}\langle\sigma^{(m)}_{s_i}(\mathbf{k})_x\sigma^{(m)}_{s_j}(-\mathbf{k})_x\rangle_0,\\
\langle\sigma^{(m)}_{ix}\sigma^{(m)}_{jy}\rangle_0 &= -\langle\sigma^{(m)}_{jy}\sigma^{(m)}_{ix}\rangle_0\\
&= \frac{1}{N^2}\sum_{\mathbf{k}} e^{i\mathbf{k}\cdot(\mathbf{r}_i-\mathbf{r}_j)}\langle\sigma^{(m)}_{s_i}(\mathbf{k})_x\sigma^{(m)}_{s_j}(\mathbf{k})_y\rangle_0,\\
\langle\sigma^{(m)}_{iy}\sigma^{(m)}_{jy}\rangle_0 &= \frac{1}{N^2}\sum_{\mathbf{k}} e^{-i\mathbf{k}\cdot(\mathbf{r}_i-\mathbf{r}_j)}\langle\sigma^{(m)}_{s_i}(\mathbf{k})_y\sigma^{(m)}_{s_j}(-\mathbf{k})_y\rangle_0. \qquad \text{(B21)}
\end{aligned}$$

The shape of first Brillouin zone that is used in the k-sum is of course arbitrary, as long as the number of $\mathbf{k}$-points used is equal to N and the total area is equal to $\frac{\sqrt{3}}{2}a^{*2}$, where $a^* = \frac{2\pi}{\sqrt{3}a}$ is the lattice constant of the reciprocal lattice, and $2a$ that of the real-space triangular Bravais lattice[22] However, since we desire the real space supercell to be fairly regular in shape (with periodic boundary conditions) for ease of future calculations, the distribution of k-points and the shape of the first Brillouin zone must be chosen correspondingly. The easiest shape to compute is a rhombus with the real space points given by $\mathbf{r}_{n_1n_2} = n_1\mathbf{a}_1 + n_2\mathbf{a}_2$, $n_1, n_2 = 0, 1, ..., L-1$, where $L = \sqrt{N}$. In

[22] We distinguish among 3 different real space lattices: 1) the kagomé latttice, with lattice constant a; 2) the triangular Bravais lattice, with lattice constant $2a$ and 3 spins in a primitive unit cell; 3) the magnetic Bravais lattice, which Zeng and Elser [15] and Harris *et al* [8] used. For the "$\sqrt{3}\times\sqrt{3}$" state, there are 9 spins in a magnetic primitive unit cell. Our reciprocal lattice is reciprocal to (2). We have no need of (3) because our spinwave Hamiltonian Eq.(3.7) is defined with respect to local coordinate axes, as emphasized in Section[3.1]. Therefore, our magnetic primitive unit cell is always identical to the atomic primitive unit cell, for *any* Potts state.

Cartesian coordinates, $\mathbf{a}_1 = 2a(\frac{\sqrt{3}}{2}, -\frac{1}{2})$ and $\mathbf{a}_2 = 2a(\frac{\sqrt{3}}{2}, \frac{1}{2})$. The corresponding first Brillouin zone also has the shape of the rhombus, with k-points given by $\mathbf{k}_{m_1 m_2} = \frac{m_1}{\sqrt{N}}\mathbf{a}_1^* + \frac{m_2}{\sqrt{N}}\mathbf{a}_2^*$, $m_1, m_2 = 0, 1, ..., \sqrt{N} - 1$, where $\mathbf{a}_1^*$ and $\mathbf{a}_2^*$ are the primitive vectors of the reciprocal lattice dual to $\mathbf{a}_1$ and $\mathbf{a}_2$. In Cartesian coordinates, they are $\mathbf{a}_1^* = a^*(\frac{1}{2}, \frac{\sqrt{3}}{2})$ and $\mathbf{a}_2^* = a^*(\frac{1}{2}, -\frac{\sqrt{3}}{2})$.

(Note that although the rhombic shape is easy to handle if we use periodic boundary condition, and well-suited for fast-Fourier transform, it lacks the full spatial 6-fold and the reflection symmetry of the kagomé lattice. This lack of symmetry entails a lot of redundant summation both in the reciprocal space and in real space. A hexagonal first Brillouin zone would be the most efficient for summing, but it is difficult to encode periodic boundary conditions for the real lattice.)

B.3 Qualitative Properties of Spin-spin Correlations

Since our later calculations depend crucially on these real-space correlation functions, it is useful to understand their spatial dependence.

The spin-spin correlations for short distances are calculated numerically for different S and J_3 and plotted in Figures B.4 and B.5 . Note that after scaling by the powers of S as predicted in Section[3.3], the magnitudes of these correlations are independent of J_3 for small $|J_3|$. This observation serves as an important justification for our effective Hamiltonian treatment in Section[3.7].

To gain understanding of correlations between spins which are far apart, one need to resort to some coarse-grained summations. For each polarization

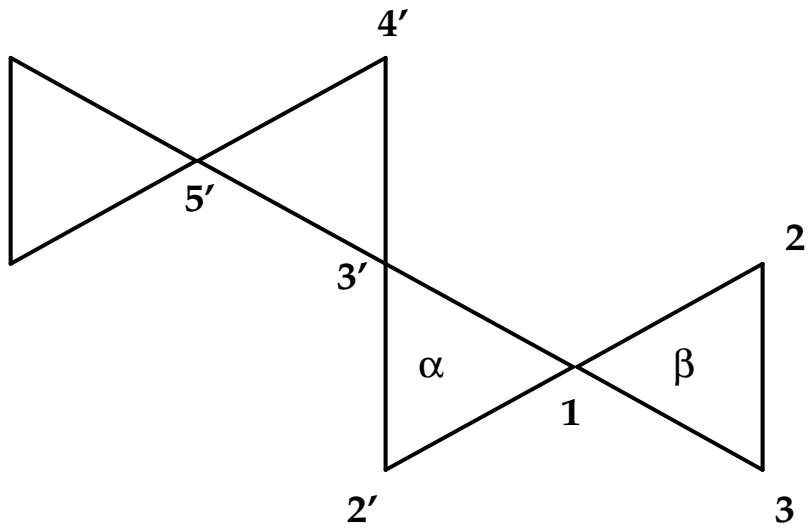

Figure B .3 The labelling of sites.

(p), we approximate the discrete sum in Eq.(B 21) as integrals:

$$\langle \sigma_x^{(p)}(\mathbf{0})\sigma_x^{(p)}(\mathbf{r})\rangle_0 \sim \int_{-\Lambda}^{\Lambda}\int_{-\Lambda}^{\Lambda} e^{-i\mathbf{k}\cdot\mathbf{r}}\langle \sigma_x(\mathbf{k})^{(p)2}\rangle_0 \mathrm{d}\mathbf{k},$$
$$\langle \sigma_y^{(p)}(\mathbf{0})\sigma_y^{(p)}(\mathbf{r})\rangle_0 \sim \int_{-\Lambda}^{\Lambda}\int_{-\Lambda}^{\Lambda} e^{i\mathbf{k}\cdot\mathbf{r}}\langle \sigma_y(\mathbf{k})^{(p)2}\rangle_0 \mathrm{d}\mathbf{k}, \qquad \text{(B22)}$$

where $\Lambda \sim a^*/2$ is approximately the half-width of the Brillouin zone.

The $\langle \sigma_x(\mathbf{k})^{(p)2}\rangle_0$ and $\langle \sigma_y(\mathbf{k})^{(p)2}\rangle_0$ are related to the quantities $\mathcal{K}^{(p)}$ and $\mathcal{M}^{(p)}$ through Eq.(B 20). For large $|\mathbf{r}|$, these integrals are dominated by the behavior of the integrands at $\mathbf{k} \sim \mathbf{0}$, assuming[23] that there are no singularities at other values of $\mathbf{k}$. (The integrals pick up very little contributions from the non-singular region of the integrand because of rapid oscillations of $e^{i\mathbf{k}\cdot\mathbf{r}}$.) The small-$\mathbf{k}$ behavior of $\mathcal{K}^{(p)}$ and $\mathcal{M}^{(p)}$ can be obtained by analytically diagonalizing the $\mathcal{K}$ and $\mathcal{M}$ matrices in Eq.(B 8) after Taylor-expanding them around $\mathbf{k} = \mathbf{0}$.

[23] Since we are implicitly assuming a "q=0" state in constructing $\tilde{\mathcal{H}}$, there are indeed no singularities in the integrands anywhere but $\mathbf{k} = \mathbf{0}$. See related comments in Section[B.1].

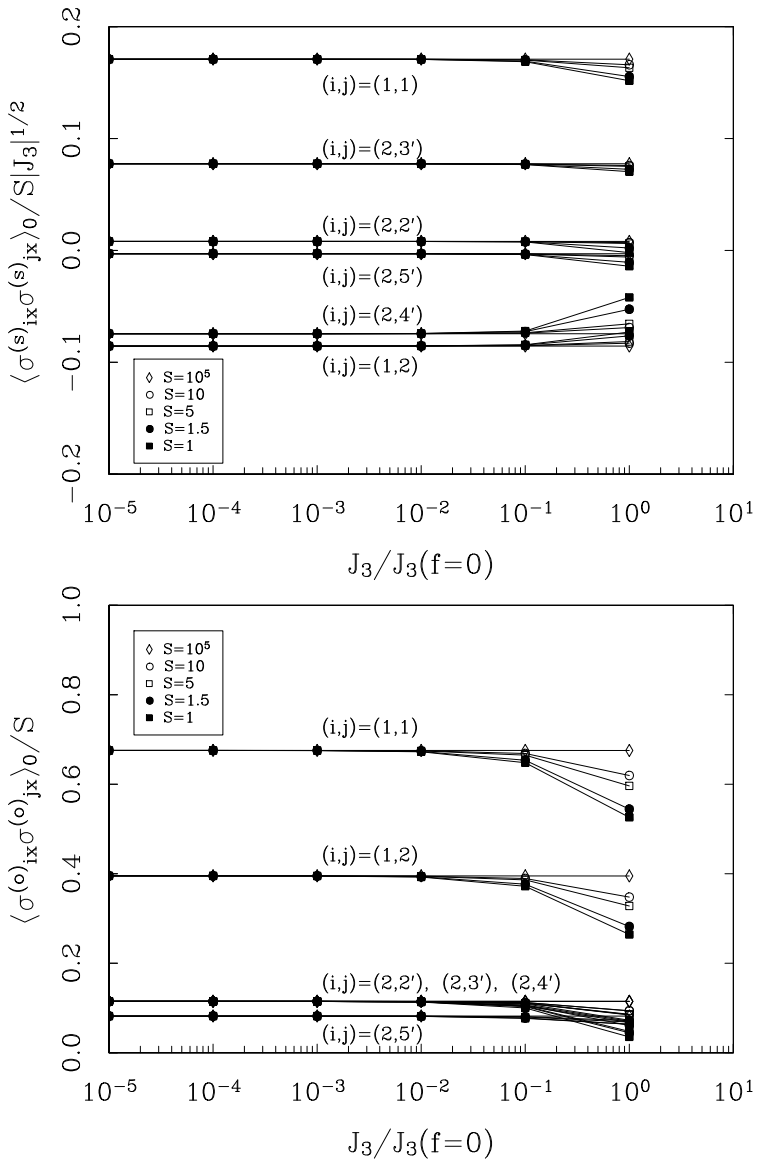

Figure B .4 $\langle\sigma^{(m)}_{ix}\sigma^{(m)}_{jx}\rangle_0$ as function of J_3 for a $L = 16$ system. J_3 is written here as sub-multiples of $J_3(f = 0)$ which minimizes the variational energy with the $\mathcal{H}_3$ term set to zero.(See Eq.(3.75).) The values of $J_3(f = 0)$ for various S are listed in Table 3.4. The top figure is for the soft modes while the bottom one is for the ordinary modes. All the soft correlations scale with $S|J_3|^{1/2}$ for large S or small $|J_3|$, while all the ordinary correlations scale with S in the same regime. The numbering scheme for the spins are depicted in Figure B .3, and the y-intercepts are listed in Table B .1.

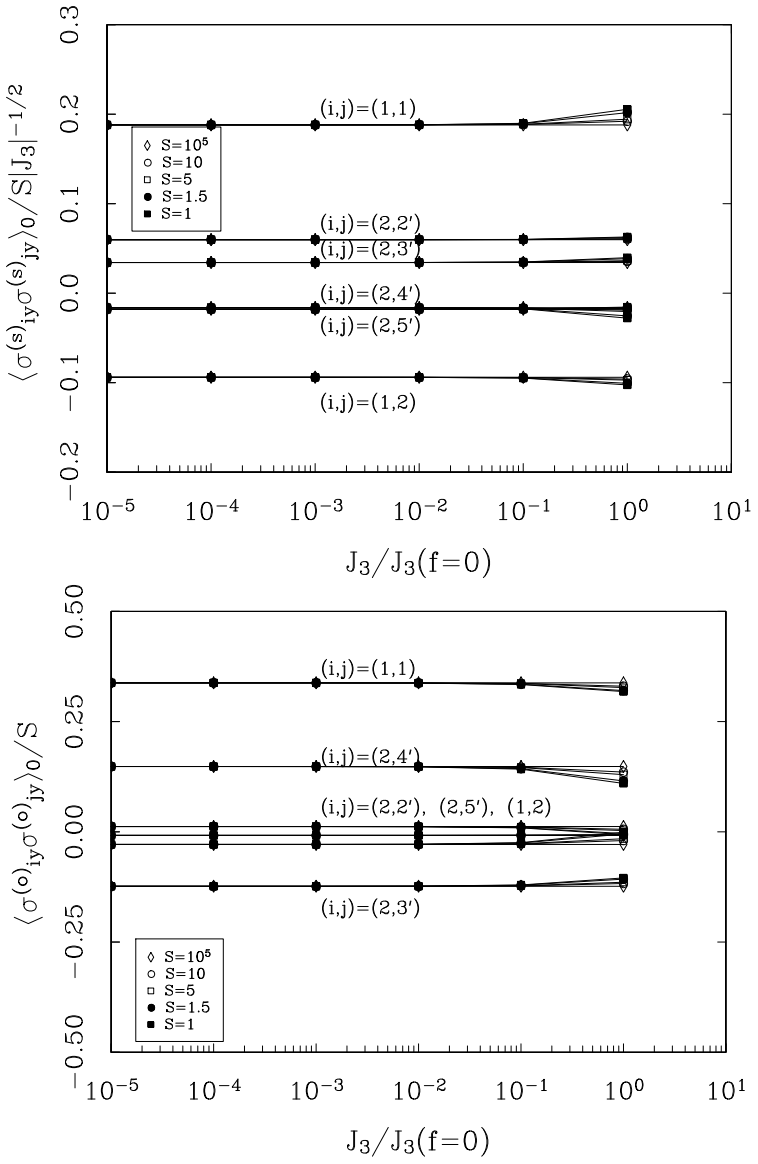

Figure B .5 $\langle\sigma^{(m)}_{iy}\sigma^{(m)}_{jy}\rangle_0$ as function of J_3 for a $L = 16$ system, similar to Figure B .4. The top figure is for the soft modes while the bottom one is for the ordinary modes. All the soft correlations scale with $S|J_3|^{-1/2}$ for large S or small $|J_3|$, while all the ordinary correlations scale with S in the same regime. The y-intercepts are listed in Table B .1.

Table B .1 Scaling of $\langle\sigma_{ix}^{(m)}\sigma_{jx}^{(m)}\rangle_0$, $\langle\sigma_{iy}^{(m)}\sigma_{jy}^{(m)}\rangle_0$, and $\langle\sigma_{ix}^{(s)}\sigma_{jy}^{(s)}\rangle_0$ with J_3 and S. The numbers quoted are for a $L = 16$ lattice, with $S = 10^5$ and $J_3 = 10^{-5}J_3(f = 0)$. The data here are derived from the y-intercepts of Figure B.4 and Figure B.5 .

Spin-spin Correlation	Scaling with S and J_3	Numerical Prefactor ($\times 10^{-1}$) for Spin Pairs (i,j) (1,1)	(1,2)	(2,3')	(2,2')	(2,4')	(2,5')
$\langle\sigma_{ix}^{(s)}\sigma_{jx}^{(s)}\rangle_0$	$S\|J_3\|^{1/2}$	1.71	-0.8549	0.7745	0.08043	-0.745	-0.02948
$\langle\sigma_{ix}^{(o)}\sigma_{jx}^{(o)}\rangle_0$	S	6.755	3.951	1.147	1.147	1.147	0.8187
$\langle\sigma_{iy}^{(s)}\sigma_{jy}^{(s)}\rangle_0$	$S\|J_3\|^{-1/2}$	1.88	-0.9401	0.3423	0.5977	-0.1625	-0.1798
$\langle\sigma_{iy}^{(o)}\sigma_{jy}^{(o)}\rangle_0$	S	3.378	-0.2868	-1.235	0.12	1.481	-0.0816
$\langle\sigma_{ix}^{(s)}\sigma_{jy}^{(s)}\rangle_0$	iS	5	0	0	-0.01961	0	0

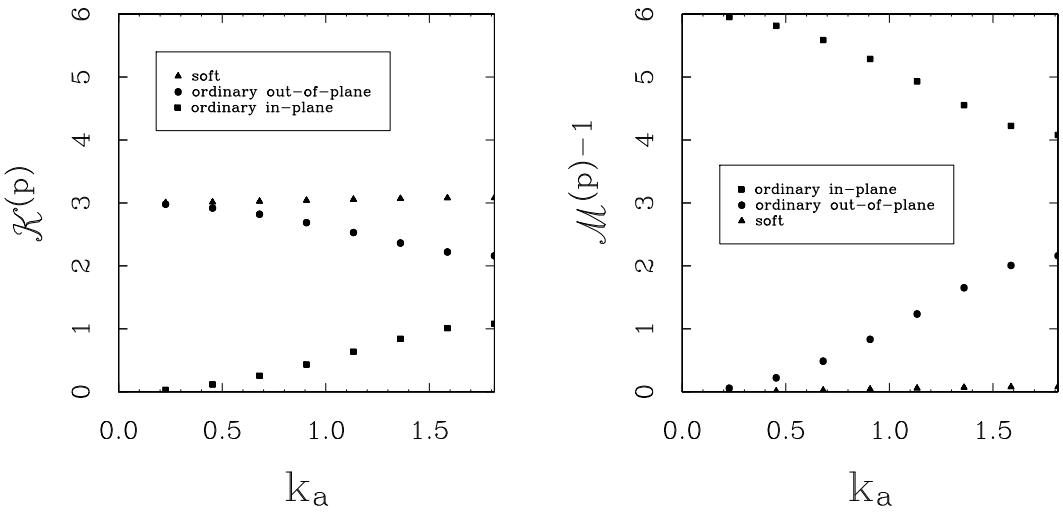

Figure B .6 Examples of the $\mathcal{K}^{(p)}$ and $\mathcal{M}^{(p)-1}$ spectrum for $L = 16, S = 1, J_3 = -0.02$. We take the $\mathbf{a}_1^*$ direction in the rhombic Brillouin zone from $\mathbf{0}$ to $(1/2)\mathbf{a}_1^*$ (see Figure B .2), and have set $a = 1$.

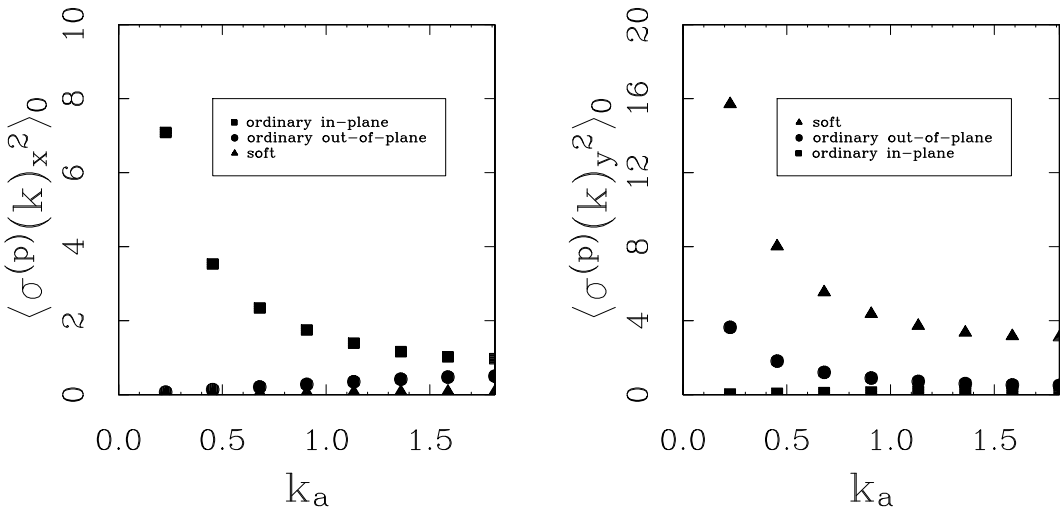

Figure B .7 Examples of the fluctuation spectrum for $\sigma^{(p)}(\mathbf{k})_x$ and $\sigma^{(p)}(\mathbf{k})_y$ in the Ψ_0 ground state. Same specifications as in Figure B .6.

We find

$$\begin{cases} \mathcal{K}^{(1)}(\mathbf{k}) \sim const. & \text{soft mode,} \\ \mathcal{K}^{(2)}(\mathbf{k}) \sim const. & \text{out-of-plane Goldstone (ordinary) mode,} \\ \mathcal{K}^{(3)}(\mathbf{k}) \sim |\mathbf{k}|^2 & \text{in-plane Goldstone mode,} \end{cases} \tag{B23}$$

and

$$\begin{cases} \mathcal{M}^{(1)-1}(\mathbf{k}) \sim |\mathbf{k}|^2 & \text{soft mode,} \\ \mathcal{M}^{(2)-1}(\mathbf{k}) \sim |\mathbf{k}|^2 & \text{out-of-plane Goldstone mode,} \\ \mathcal{M}^{(3)-1}(\mathbf{k}) \sim const. & \text{in-plane Goldstone mode,} \end{cases} \tag{B24}$$

These are illustrated in Figure B .6. Thus we get the small-$\mathbf{k}$behavior of σ_x and σ_y as

$$\begin{cases} \langle\sigma_x(\mathbf{k})^{(s)2}\rangle_0 \sim |\mathbf{k}| & \text{soft mode,} \\ \langle\sigma_x(\mathbf{k})^{(o)2}\rangle_0 \sim |\mathbf{k}| & \text{out-of-plane Goldstone,} \\ \langle\sigma_x(\mathbf{k})^{(o)2}\rangle_0 \sim 1/|\mathbf{k}| & \text{in-plane Goldstone,} \end{cases} \tag{B25}$$

and

$$\begin{cases} \langle\sigma_y(\mathbf{k})^{(s)2}\rangle_0 \sim 1/|\mathbf{k}| & \text{soft mode,} \\ \langle\sigma_y(\mathbf{k})^{(o)2}\rangle_0 \sim 1/|\mathbf{k}| & \text{out-of-plane Goldstone,} \\ \langle\sigma_y(\mathbf{k})^{(o)2}\rangle_0 \sim |\mathbf{k}| & \text{in-plane Goldstone.} \end{cases} \tag{B26}$$

See Figure B .7 for illustration.

Substituting Eq.(B 26) back into Eq.(B 22), selecting the polarizations that dominate at $\mathbf{k} = \mathbf{0}$, we get, for example,

$$\langle \sigma_x^{(s)}(\mathbf{0})\sigma_x^{(s)}(\mathbf{r})\rangle_0 \sim \int_{-\Lambda}^{\Lambda}\int_{-\Lambda}^{\Lambda} e^{-i\mathbf{k}\cdot\mathbf{r}}|\mathbf{k}|\mathrm{d}\mathbf{k},$$
$$\langle \sigma_x^{(o)}(\mathbf{0})\sigma_x^{(o)}(\mathbf{r})\rangle_0 \sim \int_{-\Lambda}^{\Lambda}\int_{-\Lambda}^{\Lambda} \frac{e^{-i\mathbf{k}\cdot\mathbf{r}}}{|\mathbf{k}|}\mathrm{d}\mathbf{k}, \qquad \text{(B27)}$$

and a similar pair of integrals for the $\sigma_y^{(m)}$'s. Since the integrals are dominated by the $|\mathbf{k}| \sim 0$ region, we can extend the lower and upper limits to $\pm\infty$ without altering the large-$|\mathbf{r}|$ behavior. The dependence on $|\mathbf{r}|$ can then be obtained by dimensional analysis[24] :

$$\langle \sigma_x^{(s)}(\mathbf{0})\sigma_x^{(s)}(\mathbf{r})\rangle_0 \sim \frac{1}{|\mathbf{r}|^3},$$
$$\langle \sigma_x^{(o)}(\mathbf{0})\sigma_x^{(o)}(\mathbf{r})\rangle_0 \sim \frac{1}{|\mathbf{r}|},$$
$$\langle \sigma_y^{(s)}(\mathbf{0})\sigma_y^{(s)}(\mathbf{r})\rangle_0 \sim \frac{1}{|\mathbf{r}|},$$
$$\langle \sigma_y^{(o)}(\mathbf{0})\sigma_y^{(o)}(\mathbf{r})\rangle_0 \sim \frac{1}{|\mathbf{r}|}. \qquad \text{(B28)}$$

These r-dependences determine the long-range behavior of the Ising coupling constants $\mathcal{J}_{\alpha\beta}$ in Eq.(3.60).

Finally, the spinwave spectrum for $\tilde{\mathcal{H}}$ is plotted in Figure B .8, to be compared with Figure 6(b) of Ref.8. Obviously, all three branches scales linearly with k for small k.

[24] This dimensional analysis can be checked by contour integrations which rotate the complex exponential to a real exponential in Eq.(B 27). It turns out that the result agrees with dimensional analysis and that the isotropic behavior of the correlations is correct in the following equations.

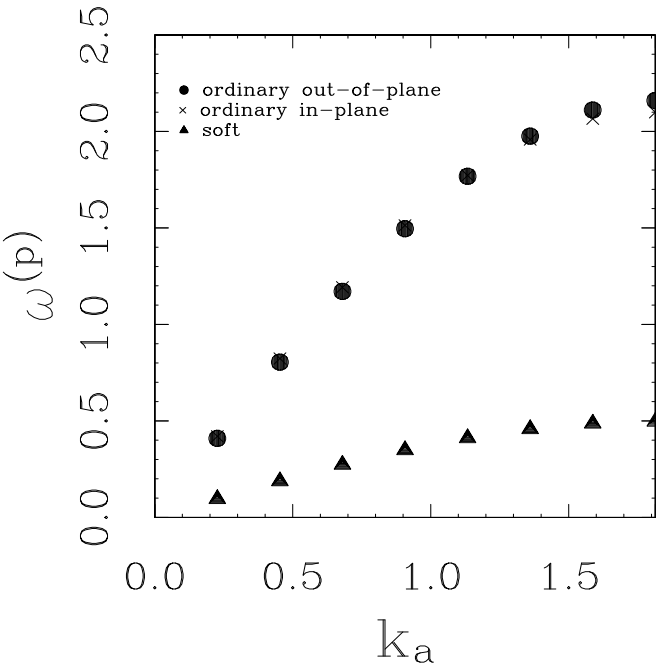

Figure B .8 Spinwave spectrum for $\tilde{\mathcal{H}}$. Same specifications as in Figure B .6. This spectrum is to be compared with Figure 6(b) of Ref.8. Note that our soft branch is almost identical to the one shown in Ref.8 despite the fact that we have $J_2 = 0$ versus their $J_2 = 0.05$. This is because $\omega^{(s)}(\mathbf{k})$ is sensitive mainly to $J_2 - J_3$, which is set to the same value in both figures.

Appendix C
Qualitative Estimate of Ground State Energy

In this Appendix we derive the relative magnitudes of successive terms in our perturbation series Eq.(3.19). We provide some detailed justifications of claims made in Section[3.4.1] and Section[3.9.3].

C.1 First Order Term

The first-order energy $\langle \mathcal{H}_2 + \mathcal{H}_4 \rangle_0$ is particularly easy. From the arguments in Section[3.3], we learned that $\mathcal{H}_2$ has a spinwave spectrum with 2 ordinary branches and 1 zero branch. The ordinary branches frequencies scale with S and thus dominate $\mathcal{H}_2$. The ordinary modes energy in $\mathcal{H}_4$ scale as $O(1)$, and can be neglected. The soft-mode contribution to $\mathcal{H}_4$ scale with $|J_3|^{-1}$. If we use the self-consistent estimate of Eq.(3.32), then $\mathcal{H}_4$ scale with $S^{2/3}$, with a smaller proportionality constant for $\tilde{\mathcal{H}}$. Thus in conclusion,

$$\langle \mathcal{H}_2 + \mathcal{H}_4 \rangle_0 \sim S.$$

C.2 Higher Order Terms

The second-order energy can be estimated as

$$-\frac{\langle V^2\rangle_0}{\Delta E}, \tag{C1}$$

where ΔE is the energy gap between the ground and excited state. We will consider V in two parts: $\mathcal{H}_3$ and $(\mathcal{H}_2 + \mathcal{H}_4 - \tilde{\mathcal{H}})$. Note that these two parts contribute to the second-order energy independently. There can be no cross-terms because $\mathcal{H}_3$ excites an odd number of magnons but $(\mathcal{H}_2+\mathcal{H}_4-\tilde{\mathcal{H}})$ excites an even number, and so there can be no common excited state.

C.2.1 Perturbation of Odd Terms

The intermediate states that $\mathcal{H}_3$ excites are 1- or 3-magnon excitations. The 1-magnon state can be either a soft or an ordinary magnon. The 3- magnon state can consist of either 3 soft magnons or a mixture of 1 ordinary and 2 soft magnons. (Other kinds of mixtures produce second-order energies that are subdominant in powers of S than the ones considered here, as we shall show in Appendix[E].) For such intermediate states, $\langle V^2\rangle_0 = \langle \mathcal{H}_3^2\rangle_0$ can be written as $\langle \sigma_y^{(s)4}\sigma_x^{(m)2}\rangle_0$, where $m = s$ for the purely soft-magnon states, and $m = o$ for the mixed soft- and ordinary-magnon states. ΔE is proportional to the respective spinwave energy ω. (This form of $\langle V^2\rangle_0$ includes the 1-magnon states, where $m = s, o$ denote the respective kind of magnons also.)

In the first case, where the magnons are all soft, we have $\Delta E \sim S\sqrt{|J_3|}$. Using Wick's theorem, we can write the second order energy schematically as

$$N_s\frac{\langle\sigma_x^{(s)2}\rangle_0\langle\sigma_y^{(s)2}\rangle_0^2/S^2}{\omega^{(s)}} \sim N_s\frac{S|J_3|^{-1/2}}{S|J_3|^{1/2}} \sim N_s|J_3|^{-1}. \tag{C2}$$

To check if perturbation theory is valid here, we need to check the magnitude of the ratio $\mathcal{R}^{(s)}$ which is defined in Eq.(3.73). We find $\mathcal{R}^{(s)} \propto S^{-1/2}|J_3|^{-3/4}$. If we use the variational estimate for J_3 from Eq.(3.32), we get the second order perturbation energy scaling as $S^{2/3}$ and $\mathcal{R}^{(s)} \propto 1$. Hence depending on the exact numerical value of $\mathcal{R}^{(s)}$, perturbation theory may or may not be valid.

Notice that in the scaling estimate Eq.(C 2) we did not take into account the cross-correlations $\langle \sigma_x^{(s)} \sigma_y^{(s)} \rangle_0$. From Eq.(B 20), it should be clear that $\langle \sigma_x^{(m)} \sigma_y^{(m)} \rangle_0 \sim \sqrt{\langle \sigma_x^{(m)2} \rangle_0 \langle \sigma_y^{(m)2} \rangle_0}$, so including such cross-correlations would not change the scaling result.

In the second case, where at least one of the magnons is ordinary, we have $\Delta E \sim S$. The excited states which will give the maximum perturbation energy are those which are created by $\sigma_y^{(s)2}$ and $\sigma_x^{(o)}$. Thus they contribute an energy of order

$$N_s \frac{\langle \sigma_x^{(o)2} \rangle_0 \langle \sigma_y^{(s)2} \rangle_0^2 / S^2}{\omega^{(o)}} \sim N_s \frac{S|J_3|^{-1}}{S} \sim N_s |J_3|^{-1}. \qquad \text{(C3)}$$

Here $\mathcal{R}^{(o)} \propto S^{-1/2}|J_3|^{-1/2}$. If we again use the variational estimate for J_3 from Eq.(3.32), then the second order perturbation energy also scales as $S^{2/3}$. However, $\mathcal{R}^{(o)} \propto S^{-1/6}$, which is guaranteed to be small for large S. Thus perturbation theory is definitely justified here for large enough S.

All the other intermediate excited states that $\mathcal{H}_3$ can create have smaller contributions to the second order energy Eq.(C 1), i.e. their contributions scale with a smaller power of S and can be neglected. This is why we define only two sets of excited wavefunctions generated by $\mathcal{Q}^{(s)}$ and $\mathcal{Q}^{(o)}$ in Section[3.2].

Now the higher order terms in the perturbation series of $\mathcal{H}_3$ can be estimated in the same way as Eq.(C 2) and Eq.(C 3). Using the notation that $E_n^{(m)}$ is the n^{th} order perturbation energy for the (m) mode, it is easy to see that

$E^{(m)}_{n+2}/E^{(m)}_n \sim \mathcal{R}^{(m)2}$. Hence

$$\frac{E^{(s)}_{n+2}}{E^{(s)}_n} \sim S^{-1}|J_3|^{-3/2} \sim 1, \tag{C4}$$

$$\frac{E^{(o)}_{n+2}}{E^{(o)}_n} \sim S^{-1}|J_3|^{-1} \sim S^{-1/3}. \tag{C5}$$

It is clear that for intermediate excited states with purely soft excited states (Eq.(C 4)), convergence of the perturbation series depends the numerical prefactors . On the other hand, for excited states with mixed soft and ordinary modes (Eq.(C 5)), the higher order perturbations always decrease in magnitude for large S, and cutting off the perturbation series at second order is justified.

C.2.2 Perturbation of Even Terms

We consider the second-order contribution of $(\mathcal{H}_2 + \mathcal{H}_4 - \tilde{\mathcal{H}})$. To simplify matters, here we only consider the intermediate states with purely soft magnons. Furthermore, we use the variational estimate for J_3 right from the beginning. From the arguments in Section[3.3], we can see that $\tilde{\mathcal{H}} - \mathcal{H}_2$ scales the same way as $\mathcal{H}_4$. Thus we have

$$\begin{aligned}\frac{\langle(\mathcal{H}_2 + \mathcal{H}_4 - \tilde{\mathcal{H}})^2\rangle_0}{\omega^{(s)}} &\sim \frac{\langle\mathcal{H}_4^2\rangle_0}{\omega^{(s)}} \\ &\sim \frac{\langle\sigma_y^{(s)2}\rangle_0^4/S^4}{S^{2/3}} \\ &\sim S^{2/3},\end{aligned}$$

and

$$\mathcal{R}^{(s)} \sim 1. \tag{C6}$$

From $\mathcal{R}^{(s)}$, we can get the higher order perturbations of $(\mathcal{H}_2 + \mathcal{H}_4 - \tilde{\mathcal{H}})$:

$$\frac{E_{n+1}^{(s)}}{E_n^{(s)}} \sim 1. \tag{C7}$$

We encountered the same problems with respect to the convergence of perturbation series as in the soft $\mathcal{H}_3$ case.

As can be shown using the same method, intermediate states consisting of ordinary magnons also result in the same scalings with S.

C.3 Conclusion

We conclude from estimating how the various perturbative terms scale with S that the perturbation series does not necessarily converge even as $S \to \infty$. This is due to the intermediate excited states which are purely soft-magnon states. In Chubukov's perturbation theory [30], he asserted that the perturbative approach is justified because all the higher order terms which have the same powers of S cancel due to a Ward identity (arising out of the Goldstone symmetry). This remains to be demonstrated rigorously.

Appendix D

Orthogonality of $\mathcal{Q}_\beta^{(m)}$ and $\Upsilon_\alpha^{(m')}$

In this Appendix we shall establish that the 2 parts of $\mathcal{H}_\alpha$ (which are the cubic terms of the spinwave Hamiltonian for one triangle, defined in Eq.(3.10))– the part proportional to $\sum(\sigma_{ix}\sigma_{jy}^2 - \sigma_{iy}^2\sigma_{jx})$ and the part proportional to $\sum(\sigma_{ix} - \sigma_{jx})^3$– are orthogonal. (The sums are over spins in the same triangle.) We have designated the former part $\mathcal{Q}_\alpha$ in Eq.(3.38). We call the latter part Υ, such that

$$\mathcal{H}_\alpha/J^* = -\frac{\sqrt{3}}{4S}\mathcal{Q}_\alpha + \Upsilon_\alpha. \tag{D1}$$

The orthogonality between the two parts of $\mathcal{H}_\alpha$ will be used in Section[3.7], especially Eq.(3.56), to simplify some terms.

We define the operators $\mathcal{H}_\alpha^{(s)}$ and $\mathcal{H}_\alpha^{(o)}$ which are the same as $\mathcal{H}_\alpha$ except we replace *one* of the σ_x's with $\sigma_x^{(s)}$'s or $\sigma_x^{(o)}$'s matching that of the $\mathcal{Q}_\alpha^{(s)}$ or $\mathcal{Q}_\alpha^{(o)}$ operators. We also replace *all* of the σ_y operators in $\mathcal{H}_\alpha$ by $\sigma_y^{(s)}$. (As in the definition of $\mathcal{Q}_\alpha^{(s)}$, we have to symmetrize the resulting terms in $\mathcal{H}_\alpha^{(s)}$ to ensure hermiticity.) Writing $\mathcal{H}_\alpha \approx \mathcal{H}_\alpha^{(s)} + \mathcal{H}_\alpha^{(o)}$ introduces errors in the resulting second order perturbative energy that are subdominant at large S, as we can check by counting the powers of S involved. We shall use the symbol "m" to denote either "s" or "o" modes below.

The orthogonality between $\mathcal{Q}_\alpha^{(m)}$ and $\Upsilon_\beta^{(m')}$ when $m \neq m'$,

$$\langle \mathcal{Q}_\alpha^{(m)} \Upsilon_\beta^{(m')} \rangle_0 = 0 \tag{D2}$$

can be shown using Wick's theorem and the orthogonality of the soft and ordinary modes. The same reasoning leads us to the result

$$\langle \mathcal{Q}_\alpha^{(m)} \mathcal{Q}_\beta^{(m')} \rangle_0 = 0, \qquad m \neq m', \tag{D3}$$

which accounts for the orthogonality between the wavefunctions $\Psi_\alpha^{(s)}$ and $\Psi_\beta^{(o)}$ defined in Eq.(3.37).

Now, to show $\langle \mathcal{Q}_\alpha^{(m)} \Upsilon_\alpha^{(m)} \rangle_0 = 0$, note that since σ_y occurs only in $\mathcal{Q}_\alpha^{(m)}$ but not in $\Upsilon_\alpha^{(m)}$, and that the contributions of the cross-correlations $\langle \sigma_{iy}^{(s)} \sigma_{jx}^{(s)} \rangle_0$ when $m = s$ turn out to be zero[25], we can employ Wick's theorem to factor out the σ_y^2's,

$$\langle \mathcal{Q}_\alpha^{(m)} \Upsilon_\beta^{(m)} \rangle_0 = \langle \sigma_{iy}^{(s)2} \rangle \Big\langle \Upsilon_\beta^{(m)} [(\sigma_{1x}^{(m)} - \sigma_{2x}^{(m)}) + (\sigma_{2x}^{(m)} - \sigma_{3x}^{(m)}) + (\sigma_{3x}^{(m)} - \sigma_{1x}^{(m)})] \Big\rangle_0$$
$$= 0. \qquad \text{(D4)}$$

(Note that we can make use of the permutation symmetry in σ_{1x}, σ_{2x}, σ_{3x} in $\mathcal{Q}_\alpha^{(m)}$ to achieve the cancellation in Eq.(D 4) only because we can factor out the σ_y's. If $\Upsilon_\beta^{(m)}$ were to contain σ_y's also, this would not have been possible.)

Equations (D 2), (D 3) and (D 4) lead to the desired Eq.(3.57).

---

[25] This cancellation of the cross-correlations can be explained because we can show that they contribute nothing to $\langle \mathcal{Q}_\alpha^{(m)} \Upsilon_\beta^{(m)} \rangle_0$. Since $\mathcal{Q}_\alpha^{(s)} \sim \sigma_x^{(s)} \sigma_y^{(s)2}$ and $\Upsilon_\beta^{(s)} \sim \sigma_x^{(s)} \sigma_x^{(o)2}$, in order to obtain a $\langle \sigma_x^{(s)} \sigma_y^{(s)} \rangle_0$ Wick's pairing, we must pair one of the $\sigma_y^{(s)}$ in $\mathcal{Q}_\alpha^{(s)}$ with the $\sigma_x^{(s)}$ within the same $\mathcal{Q}_\alpha^{(s)}$ and pair the other $\sigma_y^{(s)}$ with the $\sigma_x^{(s)}$ in $\Upsilon_\beta^{(s)}$. However, since $\mathcal{Q}_\alpha^{(s)}$ is symmetrized, and since $\langle \sigma_{ix}^{(s)} \sigma_{jy}^{(s)} \rangle_0 = -\langle \sigma_{jy}^{(s)} \sigma_{ix}^{(s)} \rangle_0$, such pairings always give a net result of zero.

Appendix E
Alternative Forms of $\mathcal{Q}_\alpha$

We have chosen $\mathcal{Q}_\alpha$ as the basis functions for our non-Gaussian wavefunction in Section[3.4.2]. As shown in Appendix[D], this $\mathcal{Q}_\alpha$ is just one part of $\mathcal{H}_3$. We want to demonstrate here that choosing the other part of $\mathcal{H}_3$, Υ (as defined in Eq.(D 1)), as the basis functions would result in a much smaller (in absolute value) second-order perturbative energy (Eq.(3.63)) at large S. In fact, we can demonstrate that all the other related choices of basis functions also result in smaller second-order energies. A smaller second-order energy implies that the basis functions are not capturing some of the important excitations created by $\mathcal{H}_4$ acting on Ψ_0.

The second-order perturbative energy has its basic form given in the third term of Eq.(3.58) or Eq.(3.63) which we display here again:

$$E_2 \sim -\sum_{m,\alpha} \frac{\langle\Psi_0|\mathcal{H}_3|\Psi_\alpha^{(m)}\rangle\langle\Psi_\alpha^{(m)}|\mathcal{H}_3|\Psi_0\rangle}{\overline{E}^{(m)} - E_0}, \tag{3.63}$$

where

$$|\Psi_\alpha^{(m)}\rangle_0 \propto \mathcal{Q}_\alpha^{(m)}|\Psi_0\rangle \tag{E1}$$

We are using the cubic Hermitian operator $\mathcal{Q}_\alpha$ as some kind of creation operator. The state it creates is a mixture of one- and three- magnon states. This raises the question: should we instead consider using an operator linear in σ's as creation operator to create one-magnon states? We find that one-magnon states $|\Psi\rangle$ created by linear operators are unsuitable because they result in a non-zero displacement[26] $\langle\Psi|\sigma_i|\Psi\rangle \neq 0$. We have argued in Appendix[A] that

[26] To show this in a simple case, suppose we create an excited state by a linear operator $|\Psi_i\rangle \sim \sigma_{ix}|\Psi_0\rangle$. The full wavefunction is $|\Psi_0\rangle \sim |\Psi_0\rangle + \sigma_{ix}|\Psi_0\rangle$. Hence the mean spin deviation is $\langle\Psi|\sigma_{ix}|\Psi\rangle \sim \langle\Psi_0|\sigma_{ix}|\Psi_0\rangle + 2\langle\Psi_0|\sigma_{ix}^2|\Psi_0\rangle + \langle\Psi_0|\sigma_{ix}^3|\Psi_0\rangle = 2\langle\sigma_{ix}^2\rangle_0 > 0$.

this is excluded by symmetry if the Potts state in question has 3-fold rotational and reflectional symmetry. Even if the Potts state does not have this symmetry, our approach has been to ignore this degree of freedom in the variational wavefunction in the interest of simplicity. Therefore, it would be inconsistent with our approximation to create states with non-zero spin displacements here. We can just focus our attention to states created by cubic operators.

One may question why we are defining the "creation" operators $\mathcal{Q}_\alpha$ to be Hermitian (see Eq.(3.38)). The reason is that we intend to create a variational subspace of excited states which are very similar to the ones that $\mathcal{H}_3$ would create, as explained in Section[3.4.1]. Designing a non-Hermitian operator that creates the same states as $\mathcal{H}_3$ would require more thought. In any case, the difference between our $\mathcal{Q}_\alpha$ and any other non-Hermitian version that one might design would be linear[27] in the σ's, which we have excluded from consideration as explained in the preceding paragraph.

We can enumerate some of the possible choices of cubic operators. Start with σ_y^3. If we apply Wick's theorem to the matrix element, we will find that there is an odd number of σ_y operators. This obviously means the matrix element is zero in Eq.(3.63). $\sigma_y^2\sigma_x$ is what we have defined to be $\mathcal{Q}_\alpha$. $\sigma_y\sigma_x^2$ will give zero matrix element in Eq.(3.63), for the same reason that σ_y^3 does. Finally, σ_x^3, which was denoted as Υ_α in Eq.(D 1), gives a second-order energy of $\mathcal{S}^0$, negligible compared with $S^{2/3}$ which is obtained with our actual choice of $\mathcal{Q}$ if we use the variational estimate of J_3 in Eq.(3.32). We can demonstrate this last result as follows. For $\Upsilon_\alpha^{(o)}$, we have

$$\Upsilon_\alpha^{(o)} \sim \sigma_x^{(o)3}. \tag{E2}$$

[27] This is because $\sigma_{ix}^{(s)}\sigma_{jy}^{(s)2} - \sigma_{jy}^{(s)2}\sigma_{ix}^{(s)} \propto \sigma_{jy}^{(s)}[\sigma_{ix}^{(s)}, \sigma_{jy}^{(s)}] \propto \sigma_{jy}^{(s)}$.

The part of $\mathcal{H}_3$ that will be relevant is

$$\mathcal{H}_\alpha \sim \frac{1}{S}\sigma_x^{(o)3}. \tag{E3}$$

Using second perturbation formula Eq.(C 1), the second order energy scales as

$$\frac{1}{\omega^{(o)}}\frac{\langle \mathcal{H}_\alpha \Upsilon_\alpha^{(o)}\rangle_0^2}{\langle \Upsilon^{(o)2}\rangle_0}. \tag{E4}$$

Using Eq.(D 1) and Eq.(D 4), one finds that

$$\langle \mathcal{H}_\alpha \Upsilon_\alpha^{(o)}\rangle_0 \sim \frac{1}{S}\langle \Upsilon_\alpha^{(o)2}\rangle_0. \tag{E5}$$

Recalling that $\omega^{(o)} \sim S$, Eq.(E 4) can be evaluated as

$$\frac{1}{S^3}\langle \sigma_x^{(o)6}\rangle_0 \sim S^0. \tag{E6}$$

Now for $\Upsilon_\alpha^{(s)}$, we have

$$\Upsilon_\alpha^{(s)} \sim \sigma_x^{(s)3}. \tag{E7}$$

The part of $\mathcal{H}_3$ that will contribute is

$$\mathcal{H}_\alpha \sim \frac{1}{S}\sigma_x^{(o)2}\sigma_x^{(s)}. \tag{E8}$$

Following similar calculations as above, this will also lead to a perturbation energy of $\mathcal{O}(S^0)$, if $J_3 \sim -S^{-2/3}$.

Appendix F

Analytic Form of $\langle\!\langle\ \mathcal{Q}_{\alpha}^{(m)}\ \mathcal{Q}_{\beta}^{(m)}\rangle\!\rangle_0$

The objective of this appendix is to explain the signs of $\mathcal{J}_{\alpha\beta}$, as displayed in Eq.(3.65), in terms of spin-spin correlation functions with respect to Ψ_0. We try to understand them qualitatively as far as possible.

Let α and β be nearest-neighbor triangles, as shown on Figure B .3. We number the triangles using the convention in Figure 3.4. We number the spins in the two triangles in a clockwise sense, also shown on the figure. After much tedious algebra, one finds that

$$\begin{aligned}\langle\langle \mathcal{Q}_0^{(m)} \mathcal{Q}_1^{(m)} \rangle\rangle_0 = & \, 4(\langle y2y3' \rangle^2 - \langle y2y2' \rangle^2)(2\langle x1x2 \rangle - \langle x1^2 \rangle) \\ & + 2(\langle x2x3' \rangle - \langle x2x2' \rangle)(4\langle y1y2 \rangle^2 - \langle y1^2 \rangle^2) \\ & + 2\langle y1^2 \rangle^2(\langle x2x2' \rangle - \langle x2x3' \rangle) \\ & + 4(\langle x2x2' \rangle \langle y2y2' \rangle^2 - \langle x2x3' \rangle \langle y2y3' \rangle^2). \qquad \text{(F1)}\end{aligned}$$

Note that we have adopted here a simpler notation $xi \equiv \sigma_{ix}^{(m)}$ and $yi \equiv \sigma_{iy}^{(s)}$ for brevity. (Note that the σ_y operators *always* refer to the soft modes in this Appendix.) For the same reason, the subscript "0", which was used to indicate that the expectations are taken with respect to Ψ_0, has also been omitted in the expectations.

Note also that we have used the notation $\langle\langle \ldots \rangle\rangle_0$ to denote correlations where we have adopted the approximation $\langle \sigma_{ix}^{(s)} \sigma_{jy}^{(s)} \rangle_0 \equiv 0$. This means that $\langle\langle \mathcal{Q}_0^{(o)} \mathcal{Q}_1^{(o)} \rangle\rangle_0 = \langle \mathcal{Q}_0^{(o)} \mathcal{Q}_1^{(o)} \rangle_0$, however, $\langle\langle \mathcal{Q}_0^{(s)} \mathcal{Q}_1^{(s)} \rangle\rangle_0 \approx \langle \mathcal{Q}_0^{(s)} \mathcal{Q}_1^{(s)} \rangle_0$ only.

F.1 Why is $\langle \mathcal{Q}_0^{(o)} \mathcal{Q}_1^{(o)} \rangle_0 = 0$?

There are certain facts about the spin-spin correlations that serve to simplify the triangle correlations. First note that the σ_y-correlations in Eq.(F 1) are all referring to the soft modes, since this is how the $\mathcal{Q}_\alpha$ is defined in Eq.(3.38). For the soft modes,

$$\langle y1^2 \rangle + 2\langle y1y2 \rangle = 0 \tag{F2}$$

for any $\tilde{\mathcal{H}}$. This can be understood by remembering that the soft σ_y fluctuations will not contribute to the energy of $\mathcal{H}_2$ at all, otherwise $\langle \mathcal{H}_2 \rangle_0$ would scale with $S^{4/3}$ as demanded by the fluctuation amplitude of $\sigma_y^{(s)}$ estimated in Section[3.3]. This $S^{4/3}$ term is obviously forbidden because the total harmonic energy should scale with S. Thus we must have perfect cancellations of all the $\sigma_y^{(s)}$ terms in $\mathcal{H}_2$:

$$\sum_\alpha \langle (\sigma_{1y}^{(s)} + \sigma_{2y}^{(s)} + \sigma_{3y}^{(s)})^2 \rangle_0 = 0. \tag{F3}$$

Obviously, this implies the summand here is also zero. Expanding the summand and setting it to zero immediately leads to Eq.(F 2). (The same argument works for $\sigma_x^{(s)}$ also, since it is the same mode as the $\sigma_y^{(s)}$. We do not emphasize this result because it is inconsequential to the signs of $\mathcal{Q}_\alpha^{(m)} \mathcal{Q}_\beta^{(m)}$.)

Second, we turn our attention to the x-correlations. We find numerically (see Table B .1) that for the ordinary modes,

$$\langle x2x2' \rangle = \langle x2x3' \rangle = \langle x2x4' \rangle. \tag{F4}$$

In other words, the ordinary x-correlations are the same for all second nearest-neighbors as well as third nearest-neighbors. Thirdly, we also find the relationship for the ordinary modes

$$\langle x1^2 \rangle - 2\langle x1x2 \rangle + \langle x2x2' \rangle = 0. \tag{F5}$$

We do not have a qualitative explanation of Eq.(F 4). It must be a basic property of $\mathcal{H}_2$ (instead of $\tilde{\mathcal{H}}$) since all the numerical relations are true only in the limit $J_3 \to 0$. However, given Eq.(F 4), we can show that Eq.(F 5) must be true. The soft modes are dominated by the "hexagon modes": $\sigma_{iy}^{(s)}$ or $\sigma_{ix}^{(s)}$ that go $(+,-,+,-,+,-)$ on a hexagon. Hence we have the relation for the soft modes

$$\langle (x_a + x_b + x_c + x_d + x_e + x_f)^2 \rangle_0 \rangle = 0, \tag{F6}$$

where we have named the sites around the hexagons $a, \ldots, f$. Since the ordinary modes are orthogonal to the soft modes, Eq.(F 6) is true for the ordinary modes also. Expanding Eq.(F 6) and reverting to the previous site labelling, we get for the ordinary modes,

$$\langle x1^2 - 2x1x2 + 2x2x3' - x2x4' \rangle = 0. \tag{F7}$$

Appling Eq.(F 4) to Eq.(F 7) immediately gives us Eq.(F 5).

If we now apply Eq.(F 2) to Eq.(F 1), the second term will be zero. If we apply Eq.(F 4) to Eq.(F 1), the third term will be zero. We can combine the first and fourth terms into a term proportional to Eq.(F 5) which also vanishes. Thus the nearest-neighbor triangle correlation for ordinary modes $\langle \mathcal{Q}_0^{(o)} \mathcal{Q}_1^{(o)} \rangle_0$ is zero.

F.2 Why is $\langle\langle \mathcal{Q}_0^{(s)} \mathcal{Q}_1^{(s)} \rangle\rangle_0 < 0$?

For the x-correlations of the soft modes, we have a qualitative argument to show why $\langle\langle \mathcal{Q}_0^{(s)} \mathcal{Q}_1^{(s)} \rangle\rangle_0 < 0$. (Recall that the notation $\langle\langle \ldots \rangle\rangle_0$ means $\langle \sigma_{ix}^{(s)} \sigma_{jy}^{(s)} \rangle_0 \equiv 0$.) Analogous to Eq.(F 2), we have for the soft x-correlations

$$\langle x1^2 \rangle + 2\langle x1x2 \rangle = 0. \tag{F8}$$

(This can be regarded as a purely numerical fact, although it is a consequence of Eq.(F 2) and the possibility of simultaneous diagonalization of the $\mathcal{K}$ and $\mathcal{M}^{-1}$ matrices in Appendix[B], which means that the x and y modes are the same.) This means that the second factor of the first term in Eq.(F 1) is zero because of Eq.(F 8), while the second factor of the second term in the same equation is zero because of Eq.(F 2). The second factor in the third term of Eq.(F 1) is dominated by $\langle x2x3' \rangle$ because it is 10 times as big as $\langle x2x2' \rangle$. Again because of the dominance of the hexagon mode correlations, the second neighbor $\langle x2x3' \rangle > 0$. So the third term in Eq.(F 1) is negative. For the same reasons the fourth term should be negative, unless $|\langle y2y3' \rangle| \gg |\langle y2y2' \rangle|$, which it isn't. Thus we have shown that $\langle\langle \mathcal{Q}_0^{(s)} \mathcal{Q}_1^{(s)} \rangle\rangle_0 < 0$.

(It is possible that this sort of argument could be generalized to include $\sigma_x^{(s)} \sigma_y^{(s)}$ cross-correlations and hence the the sign of the triangle correlation $\langle \mathcal{Q}_0^{(s)} \mathcal{Q}_1^{(s)} \rangle_0$ can be deduced, but we have not pursued that yet. As it stands, the physical relevance of $\langle\langle \mathcal{Q}_0^{(s)} \mathcal{Q}_1^{(s)} \rangle\rangle_0 < 0$ is unsure.

F.3 Conclusion

We could do a similar analysis for two next-nearest-neighbor triangles, and we would have obtained a similar justification of why $\langle \mathcal{Q}_0^{(o)} \mathcal{Q}_2^{(o)} \rangle_0 < 0$ and $\langle\langle \mathcal{Q}_0^{(s)} \mathcal{Q}_2^{(s)} \rangle\rangle_0 > 0$. Now if we look at formula (3.59) for the effective Ising coupling constant $\mathcal{J}_{\alpha\beta}$, we note that it is proportional to $2\langle \mathcal{Q}_\alpha^{(m)} \mathcal{Q}_\beta^{(m)} \rangle_0 - \overline{g}^{(m)} \langle \mathcal{Q}_\alpha^{(m)} (\tilde{\mathcal{H}} - E_0) \mathcal{Q}_\beta^{(m)} \rangle_0$. It turns out that the triangle correlation that vanishes remains zero after inserting the quantity $\tilde{\mathcal{H}} - E_0$. For the non-zero couplings, the sign cannot be easily deduced here. We find numerically that the $\langle \mathcal{Q}_\alpha^{(m)} (\tilde{\mathcal{H}} - E_0) \mathcal{Q}_\beta^{(m)} \rangle_0$ part of $\mathcal{J}_{\alpha\beta}^{(m)}$ dominates, and,

$$\begin{aligned} \mathcal{J}_{01}^{(o)} &= 0, \\ \mathcal{J}_{01}^{(s)} &< 0, \end{aligned} \tag{F9}$$

and hence

$$\mathcal{J}_{01} < 0 \tag{F10}$$

for nearest neighbors. For next-nearest neighbors,

$$\begin{aligned} \mathcal{J}_{02}^{(o)} &< 0 \\ \mathcal{J}_{02}^{(s)} &< 0. \end{aligned} \tag{F11}$$

and $\mathcal{J}_{02} > 0$.

Appendix G
Scaling with S and J_3

In this Appendix, we establish how the selection energy scales with S and J_3. The argument is very similar to the more general one given in Appendix[C]. Here we just wish to check that the specific form of the selection formula Eq.(3.59) does give the same scaling as the general results.

Besides scaling with $|J_3|$ or S, we can also inquire how $\mathcal{J}^{(m)}_{\alpha\beta}$ depends on the system size N_s and the distance between the triangles $r_{\alpha\beta}$.

G.1 Scaling of $\langle \mathcal{Q}^{(m)}_\alpha (\tilde{\mathcal{H}} - E_0) \mathcal{Q}^{(m)}_\beta \rangle_0$

First let us consider $\langle \mathcal{Q}^{(s)}_\alpha (\tilde{\mathcal{H}} - E_0) \mathcal{Q}^{(s)}_\beta \rangle_0$. One can see that part of $\langle \mathcal{Q}^{(s)}_\alpha \tilde{\mathcal{H}} \mathcal{Q}^{(s)}_\beta \rangle_0$ will cancel $E_0 \langle \mathcal{Q}^{(s)}_\alpha \mathcal{Q}^{(s)}_\beta \rangle_0$. This is because when we Wick-decompose the triangle correlations into pair correlations, we can imagine factoring out the $\tilde{\mathcal{H}}$ operator as a whole from the triangle correlation and therefore there must be a term $\langle \tilde{\mathcal{H}} \rangle_0 \langle \mathcal{Q}^{(s)}_\alpha \mathcal{Q}^{(s)}_\beta \rangle_0$ in the decomposition. Hence the only terms that remain are those in which the two σ's in each term of $\tilde{\mathcal{H}}$ are grouped into different pair correlations. Since there are only soft operators in $\mathcal{Q}^{(s)}$, only the soft part of $\tilde{\mathcal{H}}$ will survive this grouping. Because the soft fluctuations in $\tilde{\mathcal{H}}$ are prefactored[28] by J_3, we find that

$$\begin{aligned} \langle \mathcal{Q}^{(s)}_\alpha (\tilde{\mathcal{H}} - E_0) \mathcal{Q}^{(s)}_\beta \rangle_0 &\sim |J_3| \langle \sigma_y^{(s)6} \rangle_0 \langle \sigma_x^{(s)2} \rangle_0 \\ &\sim S^4, \end{aligned} \tag{G1}$$

using Eq.(3.26) and (3.27).

[28] Soft fluctuations are dominated by σ_y. However, as shown in Eq.(F 3), the soft σ_y fluctuations in $\mathcal{H}_2$ adds up to zero.

Second, we analyze $\langle \mathcal{Q}_\alpha^{(o)}(\tilde{\mathcal{H}} - E_0)\mathcal{Q}_\beta^{(o)}\rangle_0$ in a similar way. Here the $\sigma_x^{(o)}$ fluctuations in $\tilde{\mathcal{H}}$ can only pair up with the $\sigma_x^{(o)}$ in $\mathcal{Q}^{(o)}$. The soft σ_x fluctuations in $\tilde{\mathcal{H}}$ are of smaller magnitude than the ordinary (σ_x) ones (see Table 3.3) and can therefore be neglected. The ordinary fluctuations have prefactor of S which is of order unity, thus

$$\begin{aligned} \langle \mathcal{Q}_\alpha^{(o)}(\tilde{\mathcal{H}} - E_0)\mathcal{Q}_\beta^{(o)}\rangle_0 &\sim \langle {\sigma_y^{(s)}}^4\rangle_0 \langle \sigma_x^{(o)4}\rangle_0 \\ &\sim |J_3|^{-1} S^4. \end{aligned} \tag{G2}$$

G.2 Scaling of $\langle \mathcal{Q}_\alpha^{(m)}\mathcal{Q}_\beta^{(m)}\rangle_0$

It is easy to see

$$\begin{aligned} \langle \mathcal{Q}_\alpha^{(s)}\mathcal{Q}_\beta^{(s)}\rangle_0 &\sim \langle {\sigma_y^{(s)}}^4\rangle_0 \langle {\sigma_x^{(s)}}^2\rangle_0 \\ &\sim |J_3|^{-1/2} S^3, \\ \langle \mathcal{Q}_\alpha^{(o)}\mathcal{Q}_\beta^{(o)}\rangle_0 &\sim \langle {\sigma_y^{(s)}}^4\rangle_0 \langle {\sigma_x^{(o)}}^2\rangle_0 \\ &\sim |J_3|^{-1} S^3. \end{aligned} \tag{G3}$$

G.3 Scaling of $\overline{g}^{(m)}$ and $\mathcal{J}^{(m)}_{\alpha\beta}$

The $\overline{g}$'s of course scale inversely as the $\langle \mathcal{Q}_\alpha(\tilde{\mathcal{H}} - E_0)\mathcal{Q}_\beta\rangle_0$'s, except that they are normalized by $\langle \mathcal{Q}^2_\alpha\rangle_0$. Thus we find

$$\begin{aligned} \overline{g}^{(s)} &\sim |J_3|^{-1/2} S^{-1}, \\ \overline{g}^{(o)} &\sim S^{-1}. \end{aligned} \tag{G4}$$

Combining Eq.(G 1), Eq.(G 2) and Eq.(G 4) gives us

$$\begin{aligned} \mathcal{J}^{(s)}_{\alpha\beta} &\sim |J_3|^{-1}, \\ \mathcal{J}^{(o)}_{\alpha\beta} &\sim |J_3|^{-1}. \end{aligned} \tag{G5}$$

If we use the self-consistent estimate for J_3, then both of them scale with $S^{2/3}$.

Note that although both $\tilde{H}$ and E_0 scale with N_s, the difference $\langle \mathcal{Q}_\alpha(\tilde{\mathcal{H}} - E_0)\mathcal{Q}_\beta\rangle_0$ does not because Ψ_α is different from Ψ_0 only at a local set of spins.

We can check that the sum over α, β in Eq.(3.59) is of $\mathcal{O}(N_s)$. $\mathcal{J}^{(m)}_{\alpha,\beta}$ decays as $r^{-\zeta^{(m)}}$, where $\zeta^{(s)} = 5$ for the soft modes and $\zeta^{(o)} = 3$ for the ordinary modes (See Appendix[B.3] and Footnote[10]). The sum over α and β in Eq.(3.58) which gives the explicitly Ising part of the variational energy can be approximated as an integral

$$N_s \int_1^\infty \frac{1}{r^{\zeta^{(m)}}} r dr, \tag{G6}$$

which obviously is of order N_s.

Appendix H
Calculational Algorithm for $J_{\alpha\beta}$

In this appendix we describe the computer algorithm for computing the Ising coupling constants $\mathcal{J}_{\alpha\beta}$ in Eq.(3.65).

Given the variational parameters J_3, we first numerically diagonalize $\tilde{\mathcal{H}}$ using the method depicted in Appendix[B]. The calculation of the correlations then proceeds according to whether we want the soft or ordinary fluctuations. We can identify the soft modes in our program by sorting the eigenmodes of the matrix $\mathcal{K}$ according to their eigenvalues $\mathcal{K}_p$ in ascending order. The mode with the highest $\mathcal{K}_p$ is the soft mode. The real-space correlations between any two spins are then computed by summing over different $\mathbf{k}$ values of the first Brillouin zone (Eq.(B 21)). This step is a two dimensional Fourier transform. Since the shape of the first Brillouin zone that we are using is rhombic, we can in principle implement the fast Fourier transform algorithm in our summation. We did not actually do that because this is not the bottleneck in speed.

The real-space spin-spin correlations (with respect to Ψ_0) with only the soft mode and the corresponding ones with only the ordinary modes will be stored in four separate arrays in the "C++" language program,

xs[i][j], **xo[i][j]**, **ys[i][j]**, **yo[i][j]**.

We define a one-dimensional vector of indices i to denote the sites in the two-dimensional lattices. We therefore need to define arrays that contain the indices of neighbors of a given spin "**i**". These arrays, for nearest and third-nearest neighbors we called **nbrt[i][j]**, **nbrt3[i][j]**. All these are fed into subroutines which contain the triangle correlations in its Wick-decomposed form (see Appendix[I]). Correlations between triangles that are close together will then

be computed. The most time- consuming step is to compute quantities like $\langle \mathcal{Q}_\alpha \tilde{\mathcal{H}} \mathcal{Q}_\beta \rangle_0$ which require a sum over the lattice once[29] . In contrast, the term $\langle \mathcal{H}_2 + \mathcal{H}_4 \rangle_0$ requires no summation over the lattice due to its translational symmetry.

In computing the unperturbed energy E_0 and the first-order perturbation energy $\langle \mathcal{H}_2 + \mathcal{H}_4 \rangle_0$ we use either the soft fluctuations or the ordinary ones, but never a product of both kinds of correlations. However, we do need a mixture (in product form) when we compute $\langle \mathcal{Q}_\alpha^{(s)} (\tilde{\mathcal{H}} - E_0) \mathcal{Q}_\beta^{(s)} \rangle_0$, and its $\mathcal{Q}^{(o)}$ counterpart. This would have created a lot of complexity in the subroutine[30] used to compute triangle correlations. However, it is possible to convert the triangle correlations into a form which contains only $\sigma_y^{(s)}$ and either $\sigma_x^{(s)}$ or $\sigma_x^{(o)}$ but not both. To do this, it is necessary to separate $\tilde{\mathcal{H}}$ into 4 parts $\tilde{\mathcal{H}} = \tilde{\mathcal{H}}_x^{(s)} + \tilde{\mathcal{H}}_y^{(s)} + \tilde{\mathcal{H}}_x^{(o)} + \tilde{\mathcal{H}}_y^{(o)}$, each of which is respectively quadratic in $\sigma_x^{(o)}$, $\sigma_y^{(o)}$, $\sigma_x^{(s)}$, or $\sigma_y^{(s)}$. There will be some cancellations, as we shall demonstrate in the following equation, which simplify the computational algorithm. Also, we need only to pick out the terms that dominate at large S, because these dominant terms determine the selection formula Eq.(3.59). Thus, defining the shorthand $E_0^{(m)} \equiv \langle \tilde{\mathcal{H}}^{(m)} \rangle_0$,

$$
\begin{aligned}
&\langle \mathcal{Q}_\alpha^{(s)} (\tilde{\mathcal{H}} - E_0) \mathcal{Q}_\beta^{(s)} \rangle_0 \\
&= \langle \mathcal{Q}_\alpha^{(s)} (\tilde{\mathcal{H}}_x^{(s)} + \tilde{\mathcal{H}}_y^{(s)} + \tilde{\mathcal{H}}_x^{(o)} + \tilde{\mathcal{H}}_y^{(o)}) \mathcal{Q}_\beta^{(s)} \rangle_0 \\
&\quad - \langle \tilde{\mathcal{H}}_x^{(s)} + \tilde{\mathcal{H}}_y^{(s)} + \tilde{\mathcal{H}}_x^{(o)} + \tilde{\mathcal{H}}_y^{(o)} \rangle \langle \mathcal{Q}_\alpha^{(s)} \mathcal{Q}_\beta^{(s)} \rangle_0
\end{aligned}
$$

[29] In contrast, if we were to calculate second-order perturbation in the traditional way (in reciprocal space) via Eq.(3.64), we need to sum over the (reciprocal) lattice twice, a much more computationally intensive step. (We don't need to sum thrice despite the appearance of $\mathbf{k}_1, \mathbf{k}_2, \mathbf{k}_3$ in Eq.(3.64) because of the conservation of crystal momentum.)

[30] The Mathematica program (see Appendix[I]) that we use to automatically generate these C++ subroutines would have to distinguish between soft and ordinary operators. This can certainly be done, but due to historical reasons, they were not written to deal with this distinction.

$$= \langle \mathcal{Q}_\alpha^{(s)} (\tilde{\mathcal{H}}^{(s)}) \mathcal{Q}_\beta^{(s)} \rangle_0 - E_0^{(s)} \langle \mathcal{Q}_\alpha^{(s)} \mathcal{Q}_\beta^{(s)} \rangle_0, \tag{H1}$$

where the cancellations are possible because of factoring out of $\tilde{\mathcal{H}}^{(o)}$ *en masse*, as explained in the paragraph preceding Eq.(G 1). Similarly,

$$\begin{aligned}
&\langle \mathcal{Q}_\alpha^{(o)} (\tilde{\mathcal{H}} - E_0) \mathcal{Q}_\beta^{(o)} \rangle_0 \\
&= \langle \mathcal{Q}_\alpha^{(o)} (\tilde{\mathcal{H}}_x^{(s)} + \tilde{\mathcal{H}}_y^{(s)} + \tilde{\mathcal{H}}_x^{(o)} + \tilde{\mathcal{H}}_y^{(o)}) \mathcal{Q}_\beta^{(o)} \rangle_0 \\
&\quad - \langle \tilde{\mathcal{H}}_x^{(s)} + \tilde{\mathcal{H}}_y^{(s)} + \tilde{\mathcal{H}}_x^{(o)} + \tilde{\mathcal{H}}_y^{(o)} \rangle \langle \mathcal{Q}_\alpha^{(o)} \mathcal{Q}_\beta^{(o)} \rangle_0 \\
&= \langle \mathcal{Q}_\alpha^{(o)} (\tilde{\mathcal{H}}_y^{(s)} + \tilde{\mathcal{H}}_x^{(o)} + \tilde{\mathcal{H}}_y^{(o)}) \mathcal{Q}_\beta^{(o)} \rangle_0 - (E_{0y}^{(s)} + E_{0x}^{(o)} + E_{0y}^{(o)}) \langle \mathcal{Q}_\alpha^{(o)} \mathcal{Q}_\beta^{(o)} \rangle_0 \\
&\approx \langle \mathcal{Q}_\alpha^{(o)} \tilde{\mathcal{H}}^{(o)} \mathcal{Q}_\beta^{(o)} \rangle_0 - E_0^{(o)} \langle \mathcal{Q}_\alpha^{(o)} \mathcal{Q}_\beta^{(o)} \rangle_0,
\end{aligned} \tag{H2}$$

where terms with subdominant powers of S are neglected. We shall present in Section[H.1] a mathematical trick that we used to calculate the quantities $\langle \mathcal{Q}_\alpha^{(m)} (\tilde{\mathcal{H}}^{(m)} - E_0^{(m)}) \mathcal{Q}_\beta^{(m)} \rangle_0$.

We have plotted the results of the calculations of various triangle correlations in Figure 3.10 and Figure 3.11. Their limiting values at large S are listed in Table 3.2.

After the triangle correlations are computed, we can evaluate the E_g using Eq.(3.58). The J_3 that minimizes E_g is then found by standard conjugate-gradient techniques.

The computer code is written using C++. The advantage of this language is the availability of an object-oriented approach. Since our computations require a great number of operations with matrices, it is much easier to treat the matrices as a whole, rather than performing operations on their individual elements.

H.1 Calculation of $\langle \mathcal{Q}_\alpha^{(o)}(\tilde{\mathcal{H}}^{(o)} - E_0^{(o)})\mathcal{Q}_\beta^{(o)}\rangle_0$

In this section we present a trick to calculate $\langle \mathcal{Q}_\alpha^{(o)}(\tilde{\mathcal{H}}^{(o)} - E_0^{(o)})\mathcal{Q}_\beta^{(o)}\rangle_0$ without calculating the cross-correlation $\langle \sigma_{ix}^{(s)}\sigma_{jy}^{(s)}\rangle_0$. We shall show that

$$\langle \mathcal{Q}_\alpha^{(o)}(\tilde{\mathcal{H}}^{(o)} - E_0^{(o)})\mathcal{Q}_\beta^{(o)}\rangle_0 = 2\langle\langle \mathcal{Q}_\alpha^{(o)}(\tilde{\mathcal{H}}^{(o)} - E_0^{(o)})\mathcal{Q}_\beta^{(o)}\rangle\rangle_0, \tag{H3}$$

where the notation $\langle\langle \ldots\rangle\rangle_0$ was used in Appendix[F] to indicate a correlation function with $\langle \sigma_{ix}^{(s)}\sigma_{jy}^{(s)}\rangle_0 \equiv 0$.

Suppose we calculate $\langle \mathcal{Q}_\alpha^{(m)}\tilde{\mathcal{H}}^{(m)}\mathcal{Q}_\beta^{(m)}\rangle_0$ in Fourier space. We will have a sum over many terms indexed by various $\mathbf{k}$ values; schematically

$$\begin{aligned}
&\langle \mathcal{Q}(p_1\mathbf{k}_1, p_2\mathbf{k}_2, p_3\mathbf{k}_3)\tilde{\mathcal{H}}(p\mathbf{k})\mathcal{Q}(p_4 k_4, p_5\mathbf{k}_5, p_6\mathbf{k}_6)\rangle_0 \\
&\quad \propto \langle \mathcal{Q}(p_1\mathbf{k}_1, p_2\mathbf{k}_2, p_3\mathbf{k}_3)(\mathcal{K}^{(p)}(\mathbf{k})\sigma^{(p)}(\mathbf{k})_x\sigma^{(p)}(-\mathbf{k})_x \\
&\qquad + \mathcal{M}^{(p)-1}(\mathbf{k})\sigma^{(p)}(\mathbf{k})_y\sigma^{(p)}(-\mathbf{k})_y)\mathcal{Q}(p_4\mathbf{k}_4, p_5\mathbf{k}_5, p_6\mathbf{k}_6)\rangle_0
\end{aligned} \tag{H4}$$

When we apply Wick's theorem to these terms, the only terms that would not be cancelled by their counterparts in $\langle \mathcal{Q}_\alpha^{(m)}E_0^{(m)}\mathcal{Q}_\beta^{(m)}\rangle_0$ would be those which pair up the σ's in $\tilde{\mathcal{H}}$ with the σ's in the $\mathcal{Q}_\alpha^{(m)}$'s.

The essence of the demonstrations below can be expressed schematically as this:

$$\begin{aligned}
\langle \sigma_x^{(m)}(\tilde{\mathcal{H}}^{(m)} - E_0^{(m)})\sigma_x^{(m)}\rangle_0 &= 2\langle \sigma_x^{(m)}(\tilde{\mathcal{H}}_x^{(m)} - E_{0x}^{(m)})\sigma_x^{(m)}\rangle_0 \\
\langle \sigma_y^{(m)}(\tilde{\mathcal{H}}^{(m)} - E_0^{(m)})\sigma_y^{(m)}\rangle_0 &= 2\langle \sigma_y^{(m)}(\tilde{\mathcal{H}}_y^{(m)} - E_{0y}^{(m)})\sigma_y^{(m)}\rangle_0.
\end{aligned} \tag{H5}$$

Suppose we pair up the $\sigma_x^{(m)}$'s in $\mathcal{Q}_\alpha^{(m)}$ with $\tilde{\mathcal{H}}^{(m)}$. The relevant term is

$$\begin{aligned}
&\langle \ldots\rangle_0(2\mathcal{K}^{(p)}(\mathbf{k})\langle \sigma^{(p)}(-\mathbf{k})_x\sigma^{(p)}(\mathbf{k})_x\rangle_0^2 \\
&\qquad + 2\mathcal{M}^{(p)-1}(\mathbf{k})\langle \sigma^{(p)}(\mathbf{k})_x\sigma^{(p)}(\mathbf{k})_y\rangle_0\langle \sigma^{(p)}(\mathbf{k})_y\sigma^{(p)}(\mathbf{k})_x\rangle_0) \\
&\quad \propto \langle \ldots\rangle_0(\mathcal{K}^{(p)}(\mathbf{k})\sqrt{\frac{\mathcal{M}^{(p)-1}(\mathbf{k})}{\mathcal{K}^{(p)}(\mathbf{k})}}^2 + \mathcal{M}^{(p)-1}(\mathbf{k})(-i^2)) \\
&\quad = \langle \ldots\rangle_0(\mathcal{M}^{(p)-1}(\mathbf{k}) + \mathcal{M}^{(p)-1}(\mathbf{k})),
\end{aligned} \tag{H6}$$

where it is clear that if we were to set $\langle \sigma_x \sigma_y \rangle_0 \equiv 0$, we would not have the second $\mathcal{M}^{(p)-1}(\mathbf{k})$ term.

Result Eq.(H 6) immediately lead to Eq.(H 3). However, for completeness' sake, we also prove the second line of Eq.(H 5).

Suppose we pair up the $\sigma_y^{(s)}$'s in $\mathcal{Q}_\alpha^{(m)}$ with $\tilde{\mathcal{H}}^{(m)}$, (which is possible only for the $m = s$ case anyway). We would have the term

$$\begin{aligned}
&\langle \ldots \rangle_0 (2\mathcal{K}^{(p)}(\mathbf{k}) \langle \sigma^{(p)}(\mathbf{k})_y \sigma^{(p)}(\mathbf{k})_x \rangle_0 \langle \sigma^{(p)}(\mathbf{k})_x \sigma^{(p)}(\mathbf{k})_y \rangle_0 \\
&\quad + 2\mathcal{M}^{(p)-1}(\mathbf{k}) \langle \sigma^{(p)}(-\mathbf{k})_y \sigma^{(p)}(\mathbf{k})_y \rangle_0^2) \\
&\propto \langle \ldots \rangle_0 (\mathcal{K}^{(p)}(\mathbf{k})(-i^2) + \mathcal{M}^{(p)-1}(\mathbf{k}) \sqrt{\frac{\mathcal{K}^{(p)}(\mathbf{k})}{\mathcal{M}^{(p)-1}(\mathbf{k})}}^2) \\
&= \langle \ldots \rangle_0 (\mathcal{K}^{(p)}(\mathbf{k}) + \mathcal{K}^{(p)}(\mathbf{k})), \qquad \text{(H7)}
\end{aligned}$$

where, again, if we were to set $\langle \sigma_x \sigma_y \rangle_0 \equiv 0$, we would not have the first $\mathcal{K}^{(p)}(\mathbf{k})$) term.

(The reason why we cannot go on to prove that

$$\langle \mathcal{Q}_\alpha^{(s)} (\tilde{\mathcal{H}}^{(s)} - E_0^{(s)}) \mathcal{Q}_\beta^{(s)} \rangle_0 = 2 \langle \langle \mathcal{Q}_\alpha^{(s)} (\tilde{\mathcal{H}}^{(s)} - E_0^{(s)}) \mathcal{Q}_\beta^{(s)} \rangle \rangle_0$$

is because we do not know an easy result for $\langle \sigma_x^{(s)} (\tilde{\mathcal{H}}^{(s)} - E_0^{(s)}) \sigma_y^{(s)} \rangle_0$, unlike Eq.(H 5).)

Appendix I
Algorithm for Wick's Decomposition

This Appendix describes an algorithm we used to perform Wick's decomposition on high-order spin-spin correlation functions (such as the one in Eq.(3.59)) such that they can be evaluated as pair correlations.

If one has a n-spin correlation function, there are $(n-1)!!$ distinct ways to decouple it into a product of $(n/2)$ pair-correlation functions. Wick's theorem in quantum field theory states that if we have a Gaussian probability distribution, we can write the multiple correlation function as a sum of all these decoupled products,

$$\begin{aligned}\langle\sigma_1\sigma_2\sigma_3\sigma_4\ldots\rangle = &\langle\sigma_1\sigma_2\rangle\langle\sigma_3\sigma_4\rangle\langle\ldots\rangle\ldots \\ &+\langle\sigma_1\sigma_3\rangle\langle\sigma_2\sigma_4\rangle\langle\ldots\rangle\ldots+\ldots\,. \qquad \text{(I1)}\end{aligned}$$

Note that while Wick's theorem works even when the operators do not commute with each other (nor do the operators need to be time-ordered or normal-ordered as is usually assumed. See Ref.[33] for an inductive proof.) we must be careful to preserve the ordering of the operators in the correlation function. For instance, while $\langle\sigma_{ix}^{(s)}\sigma_{jx}^{(s)}\rangle_0 = \langle\sigma_{jx}^{(s)}\sigma_{ix}^{(s)}\rangle_0$, we have $\langle\sigma_{iy}^{(s)}\sigma_{jx}^{(s)}\rangle_0 = -\langle\sigma_{jx}^{(s)}\sigma_{iy}^{(s)}\rangle_0$.

When the number of operators become big, it become quite tedious to write down the analytical expression for the Wick's decomposition. Our calculation involves a product of 8 operators, and so it is quite impractical to write such an expression into the program by hand. Fortunately, we can use the symbolic manipulation ability of Mathematica to generate the C++ code computing such correlations. We describe this below.

I.1 Enumerating all the pairs

The first step is to enumerate all the possible pairings of n operators in a more abstract level before actually encoding them as functions. The list of all possible decomposition can be represented as a *nested* list of integers in Mathematica, each integer indexing one spin operator. For example, we can represent all the possible pairings of 4 operators as

$$\Big\{\Big\{\{1,2\},\{3,4\}\Big\},\ \Big\{\{1,3\},\{2,4\}\Big\},\ \Big\{\{1,4\},\{2,3\}\Big\}\Big\}. \tag{I2}$$

We call each of these pairings, such as $\Big\{\{1,2\},\{3,4\}\Big\}$, a *sublist*. (Note that this is not distinct from $\Big\{\{3,4\},\{1,2\}\Big\}$, but *is* distinct from $\Big\{\{2,1\},\{3,4\}\Big\}$. That is, order within a pair is important, since $\langle\sigma_{ix}\sigma_{jy}\rangle_0 = -\langle\sigma_{jy}\sigma_{ix}\rangle_0$.) Given the list for a product of n spin operators, we can generate the list for a product of $n+2$ spin operators by doing the following two additions *in parallel* (i.e. not sequentially) :

1) append the pair $\{n+1, n+2\}$ to each sublist of the original list. (Do this for all the sublists in the original list.) E.g.

$$\Big\{\Big\{\{1,2\},\{3,4\}\Big\},\ldots\Big\} \to \Big\{\Big\{\{1,2\},\{3,4\},\{5,6\}\Big\},\ldots\Big\}; \tag{I3}$$

2) From each pair $\{m_1, m_2\}$ in each sublist from the *original* list spawn two new sublists. The first new sublist has the pair $\{m_1, m_2\}$ replaced by $\{m_1, n+1\}$ and $\{m_2, n+2\}$. The second new sublist has this same pair $\{m_1, m_2\}$ replaced by $\{m_1, n+2\}$ and $\{m_2, n+1\}$ instead. (Do this for all the pairs in the original sublist and for all the sublists in the original list.) E.g.

$$\begin{aligned}\Big\{\Big\{\{1,2\},\{3,4\}\Big\},\ldots\Big\} \to \Big\{&\Big\{\{1,5\},\{2,6\},\{3,4\}\Big\},\Big\{\{1,6\},\{2,5\},\{3,4\}\Big\},\\ &\Big\{\{1,2\},\{3,5\},\{4,6\}\Big\},\Big\{\{1,2\},\{3,6\},\{4,5\}\Big\}\ldots\Big\}.\end{aligned} \tag{I4}$$

Concatenating the sublists generated by (1) and (2) gives us the list for $n+2$ spins. We can check that the total number of sublists in the new list equals $(n-1)!!$ from (1) plus $(n/2) \times 1 \times (n-1)!! = n(n-1)!!$ from (2), and that the sublists of the new list are distinct, giving a grand total of $(n+1)!!$, exactly the number expected for $n+2$ spins. We can therefore write a recursive procedure to create the list for $n+2$ spins starting from $n=2$. Finally, we sort the resulting list at all 3 levels with the first element in each pair or sublist as the key.

I.2 Converting spin symbols into correlation symbols

Now we try to convert the abstract list of integers obtained above into actual usable functions or array elements. The spin operators is written in Mathematica as "functions". Eg. we may write $\sigma_{ix}\sigma_{jy}$ as

```
s[x, i, ord] s[y, j, ord+1].                                    (I5)
```

The index "**ord**" is necessary because we want to treat powers of an operator as a product of identifiable operators when it comes to Wick's decomposition. Pairs of indices {ord1, ord2} are then chosen from a sublist in a list like (I 2) above, and then Mathematica will perform the substitution like

```
h[i_ , j_ , ord_]/.{s[x_, i_, ord1] s[y_, j_, ord2] → m[x, y, i, j]}/...., (I6)
```

where **h[i_ , j_ , ord_]** is some Hamiltonian operator containing a product of spin operators, and **m[x,y,i,j]** represents the pair correlation $\langle\sigma_{ix}\sigma_{jy}\rangle_0$. All the sublist of pairs will be gone through one by one, and the various ways of decomposing the product are summed up. Finally we substitute **m[x, x, i,**

j] (or **m[x, y, i, j]** etc.) by the array element **x[[i]][[j]]** (or **xy[[i]][[j]]** etc.) where **x**, **xy**, etc. are the arrays that contain the pair correlations for spin i and spin j (see Appendix[H]). Mathematica can transform its output into a format compatible with C++.

(Note that in this thesis, as we have mentioned in Section[3.9.1], we actually did not include the **xy** arrays.)

Obviously, the amount of computation necessary to compute the Wick's decomposition of n spins grows exponentially with n. This problem is compounded by the fact that symbolic manipulation programs are generally slow. We find that to decompose a product of 12 operators takes several weeks of CPU time on an IBM RS6000 workstation. In contrast, summing the resulting product over the Brillouin zone once using the C++ code takes several minutes of CPU time.

An example of a Mathematica code to decompose a sixth-order product is given in the following.

```
(*** An example of a Mma program to perform Wick's decomposition
of <s_ix^2 s_jx^2 s_jy^2>, assuming <s_ix s_jx>= 0 ***)
h[i_,j_,ord_] =s[x,i,ord] s[x,i,ord+1] s[x,j,ord+2]*
              s[x,j,ord+3] s[y,j,ord+4] s[y,j,ord+5];
              (*** Generate abstract list of integers representing all
              Wick's decomposition of 6 operators. ***)
              (*** Define recursive procedure. ***)
PairGen[n_]:=(
    prev=PairGen[n-2];
    Flatten[
        Table[
            Join[
                Flatten[
                    Table[
                        Join[
                            {
                                Join[
                                    Take[prev[[sublist]],ipair-1],
                                    Drop[prev[[sublist]],ipair],
                                    {{prev[[sublist]][[ipair]][[1]],n}},
                                    {{prev[[sublist]][[ipair]][[2]],n-1}}
                                ]
                            },
                            {
                                Join[
                                    Take[prev[[sublist]],ipair-1],
```

```
                                    Drop[prev[[sublist]],ipair],
                                    {{prev[[sublist]][[ipair]][[2]],n}},
                                    {{prev[[sublist]][[ipair]][[1]],n-1}}
                                ]
                            }
                        ],
                        {ipair,1,(n-2)/2}
                    ],
                    1
                ],
                {
                    Join[
                        prev[[sublist]],
                        {{n,n-1}}
                    ]
                }
            ],
            {sublist,1,Length[prev]}
        ],
        1
    ]
)/;n >= 4
        (*** Initialize list for 2 operators decomposition. ***)
PairGen[n_]:= {{{1,2}}} /;n == 2
        (*** Generate list for 6 operators. ***)
ListOfPairs=PairGen[6];
```

```
            (*** Sort list by first elements. ***)
SortedList=Sort[
    Table[
        Sort[
            Table[
                Sort[ListOfPairs[[sublist]][[ipair]]],
                {ipair,1,Length[ListOfPairs[[sublist]]]}
            ]
        ],
        {sublist,1,Length[ListOfPairs]}
    ]
];


            (*** The result is
            {{{1, 2}, {3, 4}, {5, 6}}, {{1, 2}, {3, 5}, {4, 6}},
             {{1, 2}, {3, 6}, {4, 5}}, {{1, 3}, {2, 4}, {5, 6}},
             {{1, 3}, {2, 5}, {4, 6}}, {{1, 3}, {2, 6}, {4, 5}},
             {{1, 4}, {2, 3}, {5, 6}}, {{1, 4}, {2, 5}, {3, 6}},
             {{1, 4}, {2, 6}, {3, 5}}, {{1, 5}, {2, 3}, {4, 6}},
             {{1, 5}, {2, 4}, {3, 6}}, {{1, 5}, {2, 6}, {3, 4}},
             {{1, 6}, {2, 3}, {4, 5}}, {{1, 6}, {2, 4}, {3, 5}},
             {{1, 6}, {2, 5}, {3, 4}}}
            ***)
            (*** Now use SortedList to generate different pairing of
            operators in h. ***)
sumterm =0;
```

```
Do[
    o1=SortedList[[ipair]][[1]][[1]];
    o2=SortedList[[ipair]][[1]][[2]];
    o3=SortedList[[ipair]][[2]][[1]];
    o4=SortedList[[ipair]][[2]][[2]];
    o5=SortedList[[ipair]][[3]][[1]];
    o6=SortedList[[ipair]][[3]][[2]];
            (*** Add to sum one particular pair
            decomposition in SortedList ***)
    sumterm=sumterm + h[i,j,1]/.
        {s[x_,i_,o1] s[y_,j_,o2] -> m[x,y,i,j]}/.
        {s[x_,i_,o3] s[y_,j_,o4] -> m[x,y,i,j]}/.
        {s[x_,i_,o5] s[y_,j_,o6] -> m[x,y,i,j]};,
            (*** For example, the last iteration uses the decomposition
            {{1, 6}, {2, 5}, {3, 4}} and generate the term
            m[x, x, j, j] m[x, y, i, j]^2, which represents
            <s_xj ^2><s_xi s_yj>^2.
            ***)
    {ipair,1,Length[SortedList]}
];
            (*** Now for illustrative purposes only,
            make all cross-correlations zero to simplify results. ***)
output = sumterm/.{m[x,y,i_,j_]->0, m[y,x,i_,j_]->0};
            (*** Put this in a Mma. function notation for later manipulation. ***)
output = output/.{m[x,x,i_,j_]->x[i][j], m[y,y,i_,j_]->y[i][j]};
            (*** Further simplify by symmetry. ***)
```

```
output = output/.{x[j][i] -> x[i][j], y[j][i] -> y[i][j]};
        (*** Convert Mma. function notation first to a Mma. matrix notation
        and then to a C program. ***)
output = output/.
    {x_[y_][z_]^n_ -> x[[y]][[z]]^n}/.
    {x_^n_ -> CForm[x^n]} >>> outputFile;
        (*** The final result, which is contained in outputFile, is
        2*(Power(x[i][j],6))*y[j][j] + x[i][i]*x[j][j]*y[j][j]
        ***)
        (*** Warning!! Mathematica may generate error messages like
        "Part::pspec: Part specification y
        is neither an integer nor a list of non-zero integers."
        These messages can be safely ignored.
        ***)
```

Appendix J
Variational and Perturbative Wavefunctions

In this Appendix, we demonstrate that the wavefunction derived from perturbation theory can also be derived from optimizing a variational wavefunction. This provides the basis for the method of Section[3.5], where we use perturbation theory to estimate the variational energy.

Both the perturbation theory and the form of the variational wavefunction we are using below assume that we have a system of finite size (a finite number of states) and the perturbation matrix element V is smaller in magnitude than the energy gap between the ground state and the excited states. This is what we meant by a "small V" in the calculation below. This assumption about finite system has been discussed in Section[3.2]). We need this assumption in order to avoid certain subtleties concerning perturbation theory in an infinite system.

Consider a Hamiltonian $\mathcal{H}$ which is divided into an unperturbed part $\tilde{\mathcal{H}}$ and a perturbation V,

$$\mathcal{H} = \tilde{\mathcal{H}} + V. \tag{J1}$$

Now let $\{|n\rangle | n = 0, 1, 2, \ldots .\}$ be the set of (orthonormal) eigenstates of $\tilde{\mathcal{H}}$, where $|0\rangle$ is the ground state. Without loss of generality, we assume that there is no diagonal matrix element of V:

$$\langle n|V|n\rangle = 0. \tag{J2}$$

Construct a variational wavefunction Ψ for the ground state of $\mathcal{H}$ as follows:

$$\Psi = \sum_n a_n |n\rangle, \tag{J3}$$

with the normalization

$$\sum_n |a_n|^2 = 1. \tag{J4}$$

Now we proceed to find the set of a_n which minimizes the ground state energy $\langle\Psi|\mathcal{H}|\Psi\rangle$:

$$\frac{\partial}{\partial a_n}(\langle\Psi|\mathcal{H}|\Psi\rangle - \lambda\langle\Psi|\Psi\rangle), \tag{J5}$$

where λ is a Lagrange multiplier. Solving this equation gives

$$a_n = \frac{1}{\lambda}\sum_{n_1} \mathcal{H}_{nn_1} a_{n_1}, \tag{J6}$$

where we use the shorthand $\mathcal{H}_{n,n_1} a_{n_1}$ to denote $\langle n|\mathcal{H}|n_1\rangle$. The Lagrange multiplier λ is found using the normalization constraint,

$$1 = \sum_n a_n a_n^* = \frac{1}{|\lambda|^2}\sum_{n,n_1,n_2} \mathcal{H}_{n_2 n}\mathcal{H}_{nn_1} a_{n_1} a_{n_2}^*. \tag{J7}$$

For small V, we expect

$$\begin{aligned} a_0 &= 1 + \mathcal{O}(V) \\ a_n &= \mathcal{O}(V), \ \text{n} \neq 0, \end{aligned} \tag{J8}$$

since we know the limit $V \to 0$. Making use of Eq.(J 2) and Eq.(J 8) and after some tedious algebra, we can solve Eq.(J 7) to get

$$\lambda = E_0 a_0 + \mathcal{O}(V^2). \tag{J9}$$

We have used the notation

$$E_n \equiv \langle n|\tilde{\mathcal{H}}|n\rangle. \tag{J10}$$

Substituting Eq.(J 9) into Eq.(J 6), we obtain first of all

$$\begin{aligned} a_0 &= \frac{1}{E_0 a_0}\sum_{n_1}(\tilde{\mathcal{H}}_{0n_1} + V_{0n_1})a_{n_1} \\ &= \frac{1}{E_0 a_0}(E_0 a_0 + \sum_{n_1 \neq 0} V_{0n_1} a_{n_1}) \\ &= 1 + \mathcal{O}(V^2), \end{aligned} \tag{J11}$$

where the absence of $\mathcal{O}(V)$ terms is demonstrated. Similarly, using Eq.(J 6), Eq.(J 9) and Eq.(J 11), we obtain

$$a_n = \frac{1}{E_0}(E_n a_n + \sum_{n_1 \neq n} V_{nn_1} a_{n_1}), \ \text{n} \neq 0, \tag{J12}$$

which can be solved to give

$$\begin{aligned} a_n &= \frac{1}{E_0 - E_n} \sum_{n_1 \neq n} V_{nn_1} a_{n_1} \\ &= \frac{1}{E_0 - E_n} V_{n0} a_0 + \mathcal{O}(V^2) \\ &= \frac{V_{n0}}{E_0 - E_n} + \mathcal{O}(V^2). \end{aligned} \tag{J13}$$

This last line is the usual second order perturbation formula, Eq.(3.16).

References

1. For a review, see C. Zeng, *Cornell University Thesis*, (1994), unpublished.

2. For an overview of ground state selection, see E. F. Shender, *Sov. Phys. JETP*, **56**, 178(1982); C. L. Henley, *Phys. Rev. Lett.*, **62**, 2056(1989); and the review article by A. B. Harris in *Disorder in Condensed Matter Physics: a Volume in Honour of Roger Elliott*, (ed. J. A. Blackman and J. Tagueña), Clarendon Press 1991. See also Q. Sheng and C. L. Henley, *J. Phys. Condens. Matt.*, **4**, 2937(1993) for another case where anharmonic perturbation is necessary for selection.

3. J. Villain, R. Bidaux, J.-P. Carton and R. Conte,*J. de Physique*, **41**, 1263(1980).

4. H. Xu and M. Baus, *J. Phys.: Condens. Matter*, **4**, L663(1992).

5. I. Ritchey, P. Coleman and P. Chandra, *Phys. Rev. B*, **47**, 15342(1993).

6. E. F. Shender, V. B. Cherepanov, P. C. W. Holdsworth and A. J. Berlinsky, *Phys. Rev. Lett.*, **70**, 3812(1993).

7. E. F. Shender, P. C. W. Holdsworth, " Order by Disorder and topology in frustrated magnetic systems", in *Fluctuations and Order: The New Synthesis*, (M. M. Millonas ed.), MIT Press 1994.

8. A. B. Harris, C. Kallin and A. J. Berlinsky, *Phys.Rev.B*, **45**, 2899(1992).

9. J. Chalker, P. C. W. Holdsworth and E. F. Shender,*Phys. Rev. Lett.*, **68**, 855(1992).

10. D. A. Huse and A. Rutenberg, *Phys. Rev. B*, **45**, 7536(1992).

11. J. N. Reimers and A. J. Berlinsky, *Phys. Rev. B*, **48**, 9539(1993).

12. J. B. Marston and C. Zeng, *J. Appl. Phys.*, **69**, 5962(1991).

13. S. Sachdev, *Phys. Rev. B*, **45**, 12377(1992).

14. V. Elser, *Phys. Rev. Lett.*, **62**, 2405(1989).

15. C. Zeng and V. Elser, *Phys. Rev. B.*, **42**, 8436(1990).

16. P. W. Leung and V. Elser, *Phys. Rev. B*, **47**, 5459(1993).

17. V. Elser and C. Zeng, *Phys. Rev. B.*, **48**, 13647(1993).

18. D. S. Greywall and P. A. Busch, *Phys. Rev. Lett.*, **62**, 1868(1989) and references therein.

19. P. Chandra, P. Coleman and I. Ritchey, *J. Physique*, **3**, 591(1993).

20. A. Chubukov, *Phys. Rev. Lett.*, **69**, 832(1992). See also A. Chubukov, *J. Appl. Phys.*, **73**, 5639(1993).

21. A. P. Ramirez, G. P. Espinosa and A.S. Cooper, *Phys. Rev. Lett.*, **64**, 2070(1990).

22. C. Broholm, G. Aeppli, G. P. Espinosa and A. S. Cooper, *Phys. Rev. Lett.*, **65**, 3173(1990).

23. C. Broholm, G. Aeppli, G. P. Espinosa and A. S. Cooper, *J. Appl. Phys.*, **69**, 4968(1990).

24. R. J. Baxter, *J. Math. Phys.*, **11**, 784(1970).

25. J. von Delft and C. L. Henley, *Phys. Rev. B*, **48**, 965(1993).

26. See for e.g., C.Kittel, *Quantum Theory of Solids*, p.49. (John Wiley & Sons, 1963).

27. C. L. Henley and B. E. Larson, *J. Appl. Phys.*, **67**, 5752(1990).

28. D. C. Mattis, Phys. Lett. A **56**, 421(1976).

29. M. Kvale, preprint 1994 (submitted to *Phys. Rev. B.*).

30. A. Chubukov, private communication.

31. See for e.g., J. M. Ziman, *Models of Disorder*, p.330. (Cambridge University Press, 1979).

32. See for e.g., N. W. Ashcroft and N. D. Nermin, *Solid State Physics*, p.187. (Saunders College, 1976).

33. C. L. Henley, private communication.

34. C. L. Henley and E. P. Chan, submitted to ICM '94 (for publication in *J. Mag. Mag. Mater.*), 1994.

ORDERING BY DISORDER
IN
KAGOMÉ QUANTUM ANTIFERROMAGNET

A Dissertation
Presented to the Faculty of the Graduate School
of Cornell University
in Partial Fulfillment of the Requirements for the Degree of
Doctor of Philosophy

by
Ernest P. Chan
August 1994

ORDERING BY DISORDER
IN
KAGOMÉ QUANTUM ANTIFERROMAGNET

Ernest P. Chan, Ph.D.
Cornell University 1994

The ground state ensemble of classical Heisenberg antiferromagnetic spins on the kagomé lattice has degeneracies which grow exponentially with system size. This large degeneracy is typical of *frustrated* systems. However, quantum fluctuations may endow these classical ground states with different quantum zero point energies, resulting in an unique quantum ground state. Ordinarily, harmonic spinwave theory suffices to determine this "selection energy"; however, in this case, a macroscopic number of degeneracies remain upto harmonic order. This thesis explores the use of spinwave theory upto quartic order in the search for the quantum ground state.

We construct a non-Gaussian variational function in order to estimate the ground state energy of a disordered Hamiltonian with quartic interactions. Localized magnons form the basis of the variational subspace. A partially analytic solution to the variational minimization is found using perturbation theory on the cubic and disordered part of the Hamiltonain. The resulting energy is written as an effective Ising Hamiltonian with the *chiralities* of the spins serving as the Ising variables. The selected ground state has perfect periodicity, of the "$\sqrt{3} \times \sqrt{3}$" kind, rendering this an example of the general phenomenon of "ordering by disorder".

Biographical Sketch

Ernest Pun Chan was born on January 11, 1966, in Hong Kong, where he received his elementary and secondary education. In 1983 he and his family emigrated to Toronto, Canada. He attended one year of high school there and 4 years of college at the University of Toronto, majoring in physics. During the summers of 1987 and 1988 he worked at the physics department of the University of British Columbia as a research assistant. He enrolled as a graduate student in the physics department of Cornell University in Fall, 1988. He will be joining the Human Language Technologies Group at IBM Thomas J. Watson Research Center as a postdoctoral fellow starting Fall, 1994.

To Chan Hung Yip and Lau Ching

Acknowledgments

I am greatly indebted to Professor Chris Henley, my thesis advisor, for introducing me to a style of thinking and research that, I am certain, will benefit me in whatever endeavor I pursue in the future. He is a person of high integrity and honesty. His concern and attention to students is much appreciated.

I am also very grateful to my two other special committee members, Professors Jim Sethna and Bobby Pohl. They both served as my research supervisors at one time or another, and have given me much guidance and support since then. Jim is forever excited to listen to his students' ideas and forever encouraging. Bobby inspires a standard of thoroughness in research that I shall always aspire to.

I thank Professor Veit Elser for suggesting, among other things, the Method of Moments which eventually lead to the form of our non-gaussian wavefunction.

A number of my colleagues in the LASSP theory group have provided great help to me in this research. Among them are Chen Zeng, Qing Sheng, and Mark Kvale. They have inspired many important ideas in this thesis and have clarified for me many complicated issues. As for help in the computational aspects of the work, I must thank Bruce Roberts and Mark Oxborrow for assisting me with their prolific knowledge of UNIX, C++, and Mathematica.

I am grateful to my former and present officemates, Bryd Edwards, Sivan Kartha, Christos Likos, Lin-Wang Wang and Lisa Wickham, for their forbearance, and to Chris Rapcewicz, Tony Basile, Ragu Raghavan and Zhiping Liu for their friendships and advices.

There are many other people in Cornell that I wish to thank for their warm friendships over the years: Jack Chan, Cho-Hoi Hui, Pak-Wo Leung, Zhi Liu, Daniel Mak, Kaikee Wong, Shu So, Tsing-Yi Tsai, and Sheng-Te Tsao. Finally, my deepest gratitude to my housemate and friend Dave Mikolas, who led me to many novel ways of looking at things, who prodded me to do things I would not imagine doing, and who is an unfailing supplier of sympathy and comfort in times of hardship.

Table of Contents

Page

1 Introduction 1
1.1 Ordering by Disorder 1
1.2 Regimes of Interest 3
1.3 Outline of Paper 6

2 Review of Kagomé Peculiarities 9
2.1 Classical Ground States 9
2.2 Coplanar Selection 13
2.3 Zero Modes 15
2.4 Effects of Anharmonicity 17

3 Calculation of In-plane Selection 20
3.1 Spinwave Hamiltonian 20
3.2 Variational Wavefunction 27
3.3 Renormalized Gaussian Wavefunction 31
3.4 Non-gaussian Part of Wavefunction 36
3.4.1 Kinds of Excited States to be Included 37
3.4.2 Definition of Non-gaussian Wavefunction 39
3.5 Partial Optimization of Wavefunction 42
3.6 Perturbation Theory in the Subspace Ξ 44
3.7 Effective Ising Hamiltonian 46
3.8 Relation to Reciprocal Space Perturbation 49
3.9 Results 51
3.9.1 In-plane Selection 51
3.9.2 Implicit Contributions to Selection Energy 57
3.9.3 Failure of Optimization 59
3.9.4 Regulated Hamiltonian 66
3.10 Discussion 68

3.10.1 Implications on Perturbative Approach 68
3.10.2 Possible Error in In-plane Selection? 70

4 Conclusion 73

Appendices

A Why a Gaussian Ψ is Inadequate 77

B Renormalized Harmonic Hamiltonian 82
B.1 Definition 82
B.2 Spin-spin correlations 85
B.3 Qualitative Properties of Spin-spin Correlations 91

C Qualitative Estimate of Ground State Energy 99
C.1 First Order Term 99
C.2 Higher Order Terms 100
C.2.1 Perturbation of Odd Terms 100
C.2.2 Perturbation of Even Terms 102
C.3 Conclusion 103

D Orthogonality of $\mathcal{Q}_{\boldsymbol{\beta}}^{(\mathbf{m})}$ and $\boldsymbol{\Upsilon}_{\boldsymbol{\alpha}}^{(\mathbf{m}')}$ 104

E Alternative Forms of $\mathcal{Q}_{\boldsymbol{\alpha}}$ 106

F Analytic Form of $\langle\!\langle \mathcal{Q}_{\boldsymbol{\alpha}}^{(\mathbf{m})}\ \mathcal{Q}_{\boldsymbol{\beta}}^{(\mathbf{m})} \rangle\!\rangle_{\mathbf{0}}$ 109
F.1 Why is $\langle \mathcal{Q}_{\mathbf{0}}^{(\mathbf{o})} \mathcal{Q}_{\mathbf{1}}^{(\mathbf{o})} \rangle_{\mathbf{0}} = \mathbf{0}$? 110
F.2 Why is $\langle\langle \mathcal{Q}_{\mathbf{0}}^{(\mathbf{s})} \mathcal{Q}_{\mathbf{1}}^{(\mathbf{s})} \rangle\rangle_{\mathbf{0}} < \mathbf{0}$? 112
F.3 Conclusion 113

G Scaling with S and J_3 114
G.1 Scaling of $\langle \mathcal{Q}_{\alpha}^{(m)} (\tilde{\mathcal{H}} - E_0) \mathcal{Q}_{\beta}^{(m)} \rangle_0$ 114
G.2 Scaling of $\langle \mathcal{Q}_{\alpha}^{(m)} \mathcal{Q}_{\beta}^{(m)} \rangle_0$ 115
G.3 Scaling of $\overline{g}^{(m)}$ and $\mathcal{J}_{\alpha\beta}^{(m)}$ 116

H Calculational Algorithm for $J_{\alpha\beta}$ 117
H.1 Calculation of $\langle \mathcal{Q}_\alpha^{(o)} (\tilde{\mathcal{H}}^{(o)} - E_0^{(o)}) \mathcal{Q}_\beta^{(o)} \rangle_0$ 120

I Algorithm for Wick's Decomposition 122
I.1 Enumerating all the pairs 123
I.2 Converting spin symbols into correlation symbols 124

J Variational and Perturbative Wavefunctions 131

References 134

List of Tables

Page

3.1 Soft and Ordinary Modes Contributions to $\mathcal{J}_{\alpha\beta}$ 56

3.2 Numerical values of triangle correlations 63

3.3 Numerical values of energy expectations and Green's functions . 65

3.4 $J_3(f = 0)$ as function of S 68

B .1 Numerical values of $\langle \sigma_{ix}^{(m)} \sigma_{jx}^{(m)} \rangle_0$, $\langle \sigma_{iy}^{(m)} \sigma_{jy}^{(m)} \rangle_0$ and $\langle \sigma_{ix}^{(s)} \sigma_{jy}^{(s)} \rangle_0$ . . 95

List of Figures

Page

1.1 Illustration of quantum and thermal selection 2
1.2 Ground states of the classical kagomé Hamiltonian 4
2.1 Mapping coplanar states to Potts states 10
2.2 Creating a non-coplanar state 12
2.3 Schematic harmonic spinwave spectrum 14
2.4 Hexagon mode 15
2.5 Spin deviation vector 16
3.1 Definition of local coordinate axes 21
3.2 Definition of chirality 24
3.3 Mapping of Potts States to Ising Model 25
3.4 Labelling of triangles 52
3.5 $\mathcal{J}_{\alpha\beta}$ as functions of J_3 53
3.6 Finite size scaling of $\mathcal{J}_{\alpha\beta}$ 54
3.7 $\mathcal{J}^{(m)}_{\alpha\beta}$ as functions of $|J_3|$ 55
3.8 $\langle\tilde{\mathcal{H}}^{(m)}\rangle_0$, $\langle\mathcal{H}^{(m)}_2\rangle_0$ and $\langle\mathcal{H}^{(m)}_4\rangle_0$ as functions of J_3 and S 60
3.9 $\overline{g}^{(m)}$ as functions of J_3 and S 61
3.10 $\langle\mathcal{Q}^{(m)}_\alpha\mathcal{Q}^{(m)}_\beta\rangle_0$ as function of J_3 and S. 62
3.11 $\langle\mathcal{Q}^{(m)}_\alpha(\tilde{\mathcal{H}}-E_0)\mathcal{Q}^{(m)}_\beta\rangle_0$ as function of J_3 and S. 64
3.12 $J_3(f=0)$ as function of S 67
3.13 Comparison between exact and approximate variational energy . 70
A .1 The equivalence of all spins in a symmetric Potts state 78
A .2 Reflection symmetry of a symmetric Potts state 79
B .1 Next-nearest-neighbor couplings used in $\tilde{\mathcal{H}}$ 82
B .2 Shape of lattices used in computation 88
B .3 Labelling of sites 92
B .4 $\langle\sigma^{(m)}_{ix}\sigma^{(m)}_{jx}\rangle_0$ as function of J_3 93
B .5 $\langle\sigma^{(m)}_{iy}\sigma^{(m)}_{jy}\rangle_0$ as function of J_3 94

B .6 Plot of $\mathcal{K}^{(p)}(\mathbf{k})$ and $\mathcal{M}^{(p)-1}(\mathbf{k})$ 95
B .7 Plot of $\langle \sigma^{(p)}(\mathbf{k})_x \sigma^{(p)}(\mathbf{k})_x \rangle_0$ and $\langle \sigma^{(p)}(\mathbf{k})_y \sigma^{(p)}(\mathbf{k})_y \rangle_0$ 96
B .8 Plot of $\omega^{(p)}(\mathbf{k})$ 98